

# Climate4you update September 2020



1

Climate4you.com

## Summary of observations:

- 1: Observed average global air temperature change last 30 years is about  $+0.15^{\circ}\text{C}$  per decade.  
If unchanged, additional average global air temperature increase by year 2100 will be about  $+1.2^{\circ}\text{C}$ .
- 2: Tide gauges along coasts indicate a typical global sea level increase of about 1-2 mm/yr.  
Coastal sea level change rate last 100 year has essential been stable, without recent acceleration.  
If unchanged, global sea level at coasts will typically increase 8-16 cm by year 2100, although many locations in regions affected by glaciation 20,000 years ago, will experience a relative sea level drop.
- 3: Since 2004 the global oceans above 1900 m depth on average have warmed about  $0.07^{\circ}\text{C}$ .  
The maximum warming (about  $0.2^{\circ}\text{C}$ , 0-100 m depth) mainly affects oceans near Equator,  
where the incoming solar radiation is at maximum.
- 4: Changes in atmospheric CO<sub>2</sub> follow changes in global air temperature.  
Changes in global air temperature follow changes in ocean surface temperature.
- 5: There is no perceptible effect on atmospheric CO<sub>2</sub> due to the COVID-related drop in GHG emissions. Natural sinks and sources for atmospheric CO<sub>2</sub> far outweigh human contributions.

## Contents:

- Page 3: September 2020 global surface air temperature overview
- Page 4: September 2020 global surface air temperature overview versus September last 10 years
- Page 5: September 2020 global surface air temperature compared to September 2019
- Page 6: Temperature quality class 1: Lower troposphere temperature from satellites
- Page 7: Temperature quality class 2: HadCRUT global surface air temperature
- Page 8: Temperature quality class 3: GISS and NCDC global surface air temperature
- Page 11: Comparing global surface air temperature and satellite-based temperatures
- Page 12: Global air temperature linear trends
- Page 13: Global temperatures: All in one, Quality Class 1, 2 and 3
- Page 15: Global sea surface temperature
- Page 18: Ocean temperature in uppermost 100 m
- Page 20: North Atlantic heat content uppermost 700 m
- Page 21: North Atlantic temperatures 0-800 m depth along 59N, 30-0W
- Page 22: Global ocean temperature 0-1900 m depth summary
- Page 23: Global ocean net temperature change since 2004 at different depths
- Page 24: La Niña and El Niño episodes
- Page 25: Troposphere and stratosphere temperatures from satellites
- Page 26: Zonal lower troposphere temperatures from satellites
- Page 27: Arctic and Antarctic lower troposphere temperatures from satellites
- Page 28: Temperature over land versus over oceans
- Page 29: Arctic and Antarctic surface air temperatures
- Page 32: Arctic and Antarctic sea ice
- Page 36: Sea level in general
- Page 36: Global sea level from satellite altimetry
- Page 38: Global sea level from tide gauges
- Page 39: Snow cover; Northern Hemisphere weekly and seasonal
- Page 41: Atmospheric specific humidity
- Page 42: Atmospheric CO<sub>2</sub>
- Page 43: Relation between annual change of atm. CO<sub>2</sub> and La Niña and El Niño episodes
- Page 44: Phase relation between atmospheric CO<sub>2</sub> and global temperature
- Page 45: Global air temperature and atmospheric CO<sub>2</sub>
- Page 49: Latest 20-year QC1 global monthly air temperature change
- Page 50: Sunspot activity and QC1 average satellite global air temperature
- Page 51: Climate and history: *The Zweite Mandrenke 1634 AD*.

## September 2020 global surface air temperature overview

General: This newsletter contains graphs and diagrams showing a selection of key meteorological variables, if possible updated to the most recent past month. All temperatures are given in degrees Celsius.

In the maps on pages 4-5, showing the geographical pattern of surface air temperature anomalies, the last previous 10 years are used as reference period.

The rationale for comparing with this recent period instead of the official WMO so-called ‘normal’ period 1961-1990, is that the latter period is affected by the cold period 1945-1980. Most comparisons with this period will inevitably appear as warm, and it will be difficult to decide if modern temperatures are increasing or decreasing. Comparing instead with the last previous 10 years overcomes this problem and clearer displays the modern dynamics of ongoing change. This decadal approach also corresponds well to the typical memory horizon for many people and is now also adopted as reference period by other institutions, e.g. the Danish Meteorological Institute (DMI).

3

In addition, most temperature databases display temporal instability for data before the turn of the century (see, e.g., p. 9). Any comparison with the WMO reference period 1961-1990 will therefore be influenced by such ongoing monthly changes of mainly administrative nature. An unstable value is clearly not suited as reference value. Simply comparing with the last previous 10 years is more useful as reference for modern changes. See also additional reflections on page 47.

The different air temperature records have been divided into three quality classes, QC1, QC2 and QC3, respectively, as described on page 9.

In many diagrams shown in this newsletter the thin line represents the monthly global average value, and the thick line indicate a simple running average, in most cases a simple moving 37-month average, nearly corresponding to a three-year average. The 37-month average is calculated from values covering a range from 18 months before to

18 months after, with equal weight given to all individual months.

The year 1979 has been chosen as starting point in many diagrams, as this roughly corresponds to both the beginning of satellite observations and the onset of the late 20<sup>th</sup> century warming period. However, several of the data series have a much longer record length, which may be inspected in greater detail on [www.climate4you.com](http://www.climate4you.com).

### September 2020 surface air temperature

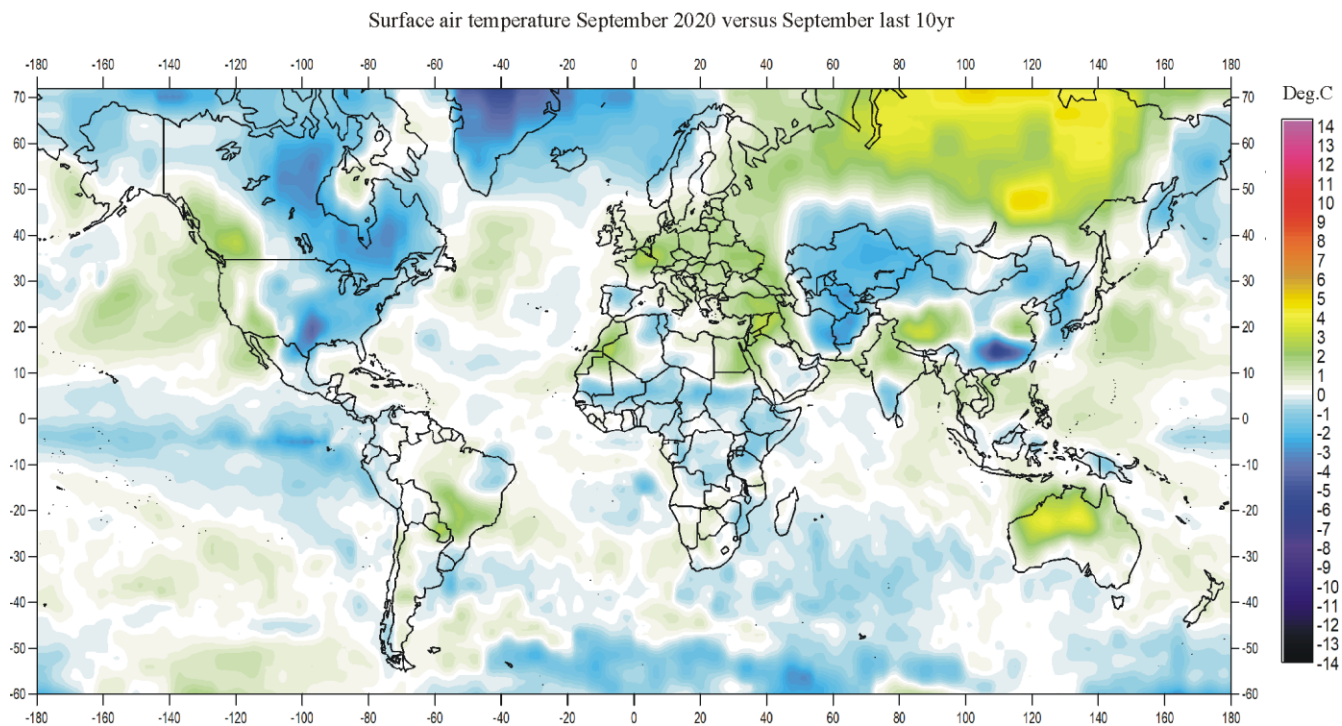
General: For September 2020 GISS supplied 16200 AIRS interpolated surface air data points. According to most temperature databases, the September 2020 global average air temperature anomaly was somewhat higher than in the previous month.

The Northern Hemisphere 10-yr temperature anomaly pattern (p.4) was characterised by regional contrasts, mainly controlled by the dominant jet stream configuration. Most of North America and Greenland was relatively cold, as were parts of Asia. In contrast, most of Europe and northern Russia and Siberia had temperatures above the 10-yr average. Ocean wise, the NE Pacific was relatively warm, while the Greenland- and Norwegian Sea were relatively cold. In the Arctic, the Alaska-, Canada-, and Greenland sectors were relatively cold, while the Russia-Siberian sectors were relatively warm.

Near the Equator temperatures were mostly near or below (especially in the Pacific Ocean) the 10-year average.

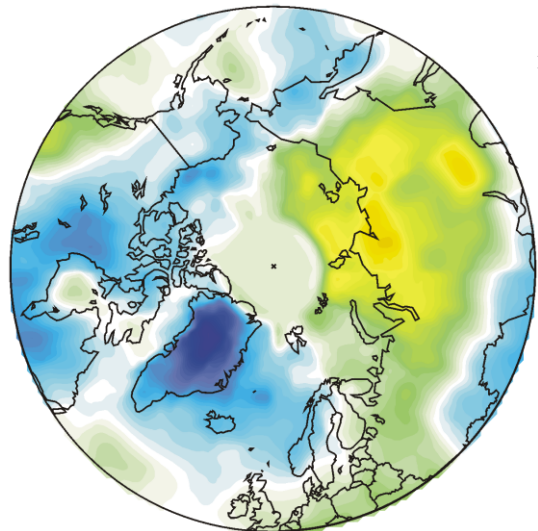
The Southern Hemisphere temperatures were largely near or below the average for the previous 10 years. Only NW Australia and parts of southern Brazil had temperatures clearly above the 10-yr average. In the Antarctic, most of East Antarctica was relatively warm, while parts of West Antarctica were relatively cold. The remaining part of the continent was a mixture of relatively warm and cold areas.

## September 2020 global surface air temperature overview versus average September last 10 years

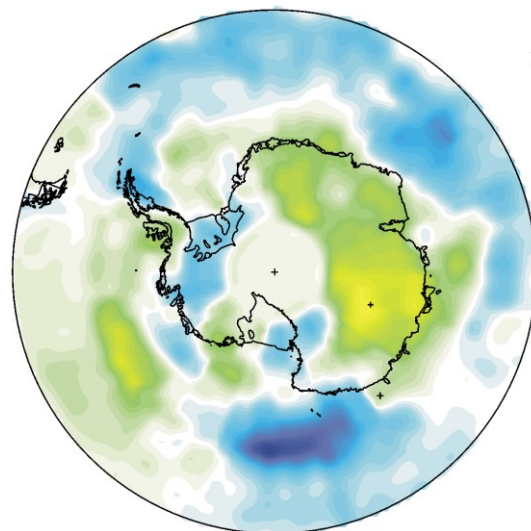


4

Surface air temperature September 2020 versus September last 10 yr

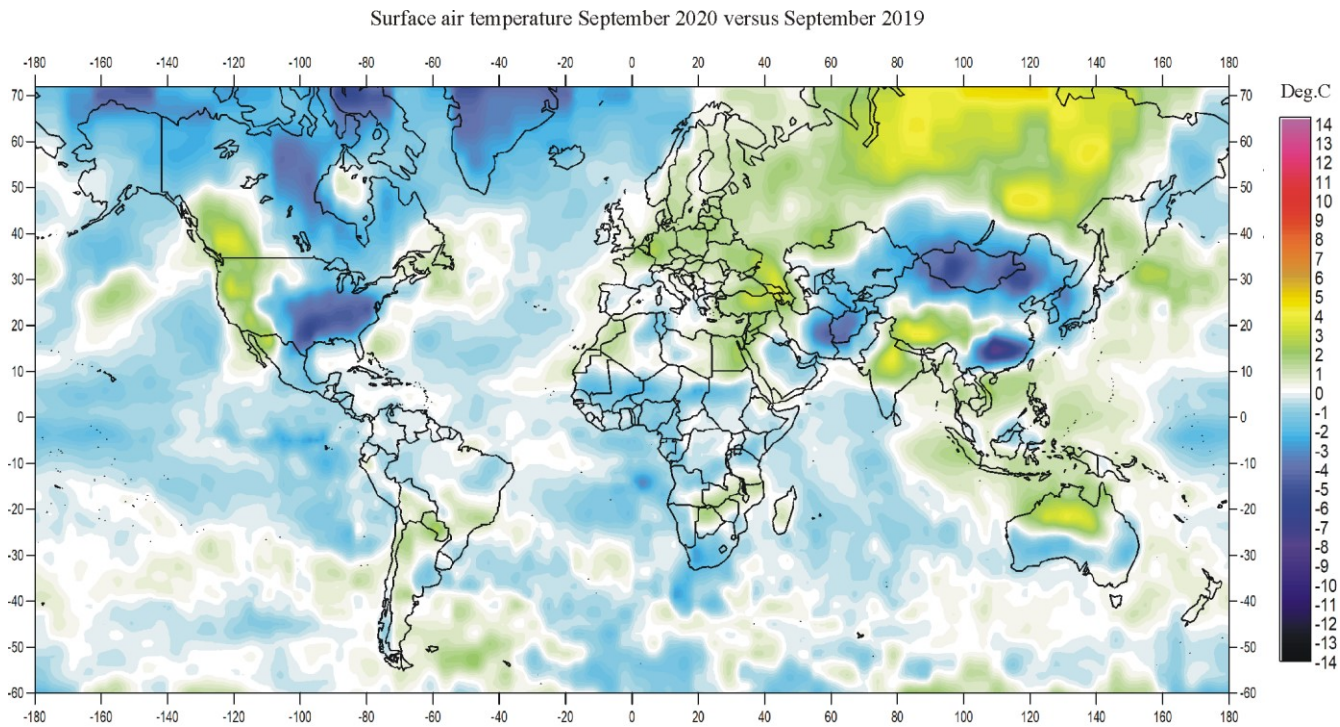


Surface air temperature September 2020 versus September last 10 yr



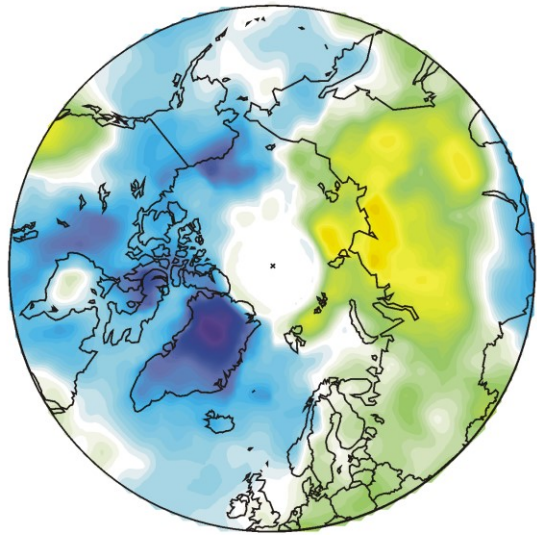
*September 2020 surface air temperature compared to the average of September over the last 10 years. Green-yellow-red colours indicate areas with higher temperature than the 10-year average, while blue colours indicate lower than average temperatures. Data source: Remote Sensed Surface Temperature Anomaly, AIRS/Aqua L3 Monthly Standard Physical Retrieval 1 degree x 1 degree V006 (<https://airs.jpl.nasa.gov/>), obtained from the GISS data portal ([https://data.giss.nasa.gov/gistemp/maps/index\\_v4.html](https://data.giss.nasa.gov/gistemp/maps/index_v4.html)).*

## September 2020 global surface air temperature compared to September 2019

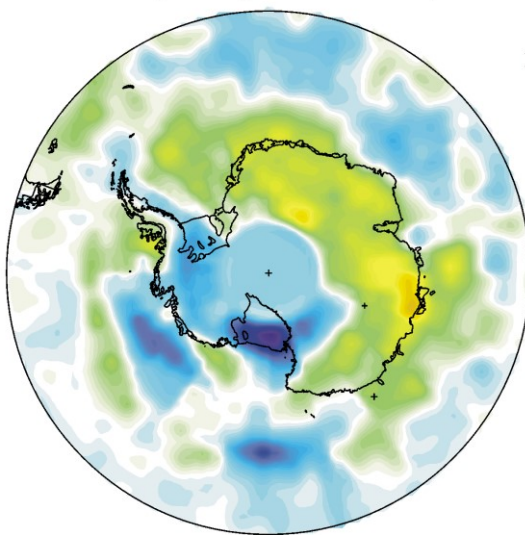


5

Surface air temperature September 2020 versus September 2019

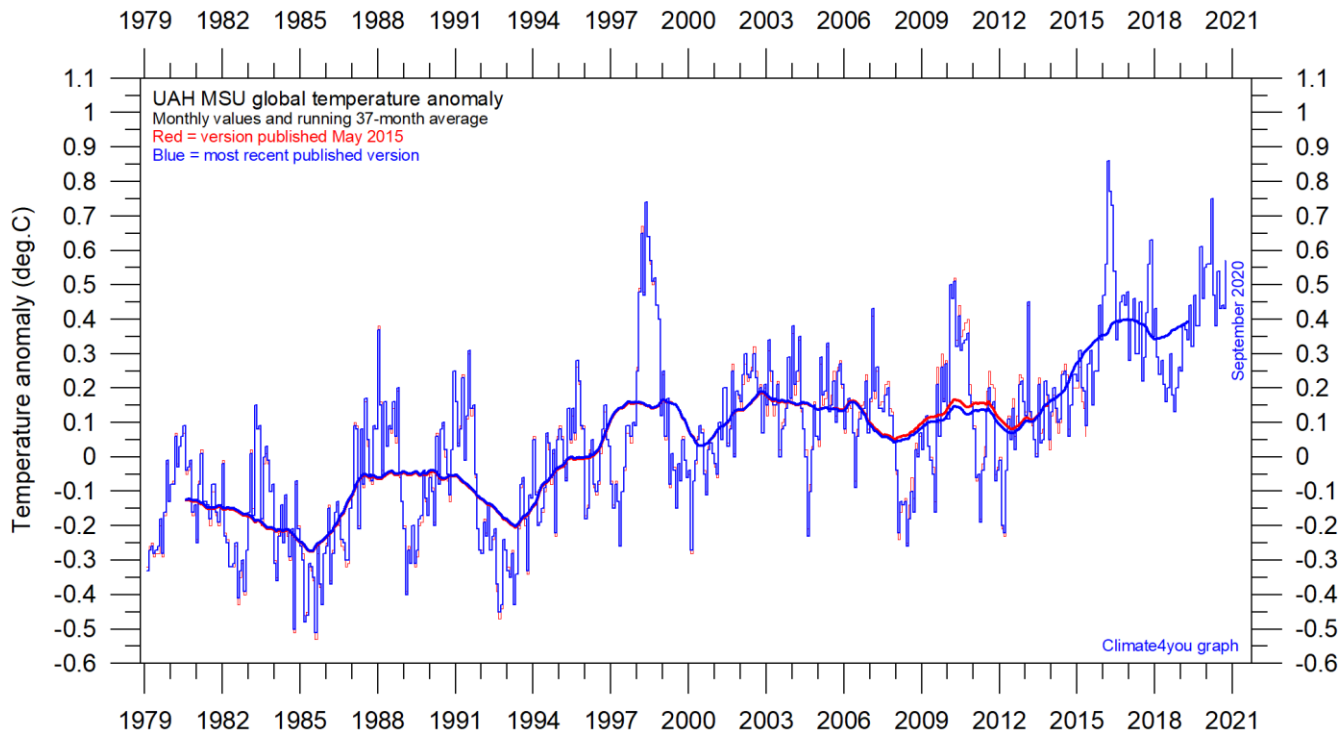


Surface air temperature September 2020 versus September 2019

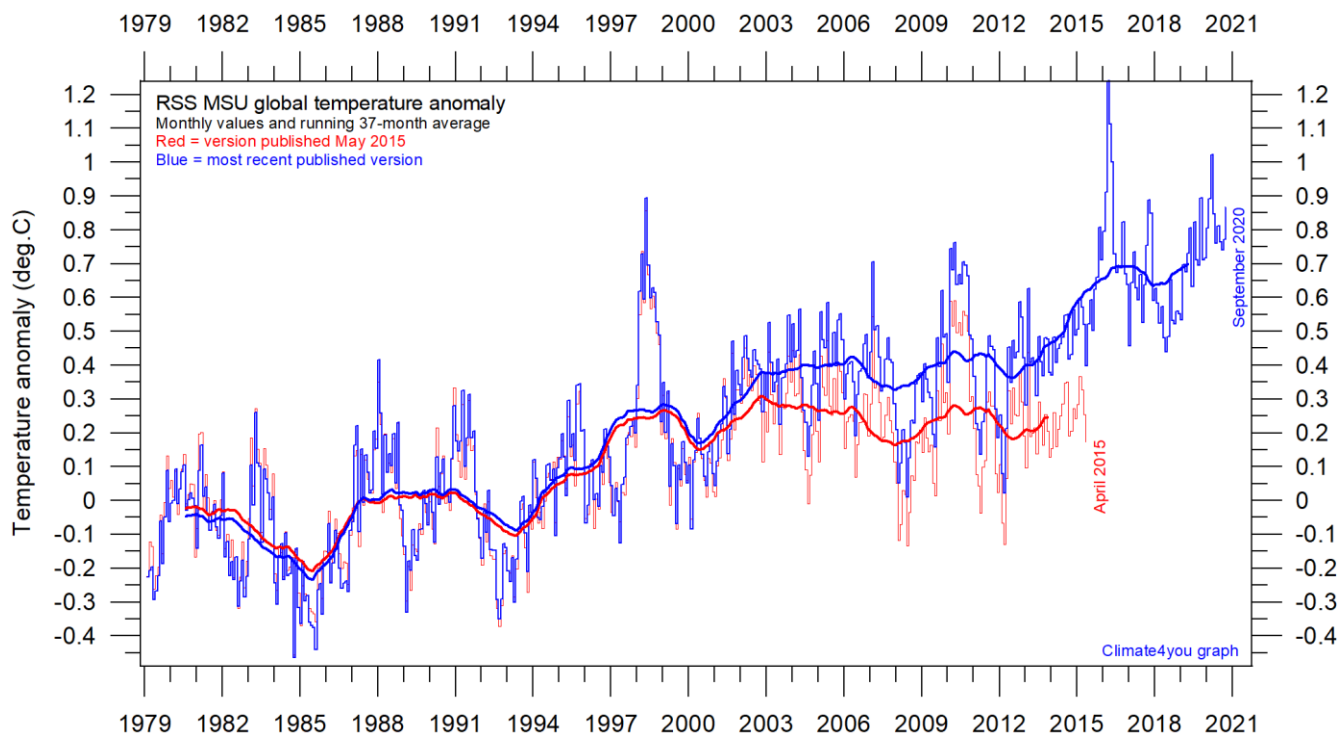


*September 2020 surface air temperature compared to September 2019. Green-yellow-red colours indicate regions where the present month was warmer than last year, while blue colours indicate regions where the present month was cooler than last year. Variations in monthly temperature from one year to the next has no tangible climatic importance but may nevertheless be interesting to study. Data source: Remote Sensed Surface Temperature Anomaly, AIRS/Aqua L3 Monthly Standard Physical Retrieval 1 degree x 1 degree V006 (<https://airs.jpl.nasa.gov/>), obtained from the GISS data portal ([https://data.giss.nasa.gov/gistemp/maps/index\\_v4.html](https://data.giss.nasa.gov/gistemp/maps/index_v4.html)).*

**Temperature quality class 1: Lower troposphere temperature from satellites, updated to September 2020**

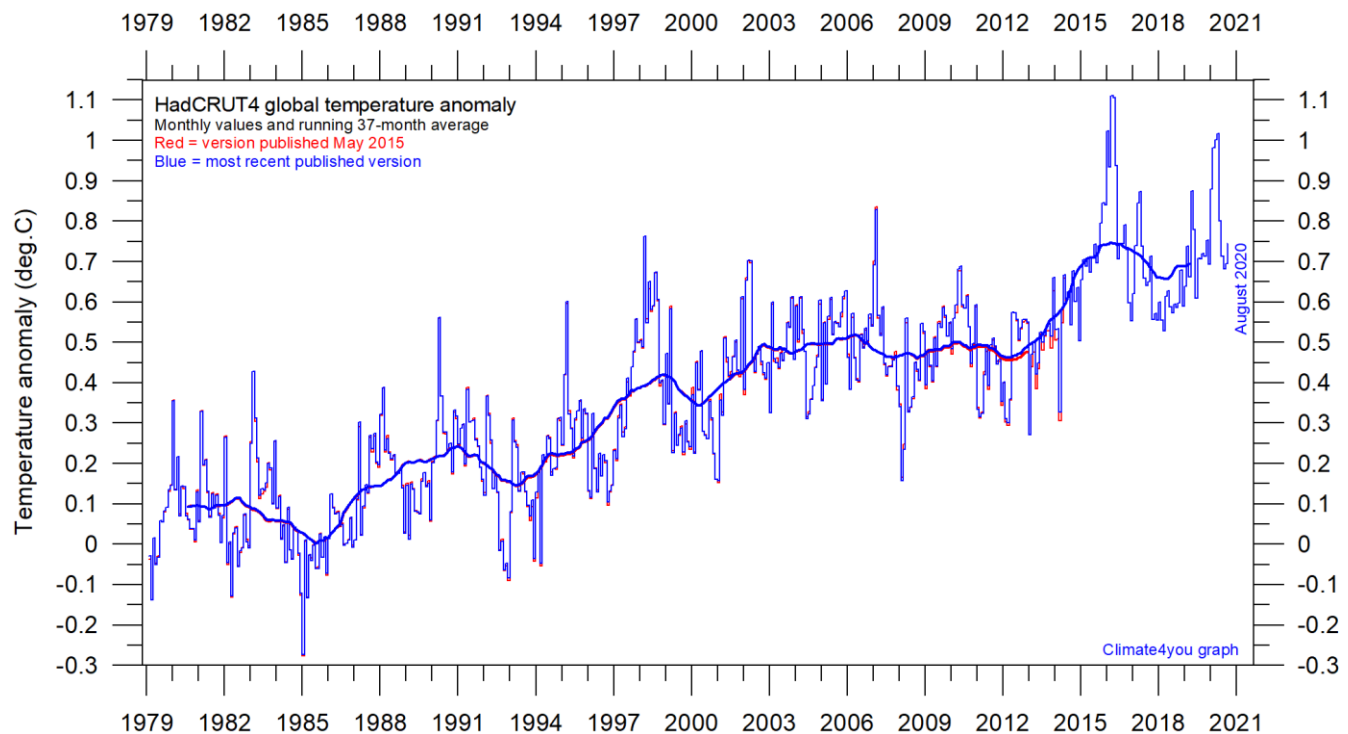


Global monthly average lower troposphere temperature (thin line) since 1979 according to [University of Alabama](#) at Huntsville, USA. The thick line is the simple running 37-month average.



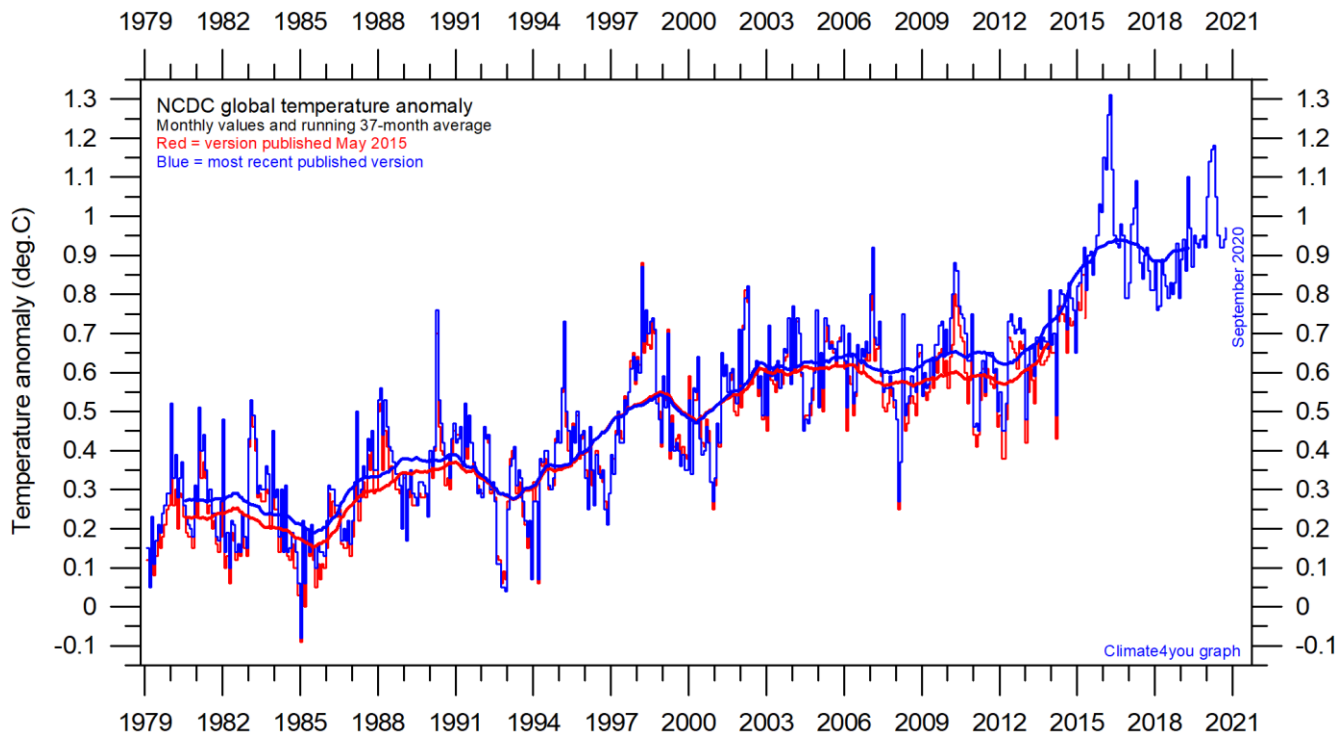
Global monthly average lower troposphere temperature (thin line) since 1979 according to [Remote Sensing Systems \(RSS\)](#), USA. The thick line is the simple running 37-month average.

## Temperature quality class 2: HadCRUT global surface air temperature, updated to August 2020

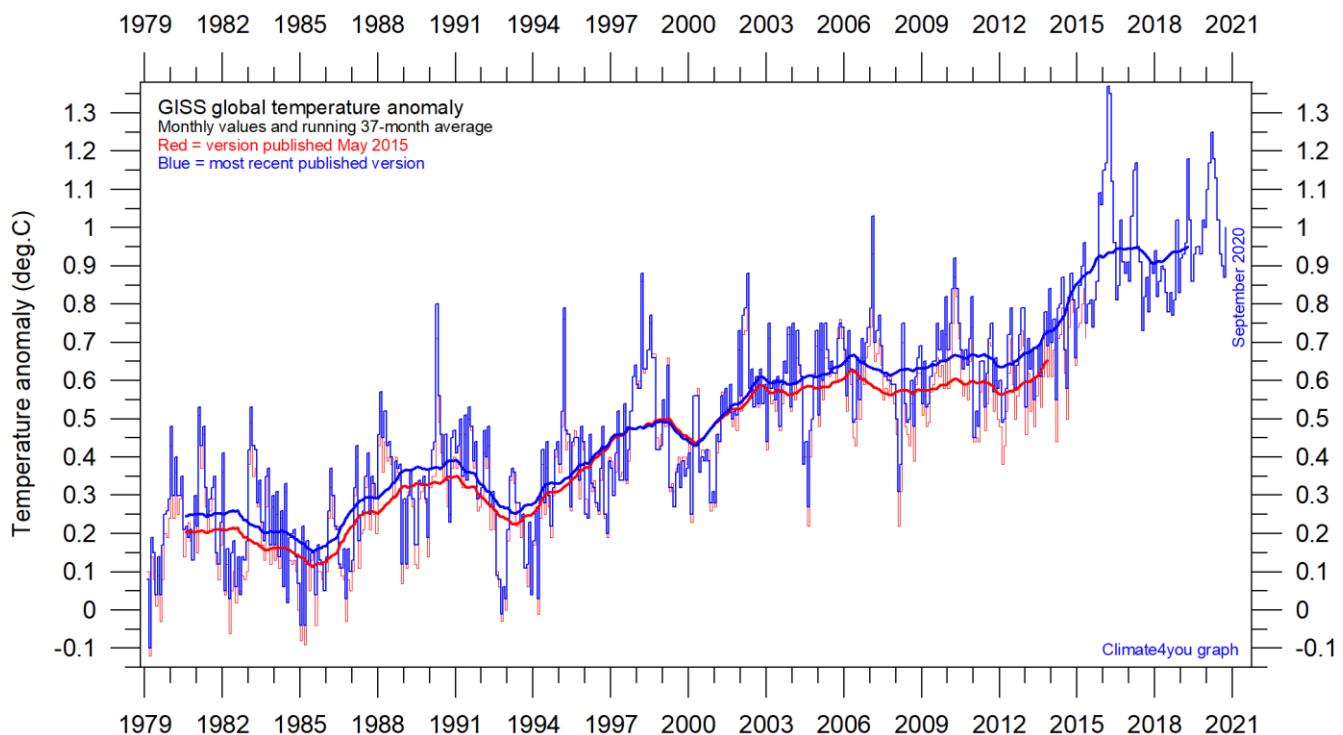


Global monthly average surface air temperature (thin line) since 1979 according to the Hadley Centre for Climate Prediction and Research and the University of East Anglia's [Climatic Research Unit \(CRU\)](#), UK. The thick line is the simple running 37-month average.

**Temperature quality class 3: GISS and NCDC global surface air temperature, updated to September 2020**



Global monthly average surface air temperature since 1979 according to according to the [National Climatic Data Center \(NCDC\), USA](#). The thick line is the simple running 37-month average.



Global monthly average surface air temperature (thin line) since 1979 according to according to the [Goddard Institute for Space Studies \(GISS\)](#), at Columbia University, New York City, USA, using ERSST\_v4 ocean surface temperatures. The thick line is the simple running 37-month average.

### A note on data record stability and -quality:

The temperature diagrams shown above all have 1979 as starting year. This roughly marks the beginning of the recent episode of global warming, after termination of the previous episode of global cooling from about 1940. In addition, the year 1979 also represents the starting date for the satellite-based global temperature estimates (UAH and RSS). For the three surface air temperature records (HadCRUT, NCDC and GISS), they begin much earlier (in 1850 and 1880, respectively), as can be inspected on [www.climate4you.com](http://www.climate4you.com).

For all three surface air temperature records, but especially NCDC and GISS, administrative changes to anomaly values are quite often introduced, even affecting observations many years back in time. Some changes may be due to the delayed addition of new station data or change of station location, while others probably have their origin in changes of the technique implemented to calculate average values. It is clearly impossible to evaluate the validity of such administrative changes for the outside user of these records; it is only possible to note that such changes quite often are introduced (see example diagram next page).

In addition, the three surface records represent a blend of sea surface data collected by moving ships or by other means, plus data from land stations of partly unknown quality and unknown degree of representativeness for their region. Many of the land stations also have been moved geographically during their period of operation, instrumentation have been changed, and they are influenced by changes in their near surroundings (vegetation, buildings, etc.).

The satellite temperature records also have their problems, but these are generally of a more technical nature and therefore better correctable. In addition, the temperature sampling by satellites is more regular and complete on a global basis than that represented by the surface records. It is also

important that the sensors on satellites measure temperature directly by emitted radiation, while most modern surface temperature measurements are indirect, using electronic resistance.

Everybody interested in climate science should gratefully acknowledge the big efforts put into maintaining the different temperature databases referred to in the present newsletter. At the same time, however, it is also important to realise that all temperature records cannot be of equal scientific quality. The simple fact that they to some degree differ shows that they cannot all be correct.

On this background, and for practical reasons, Climate4you therefore operates with three quality classes (1-3) for global temperature records, with 1 representing the highest quality level:

Quality class 1: The satellite records (UAH and RSS).

Quality class 2: The HadCRUT surface record.

Quality class 3: The NCDC and GISS surface records.

The main reason for discriminating between the three surface records is the following:

While both NCDC and GISS often experience quite large administrative changes (see example on p.10), and therefore essentially are unstable temperature records, the changes introduced to HadCRUT are fewer and smaller. For obvious reasons, as the past does not change, any record undergoing continuing changes cannot describe the past correctly all the time. Frequent and large corrections in a database inevitably signal a fundamental doubt about what is likely to represent the correct values.

You can find more on the issue of lack of temporal stability on [www.climate4you.com](http://www.climate4you.com) (go to: *Global Temperature*, and then proceed to *Temporal Stability*).

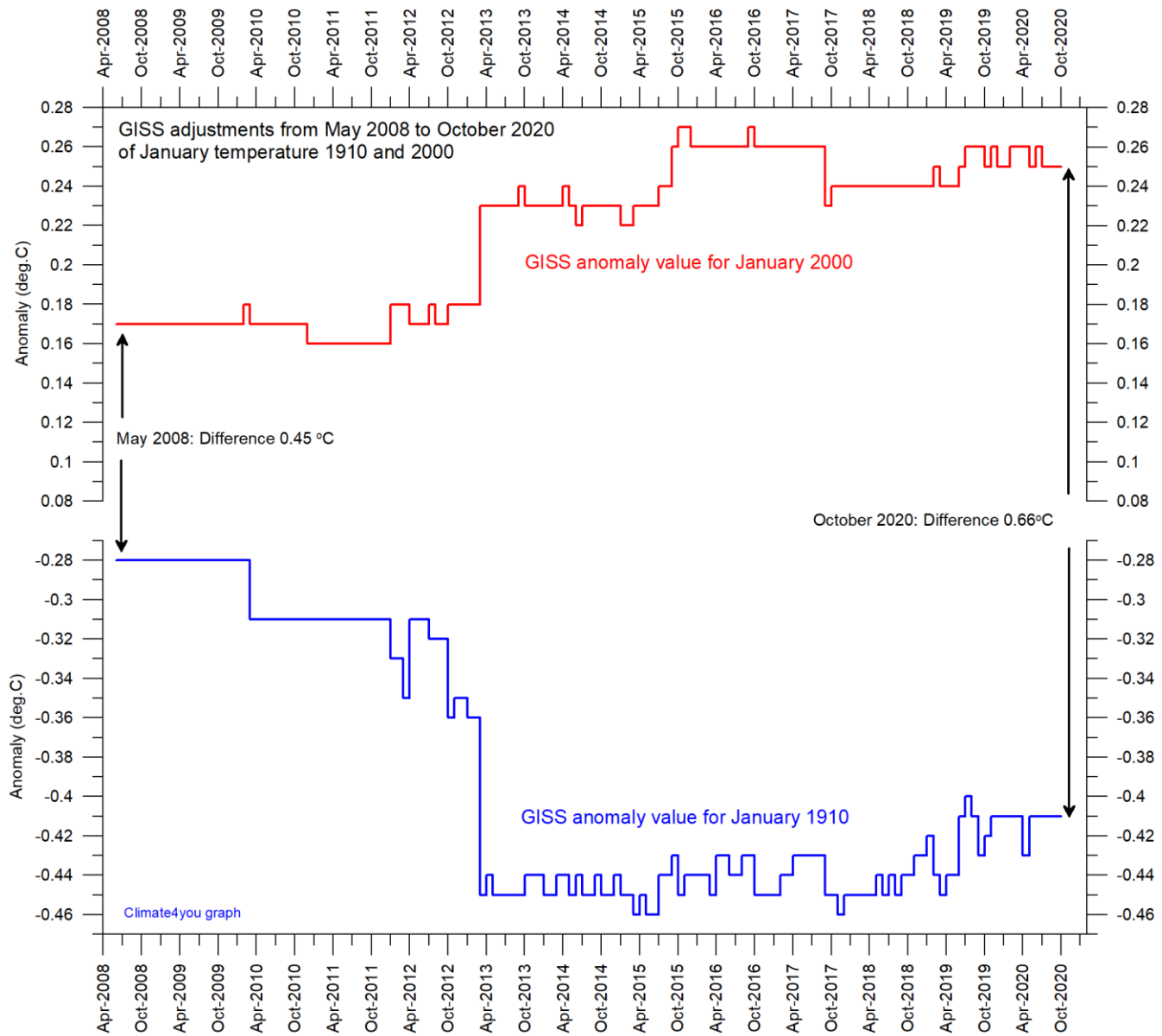
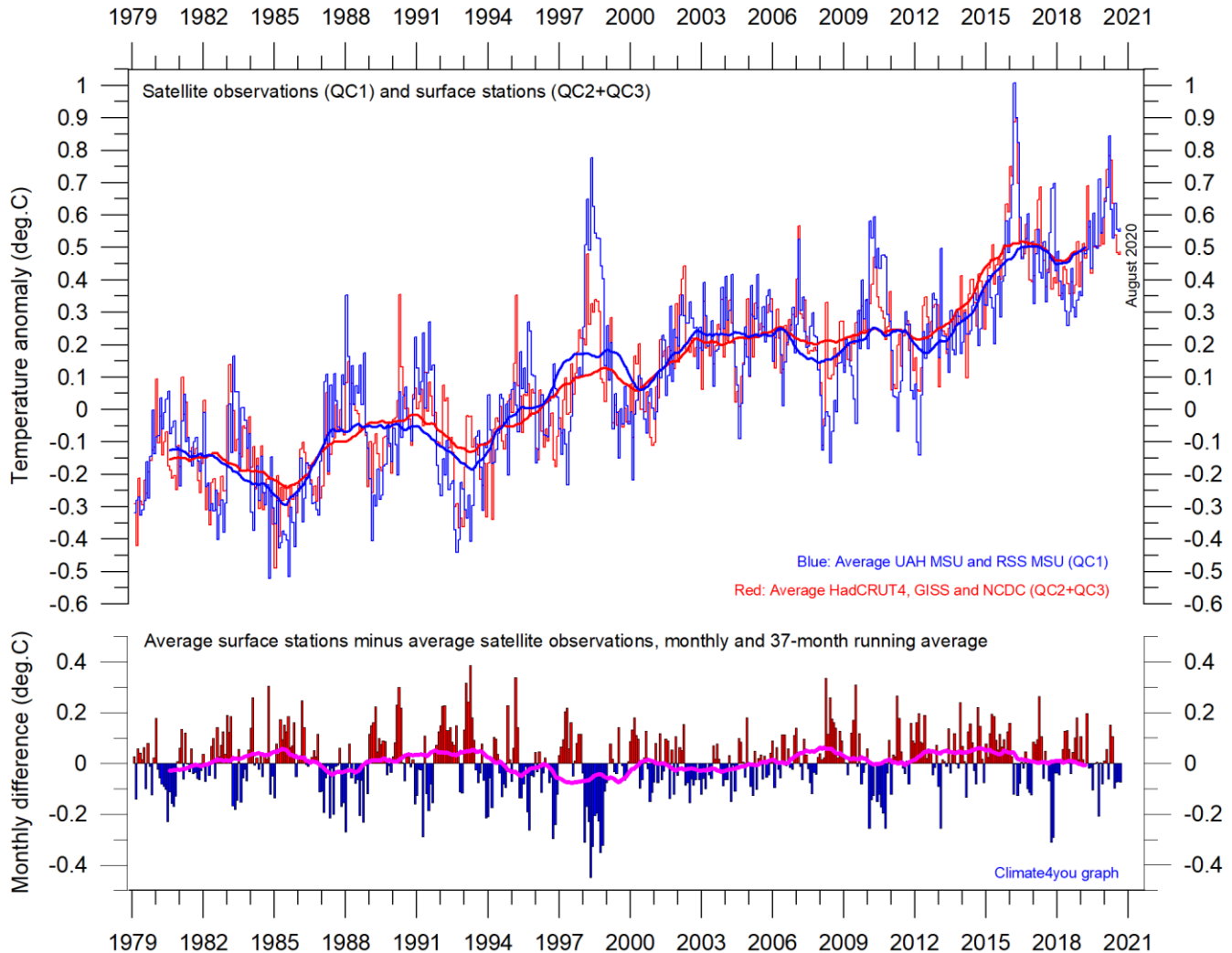


*Diagram showing the adjustments made since May 2008 by the [Goddard Institute for Space Studies \(GISS\)](#), USA, in published anomaly values for the months January 1910 and January 2000.*

The administrative upsurge of the temperature increase from January 1915 to January 2000 has grown from 0.45 (reported May 2008) to 0.66°C (reported October 2020). This represents an about 47% administrative temperature increase over this period, meaning that almost half of the apparent global temperature increase from January 1910 to January 2000 (as reported by GISS) is due to administrative changes of the original data since May 2008.

[Comparing global surface air temperature and lower troposphere satellite temperatures; updated to August 2020](#)



Plot showing the average of monthly global surface air temperature estimates (HadCRUT4, GISS and NCDC) and satellite-based temperature estimates (RSS MSU and UAH MSU). The thin lines indicate the monthly value, while the thick lines represent the simple running 37-month average, nearly corresponding to a running 3-yr average. The lower panel shows the monthly difference between average surface air temperature and satellite temperatures. As the base period differs for the different temperature estimates, they have all been normalised by comparing to the average value of 30 years from January 1979 to December 2008.

## Global air temperature linear trends updated to August 2020

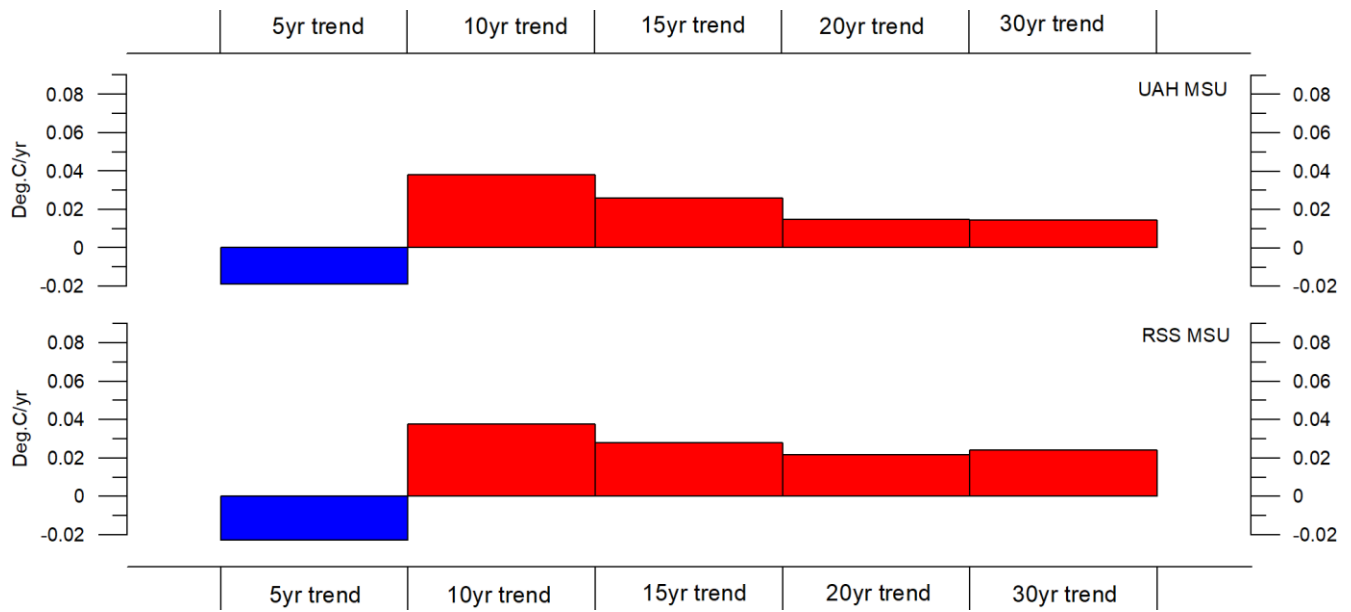


Diagram showing the latest 5, 10, 20 and 30-yr linear annual global temperature trend, calculated as the slope of the linear regression line through the data points, for two satellite-based temperature estimates (UAH MSU and RSS MSU).

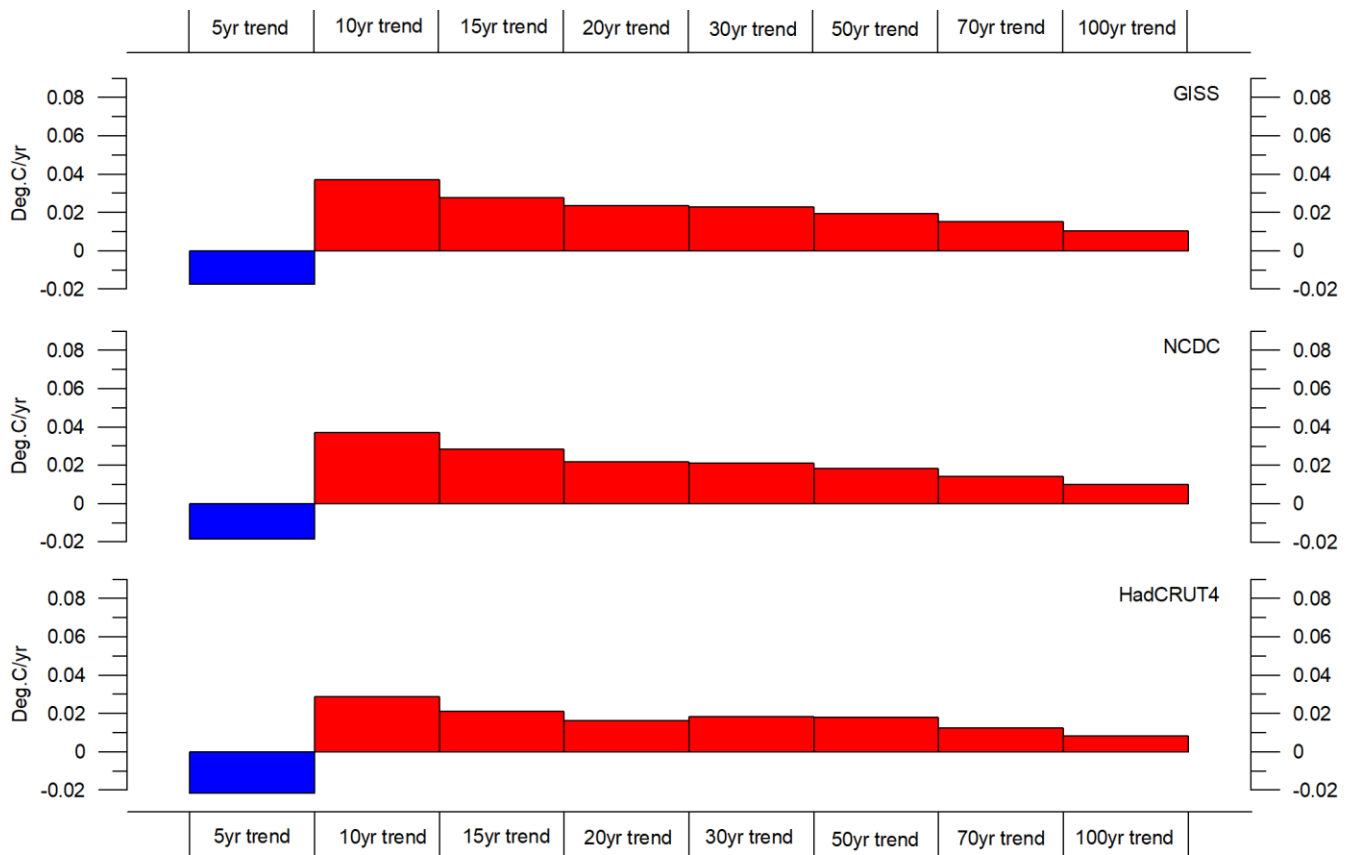
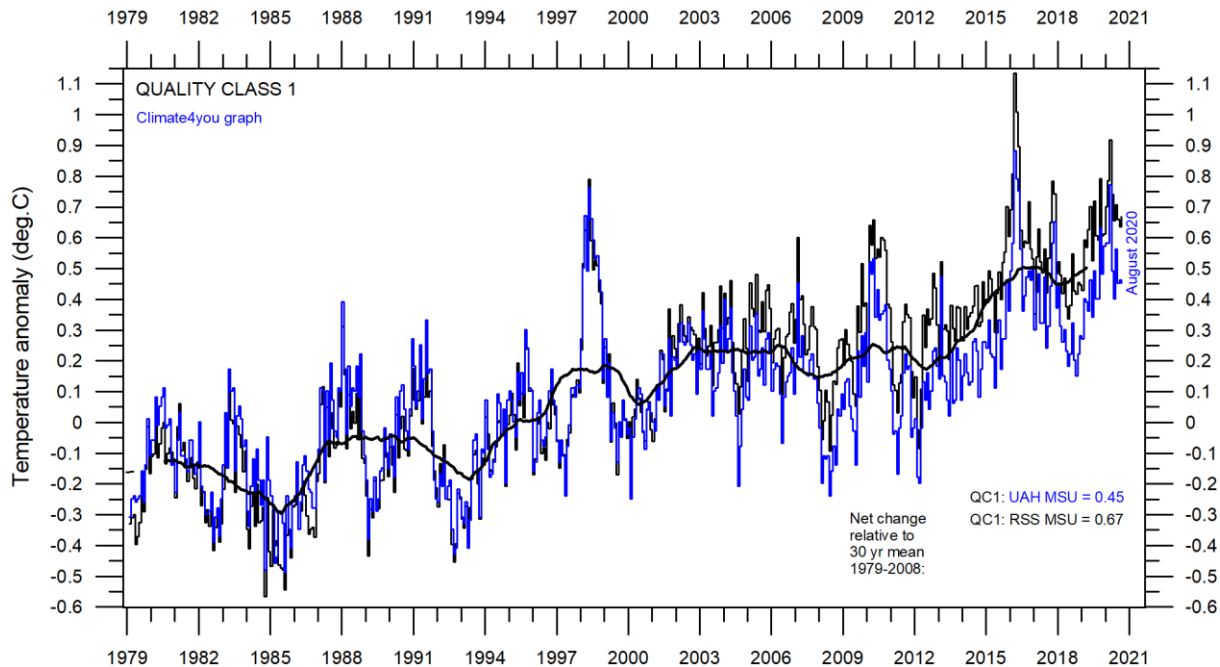


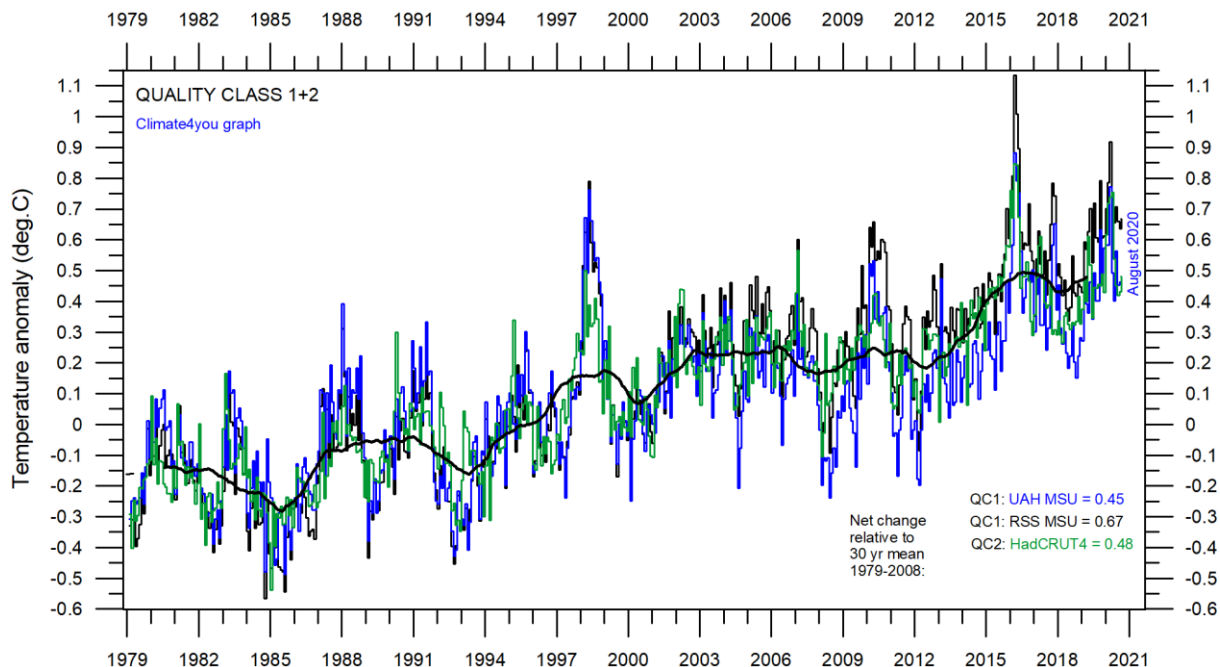
Diagram showing the latest 5, 10, 20, 30, 50, 70 and 100-year linear annual global temperature trend, calculated as the slope of the linear regression line through the data points, for three surface-based temperature estimates (GISS, NCDC and HadCRUT4).

## All in one, Quality Class 1, 2 and 3; updated to August 2020

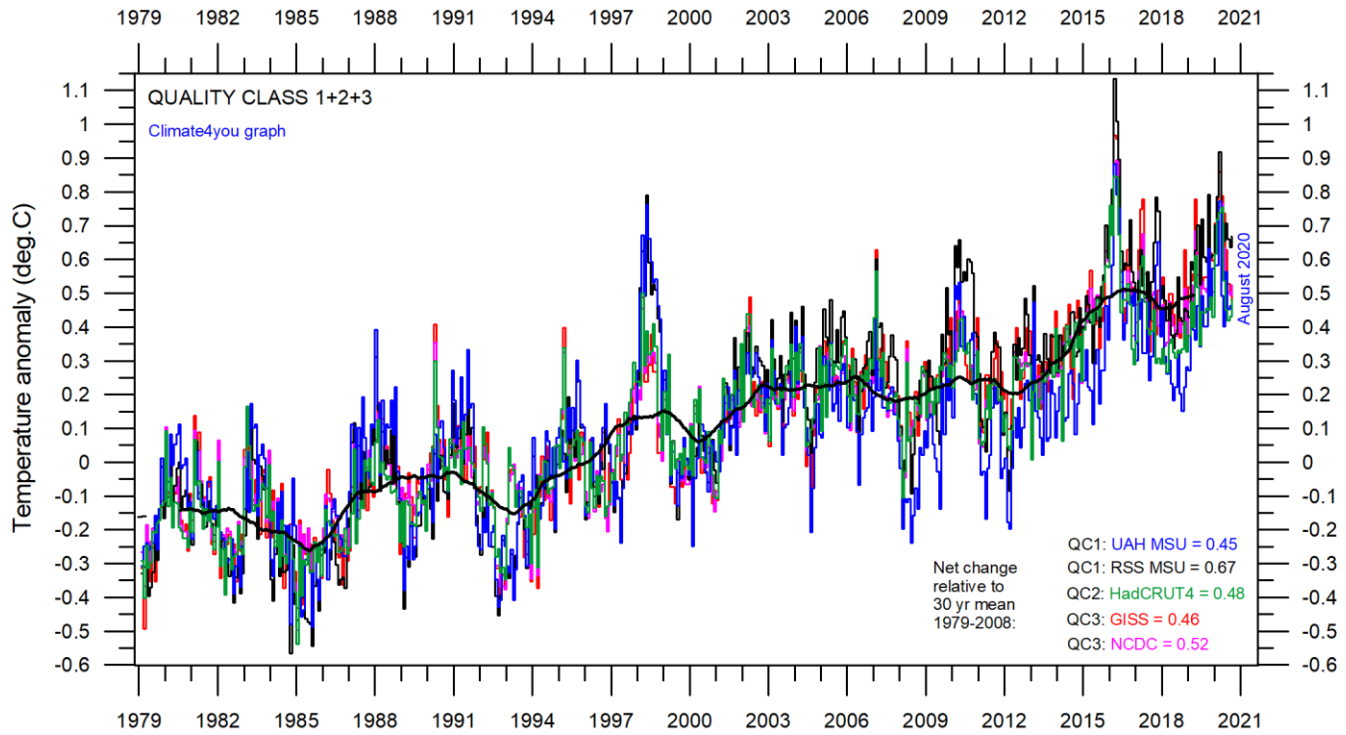


*Superimposed plot of Quality Class 1 (UAH and RSS) global monthly temperature estimates. As the base period differs for the individual temperature estimates, they have all been normalised by comparing with the average value of the initial 120 months (30 years) from January 1979 to December 2008. The heavy black line represents the simple running 37 month (c. 3 year) mean of the average of both temperature records. The numbers shown in the lower right corner represent the temperature anomaly relative to the individual 1979-2008 averages.*

13



*Superimposed plot of Quality Class 1 and 2 (UAH, RSS and HadCRUT4) global monthly temperature estimates. As the base period differs for the individual temperature estimates, they have all been normalised by comparing with the average value of the initial 120 months (30 years) from January 1979 to December 2008. The heavy black line represents the simple running 37 month (c. 3 year) mean of the average of all three temperature records. The numbers shown in the lower right corner represent the temperature anomaly relative to the individual 1979-2008 averages.*



*Superimposed plot of Quality Class 1, 2 and 3 global monthly temperature estimates (UAH, RSS, HadCRUT4, GISS and NCDC). As the base period differs for the individual temperature estimates, they have all been normalised by comparing with the average value of the initial 120 months (30 years) from January 1979 to December 2008. The heavy black line represents the simple running 37 month (c. 3 year) mean of the average of all five temperature records. The numbers shown in the lower right corner represent the temperature anomaly relative to the individual 1979-2008 averages.*

14

Please see notes on page 8 relating to the above three quality classes.

Satellite- and surface-based temperature estimates are derived from different types of measurements and comparing them directly as in the above diagrams therefore may be somewhat dubious.

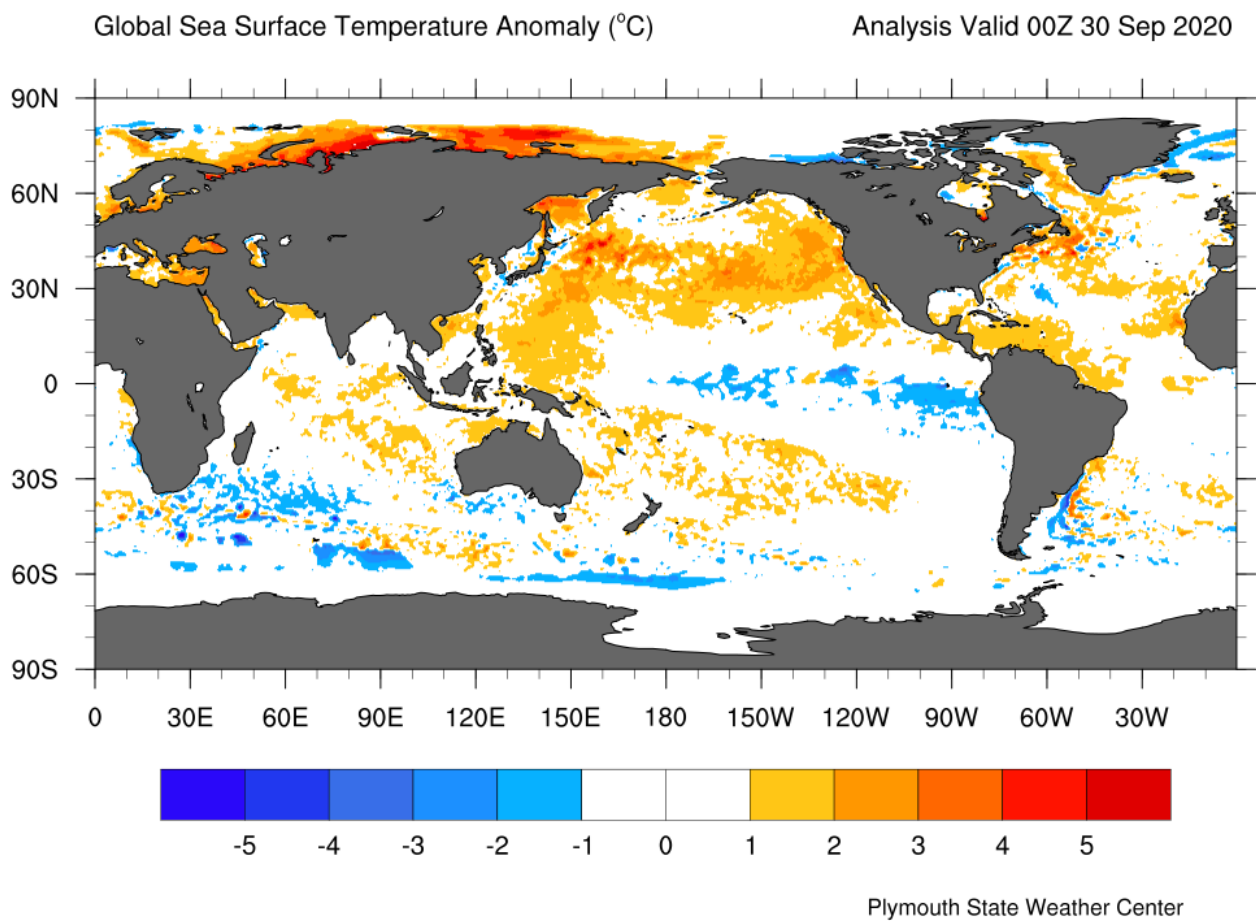
However, as both types of estimate often are discussed together in various news media, the above composite diagrams may nevertheless be of interest. In fact, the different types of temperature estimates appear to agree as to the overall temperature variations on a 2-3-year scale, although on a shorter time scale there are often considerable differences between the individual records. However, since about 2003 the surface records used to be drifting towards higher temperatures than the combined satellite record, but this overall tendency was much removed by the major adjustment of the RSS satellite series in 2015 (see lower diagram on page 5).

The combined records (diagram above) suggest a modest global air temperature increase over the last 30 years, about  $0.15^{\circ}\text{C}$  per decade. It should be noted that the apparent temperature increase since about 2003 at least partly is the result of ongoing administrative adjustments (page 5-9). At the same time, the temperature records considered here do not indicate any temperature decrease over the last 20 years. See also diagram on page 49.

The present temperature development does not exclude the possibility that global temperatures may begin to increase significantly later. On the other hand, it also remains a possibility that Earth just now is passing an overall temperature peak, and that global temperatures may begin to decrease during the coming years.

As always, time will show which of these possibilities is correct.

## [Global sea surface temperature, updated to September 2020](#)



15

*Sea surface temperature anomaly on 30 September 2020. Map source: Plymouth State Weather Center. Reference period: 1977-1991.*

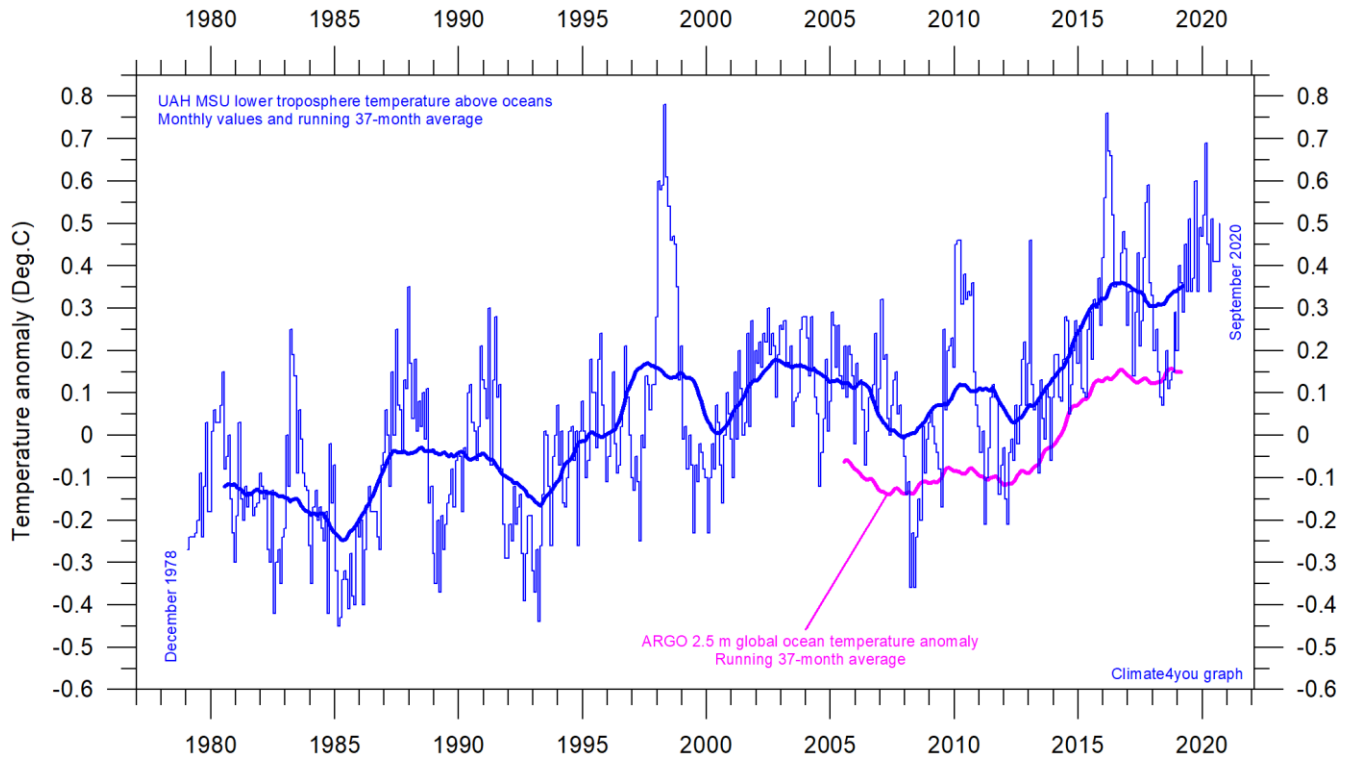
Because of the large surface areas near Equator, the temperature of the surface water in these regions is especially important for the global atmospheric temperature (p. 6-8). In fact, no less than 50% of planet Earth's surface area is located within  $30^{\circ}\text{N}$  and  $30^{\circ}\text{S}$ . Now, relatively warm surface water is mainly found in the northern hemisphere.

A mixture of relatively warm and cold water dominates much of the ocean surface, but with notable differences from month to month. All such ocean surface temperature changes will be influencing global air temperatures in the months to come.

The significance of any short-term cooling or warming reflected in air temperatures should not be

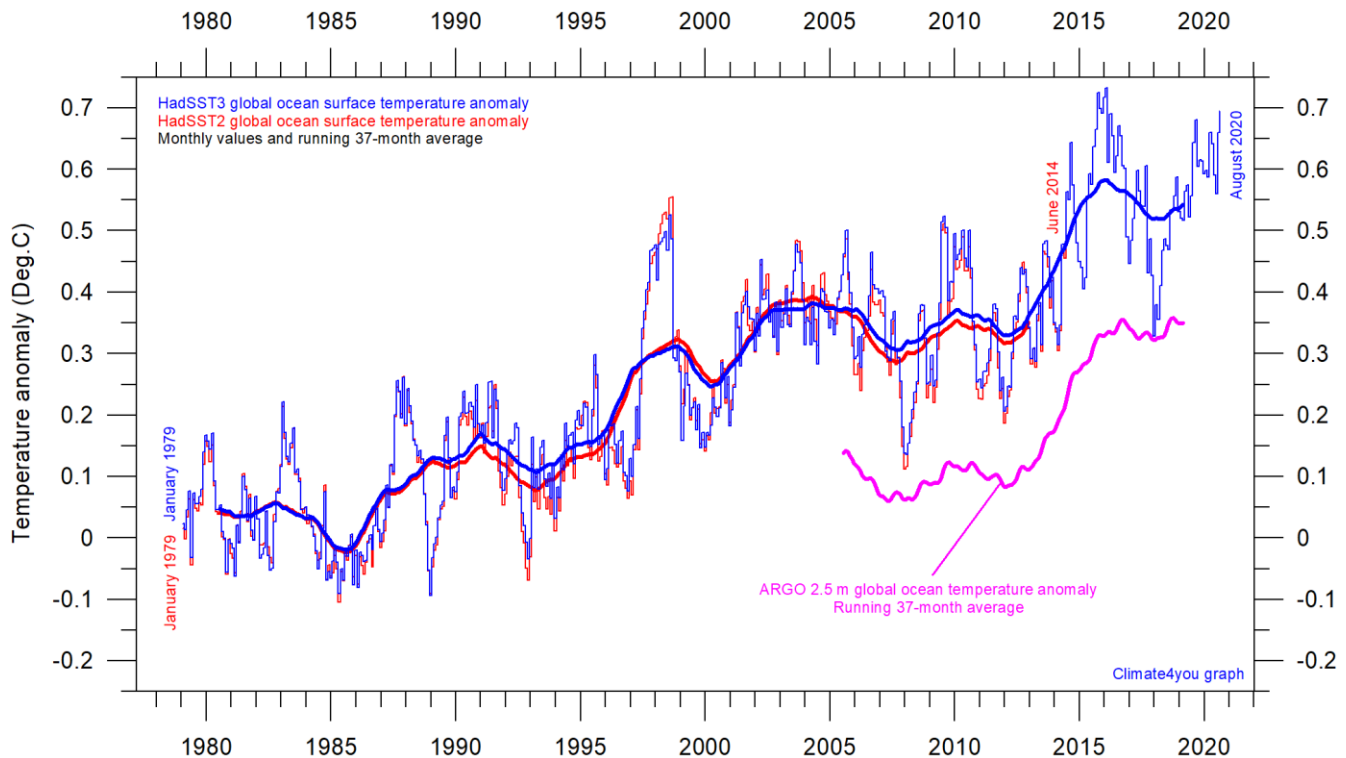
overstated. Whenever Earth experiences cold La Niña or warm El Niño episodes (Pacific Ocean, see p.24) major heat exchanges take place between the Pacific Ocean and the atmosphere above, sooner or later showing up in estimates of the global air temperature.

However, this does not necessarily reflect similar changes in the total heat content of the atmosphere-ocean system. In fact, global net changes can be small and such heat exchanges may mainly reflect redistribution of energy between ocean and atmosphere. What matters is the overall temperature development when seen over several years.

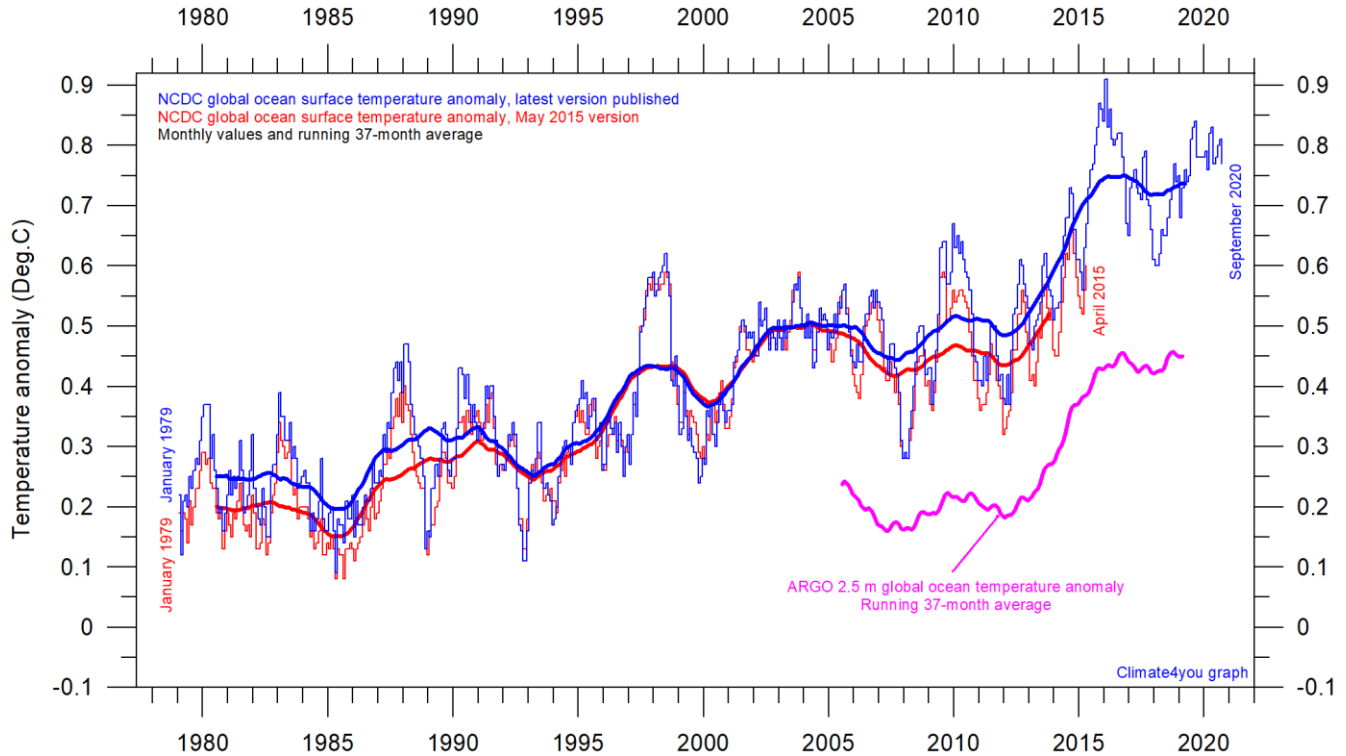


Global monthly average lower troposphere temperature over oceans (thin line) since 1979 according to [University of Alabama](#) at Huntsville, USA. The thick line is the simple running 37-month average. Insert: Argo global ocean temperature anomaly from floats, displaced vertically to make visual comparison easier.

16



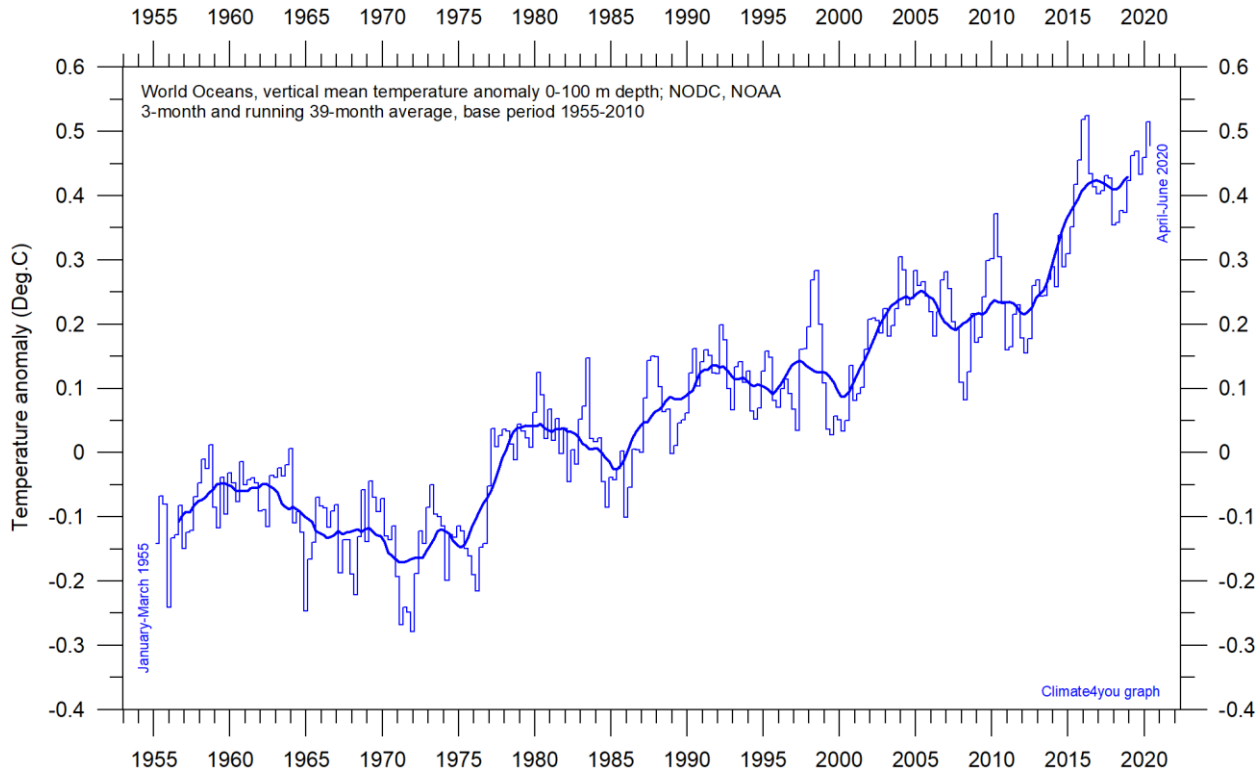
Global monthly average sea surface temperature since 1979 according to University of East Anglia's [Climatic Research Unit \(CRU\)](#), UK. Base period: 1961-1990. The thick line is the simple running 37-month average. Insert: Argo global ocean temperature anomaly from floats, displaced vertically to make visual comparison easier.



Global monthly average sea surface temperature since 1979 according to the [National Climatic Data Center](#) (NCDC), USA. Base period: 1901-2000. The thick line is the simple running 37-month average. Insert: Argo global ocean temperature anomaly from floats, displaced vertically to make visual comparison easier.

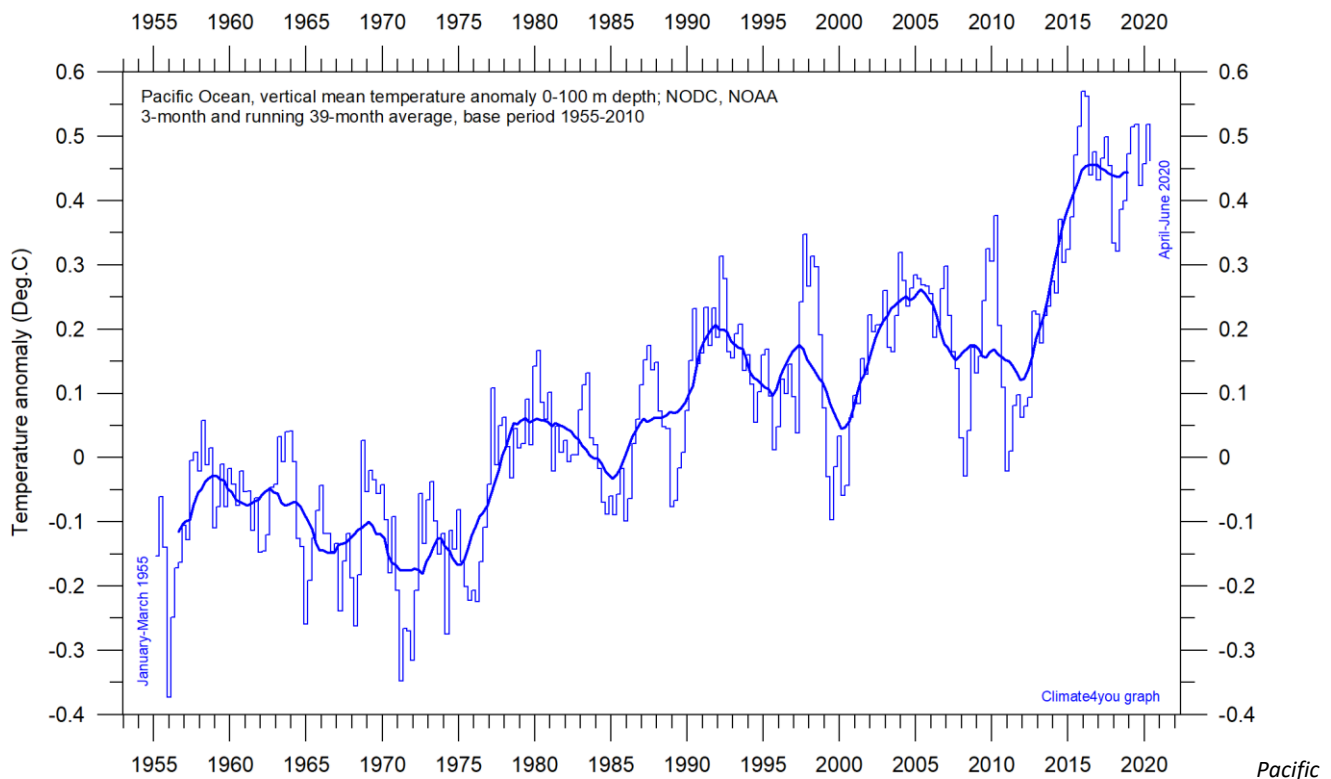
**June 18, 2015:** NCDC has introduced several rather large administrative changes to their sea surface temperature record. The overall result is to produce a record giving the impression of a continuous temperature increase, also in the 21<sup>st</sup> century. As the oceans cover about 71% of the entire surface of planet Earth, the effect of this adjustment is clearly reflected in the NCDC record for global surface air temperature (p. 7). The pre-adjustment record is shown in red in the above diagram.

## Ocean temperature in uppermost 100 m, updated to June 2020

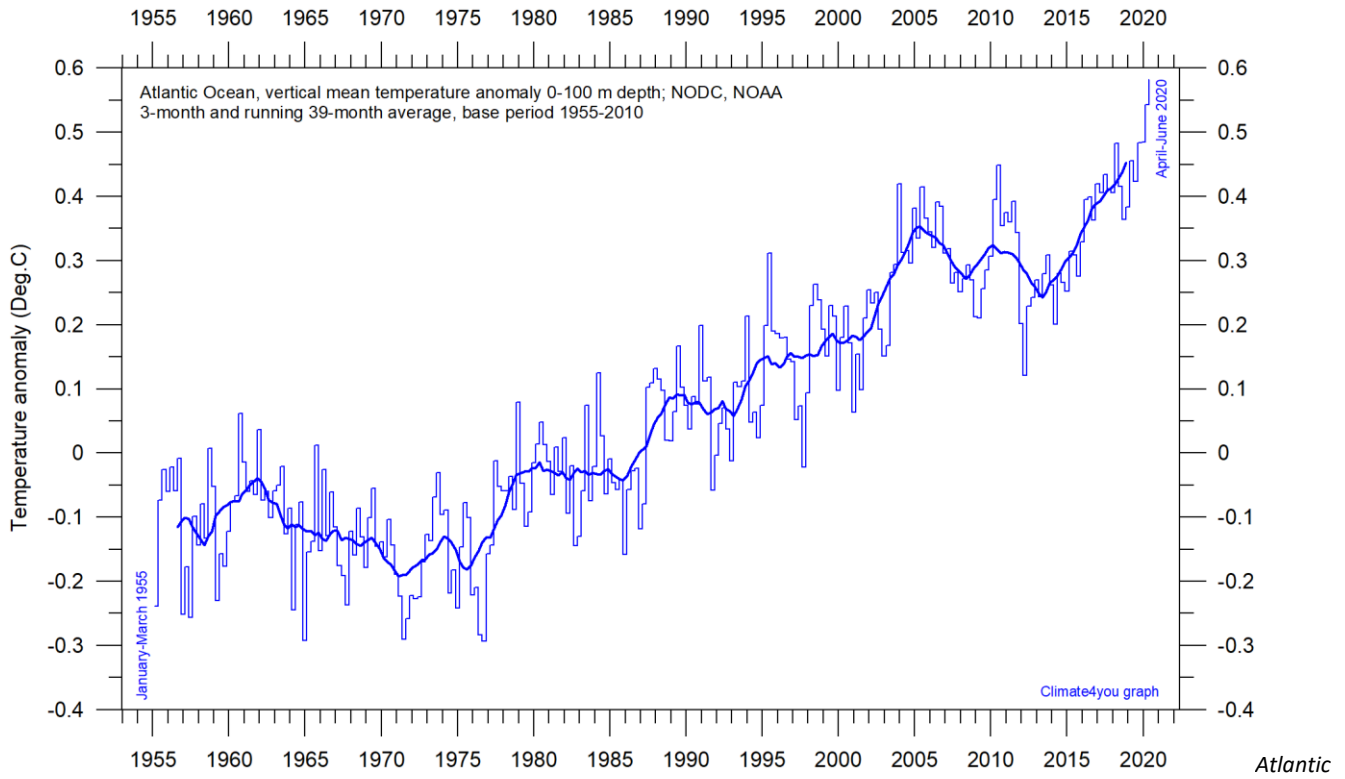


World Oceans vertical average temperature 0-100 m depth since 1955. The thin line indicates 3-month values, and the thick line represents the simple running 39-month (c. 3 year) average. Data source: [NOAA National Oceanographic Data Center](#) (NODC). Base period 1955-2010.

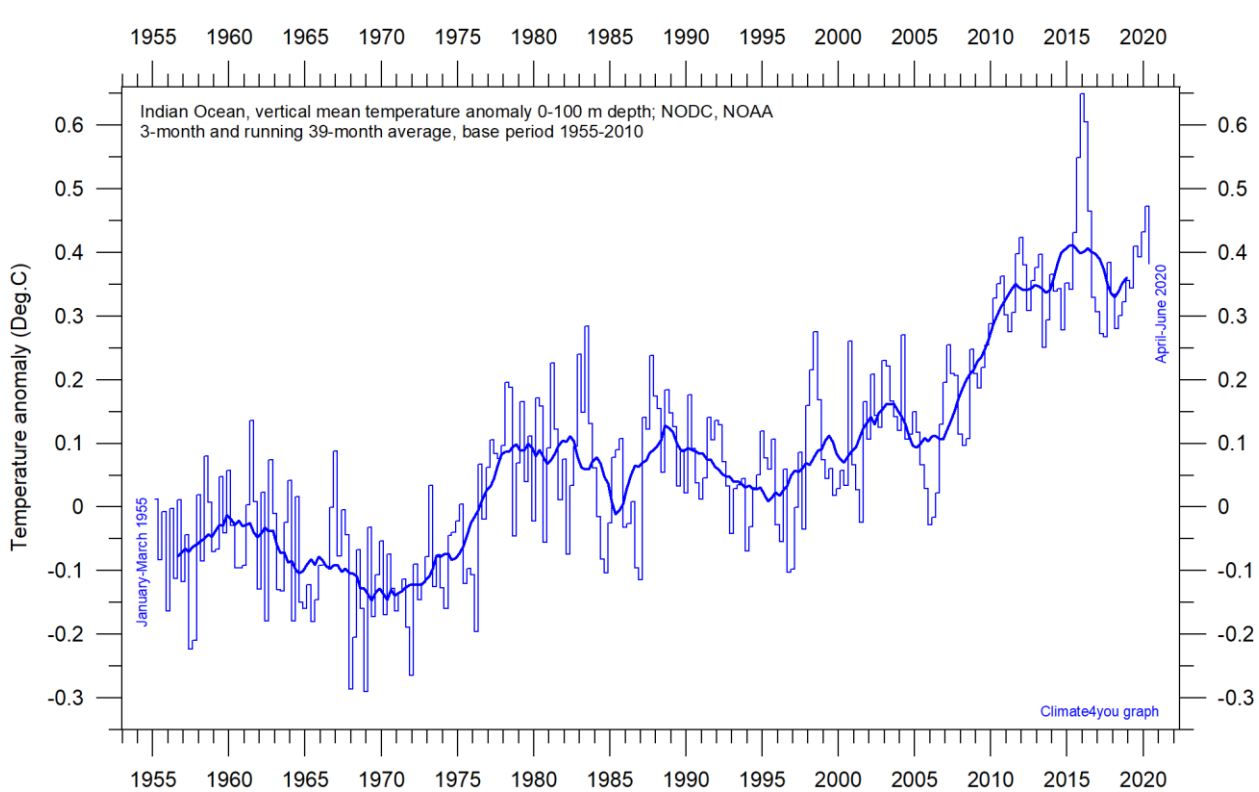
18



Ocean vertical average temperature 0-100 m depth since 1955. The thin line indicates 3-month values, and the thick line represents the simple running 39-month (c. 3 year) average. Data source: [NOAA National Oceanographic Data Center](#) (NODC). Base period 1955-2010.

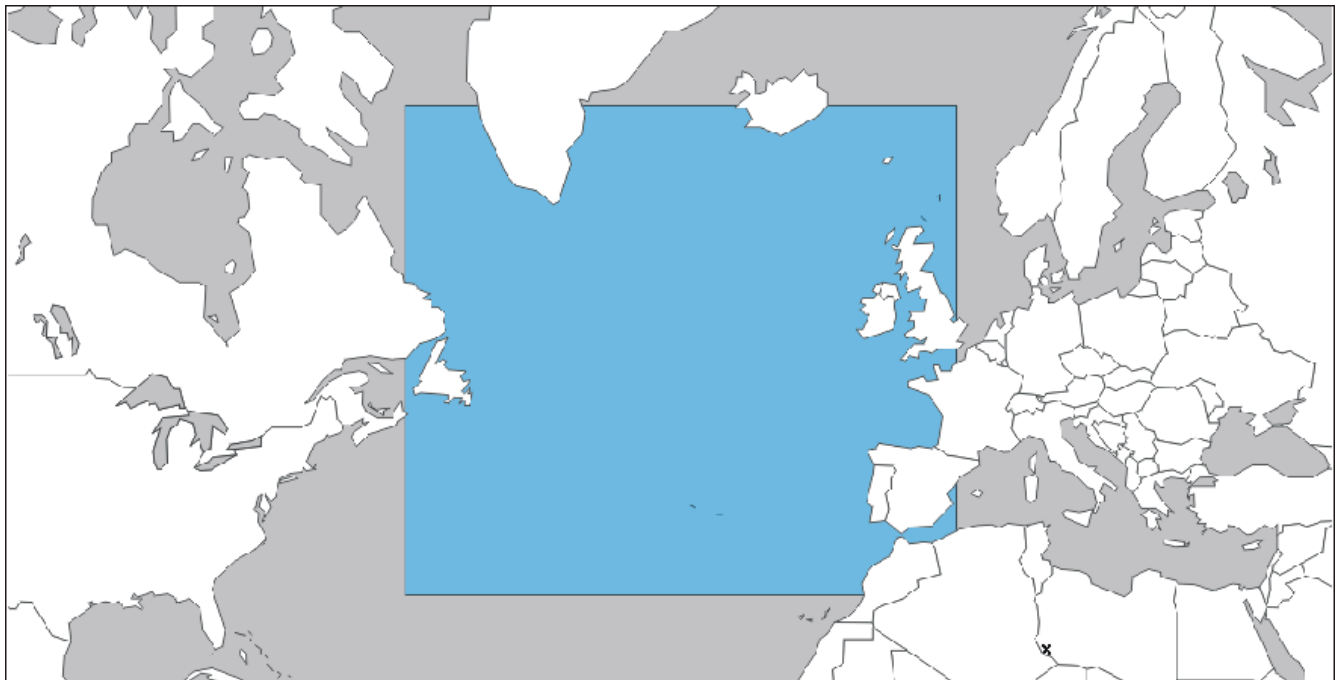


Ocean vertical average temperature 0-100 m depth since 1955. The thin line indicates 3-month values, and the thick line represents the simple running 39-month (c. 3 year) average. Data source: [NOAA National Oceanographic Data Center \(NODC\)](#). Base period 1955-2010.

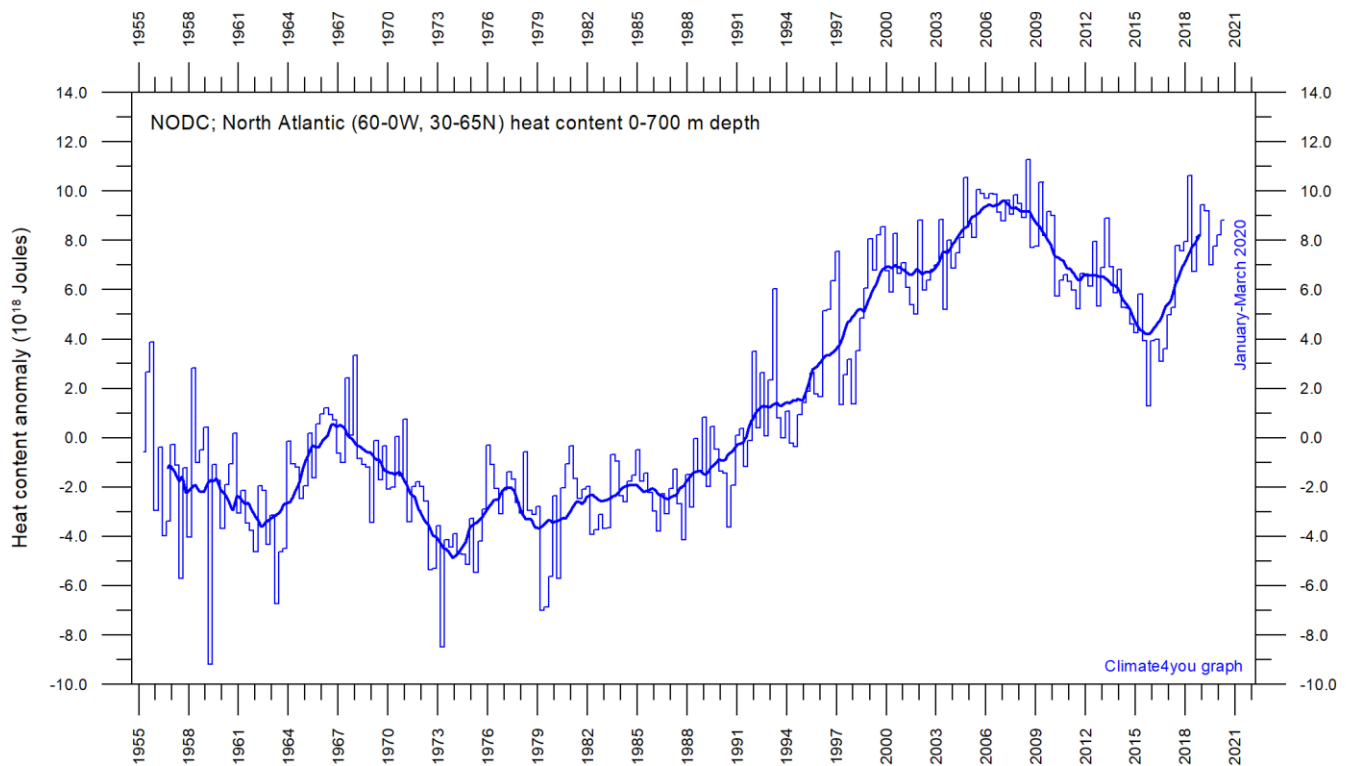


*Indian Ocean vertical average temperature 0-100 m depth since 1955. The thin line indicates 3-month values, and the thick line represents the simple running 39-month (c. 3 year) average. Data source: [NOAA National Oceanographic Data Center](#) (NODC). Base period 1955-2010.*

## North Atlantic heat content uppermost 700 m, updated to March 2020

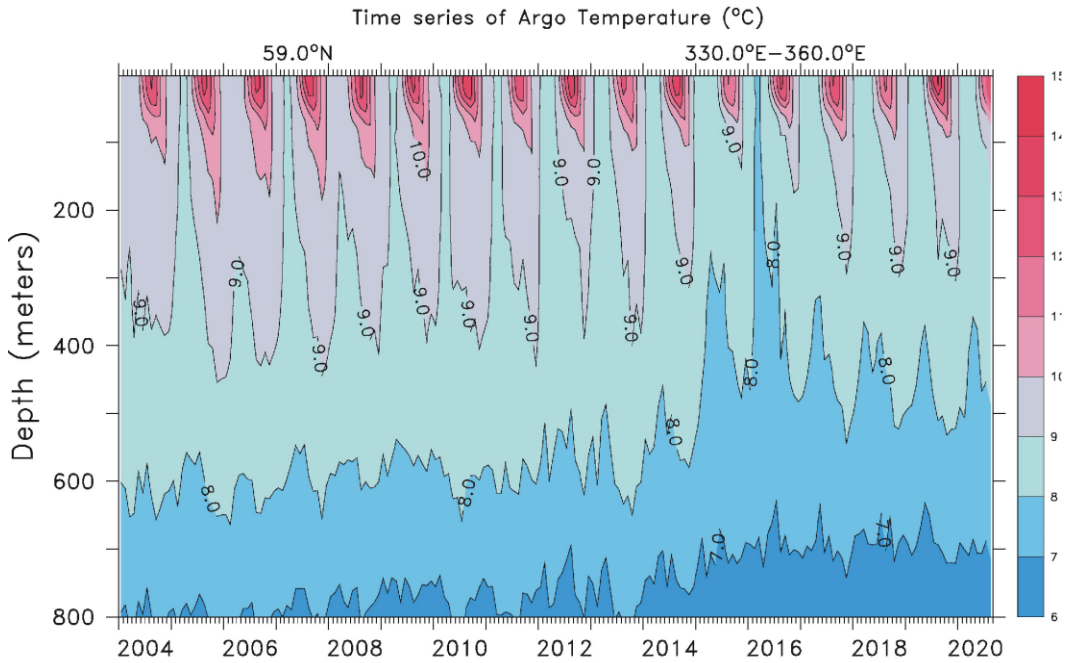


20



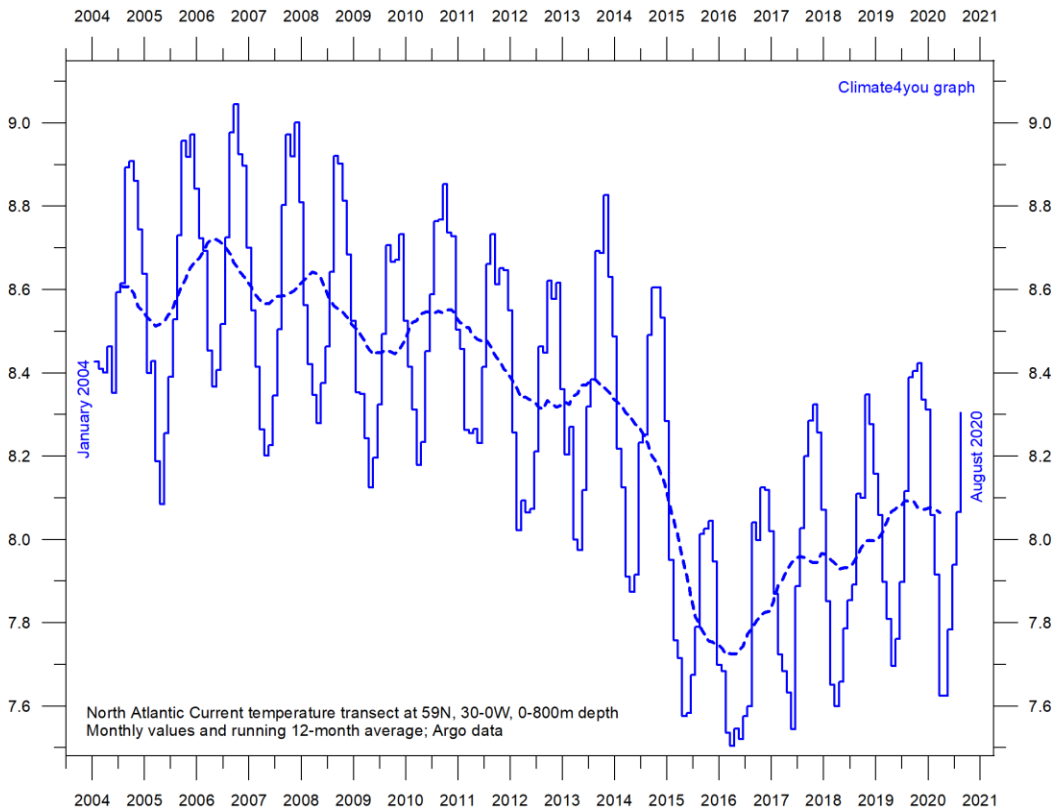
Global monthly heat content anomaly ( $10^{18}$  Joules) in the uppermost 700 m of the North Atlantic (60-0W, 30-65N; see map above) ocean since January 1955. The thin line indicates monthly values, and the thick line represents the simple running 37-month (c. 3 year) average. Data source: [National Oceanographic Data Center \(NODC\)](#).

## North Atlantic temperatures 0-800 m depth along 59°N, 30-0W, updated to August 2020



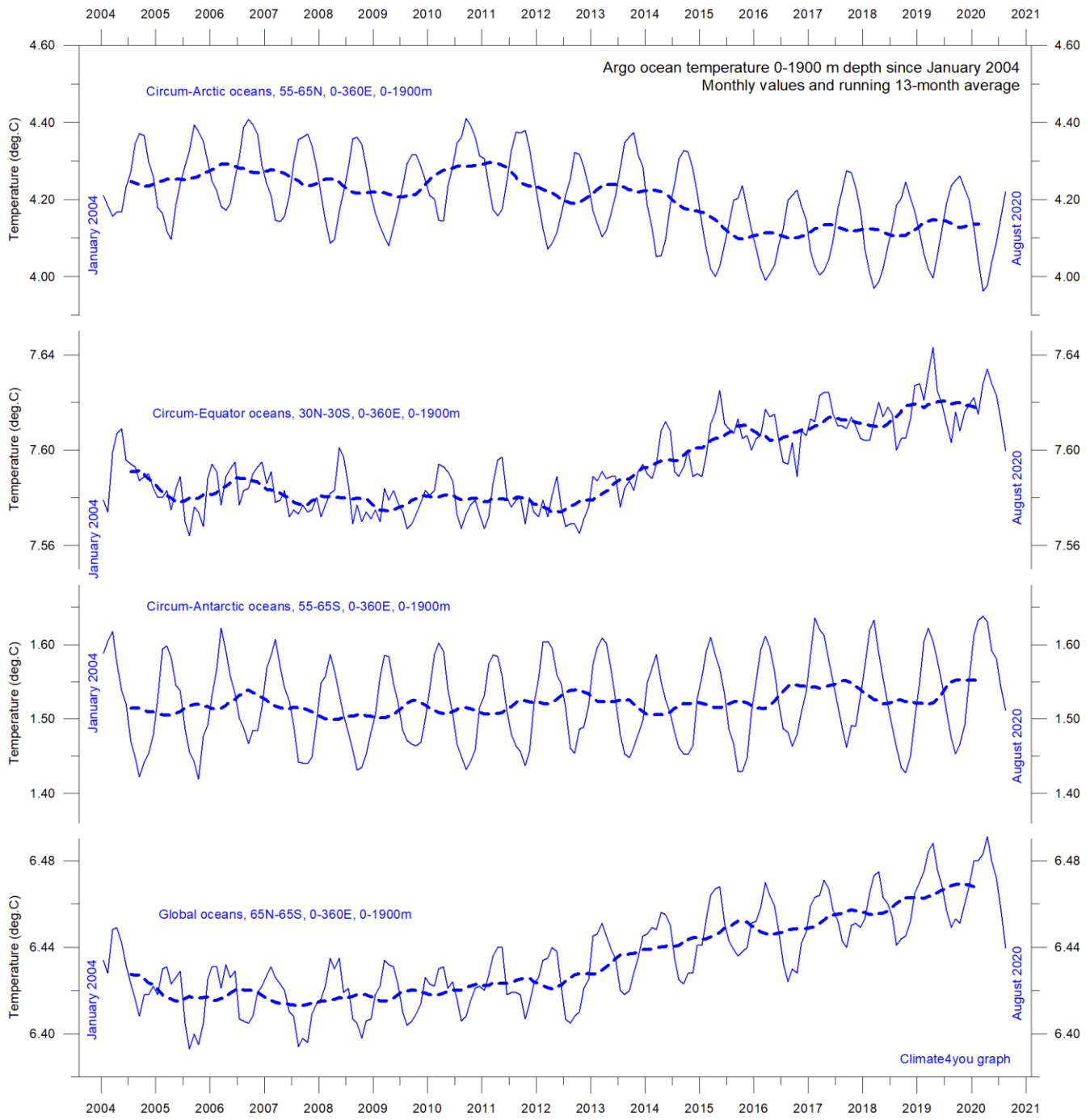
Time series depth-temperature diagram along 59 N across the North Atlantic Current from 30°W to 0°W, from surface to 800 m depth. Source: [Global Marine Argo Atlas](#). See also the diagram below.

21



Average temperature along 59 N, 30-0W, 0-800m depth, corresponding to the main part of the North Atlantic Current, using Argo-data. Source: [Global Marine Argo Atlas](#). Additional information can be found in: Roemmich, D. and J. Gilson, 2009. The 2004-2008 mean and annual cycle of temperature, salinity, and steric height in the global ocean from the Argo Program. *Progress in Oceanography*, 82, 81-100.

## Global ocean temperature 0-1900 m depth summary, updated to August 2020

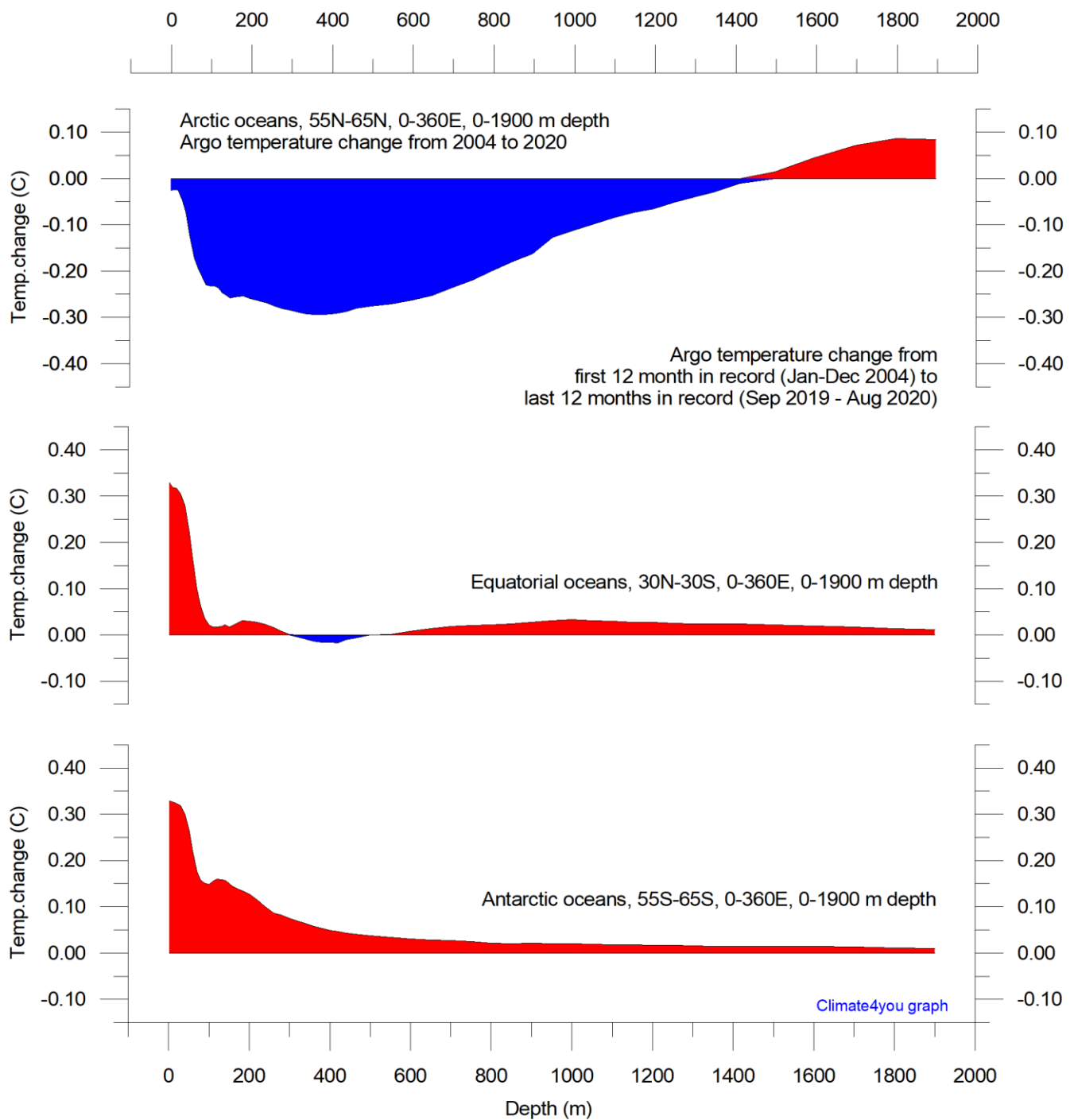


Summary of average temperature in uppermost 1900 m in different parts of the global oceans, using [Argo](#)-data. Source: [Global Marine Argo Atlas](#). Additional information can be found in: Roemmich, D. and J. Gilson, 2009. The 2004-2008 mean and annual cycle of temperature, salinity, and steric height in the global ocean from the Argo Program. [Progress in Oceanography](#), 82, 81-100.

The global summary diagram above shows that, on average, the temperature of the global oceans down to 1900 m depth has been increasing since about 2011. It is also seen that this increase since 2013 dominantly is due to oceanic changes occurring near the Equator, between

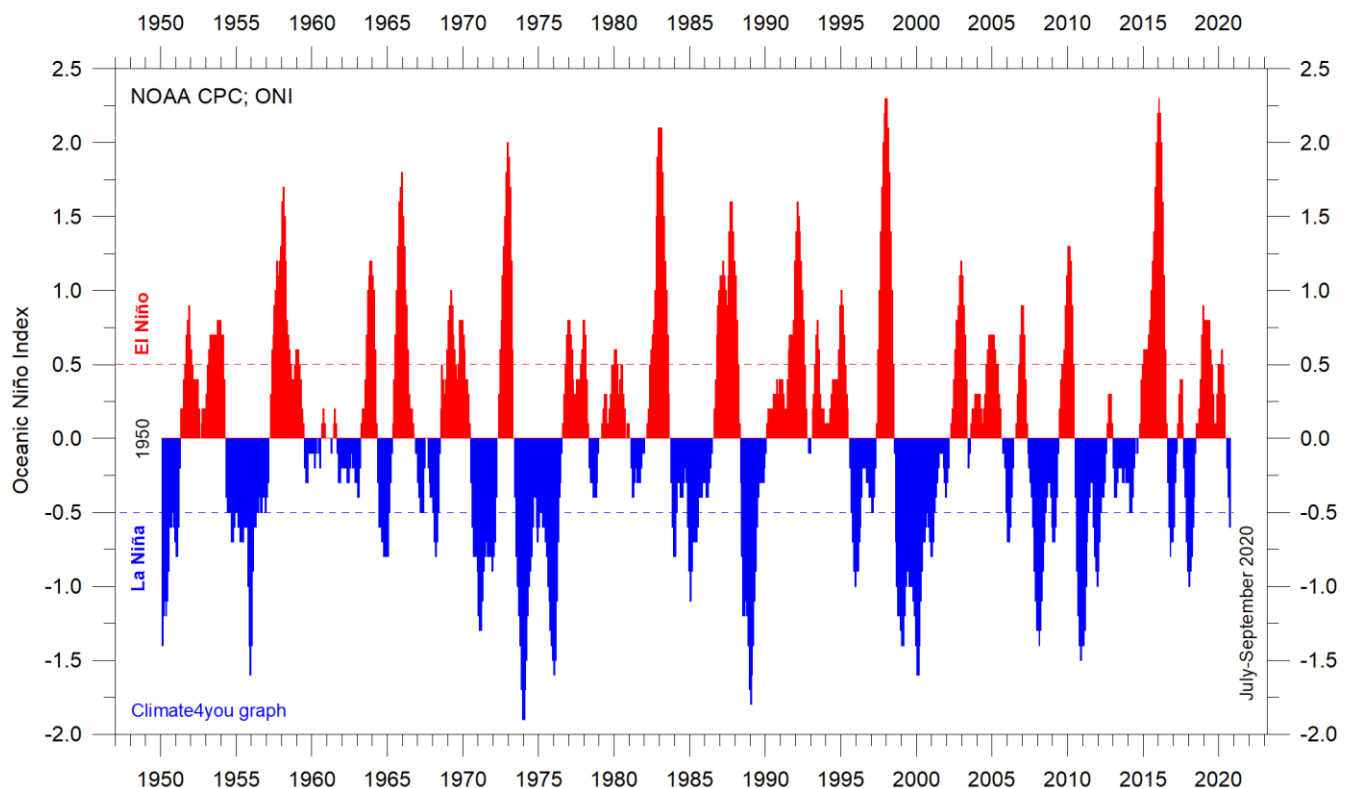
30°N and 30°S. In contrast, for the circum-Arctic oceans north of 55°N, depth-integrated ocean temperatures have been decreasing since 2011. Near the Antarctic, south of 55°S, temperatures have essentially been stable. At most latitudes, a clear annual rhythm is seen.

## Global ocean net temperature change since 2004 at different depths, updated to August 2020



Net temperature change since 2004 from surface to 1900 m depth in different parts of the global oceans, using [Argo](#)-data.  
 Source: [Global Marine Argo Atlas](#). Additional information can be found in: Roemmich, D. and J. Gilson, 2009. The 2004-2008 mean and annual cycle of temperature, salinity, and steric height in the global ocean from the Argo Program. [Progress in Oceanography](#), 82, 81-100. Please note that due to the spherical form of Earth, northern and southern latitudes represent only small ocean volumes, compared to latitudes near the Equator.

## La Niña and El Niño episodes, updated to September 2020



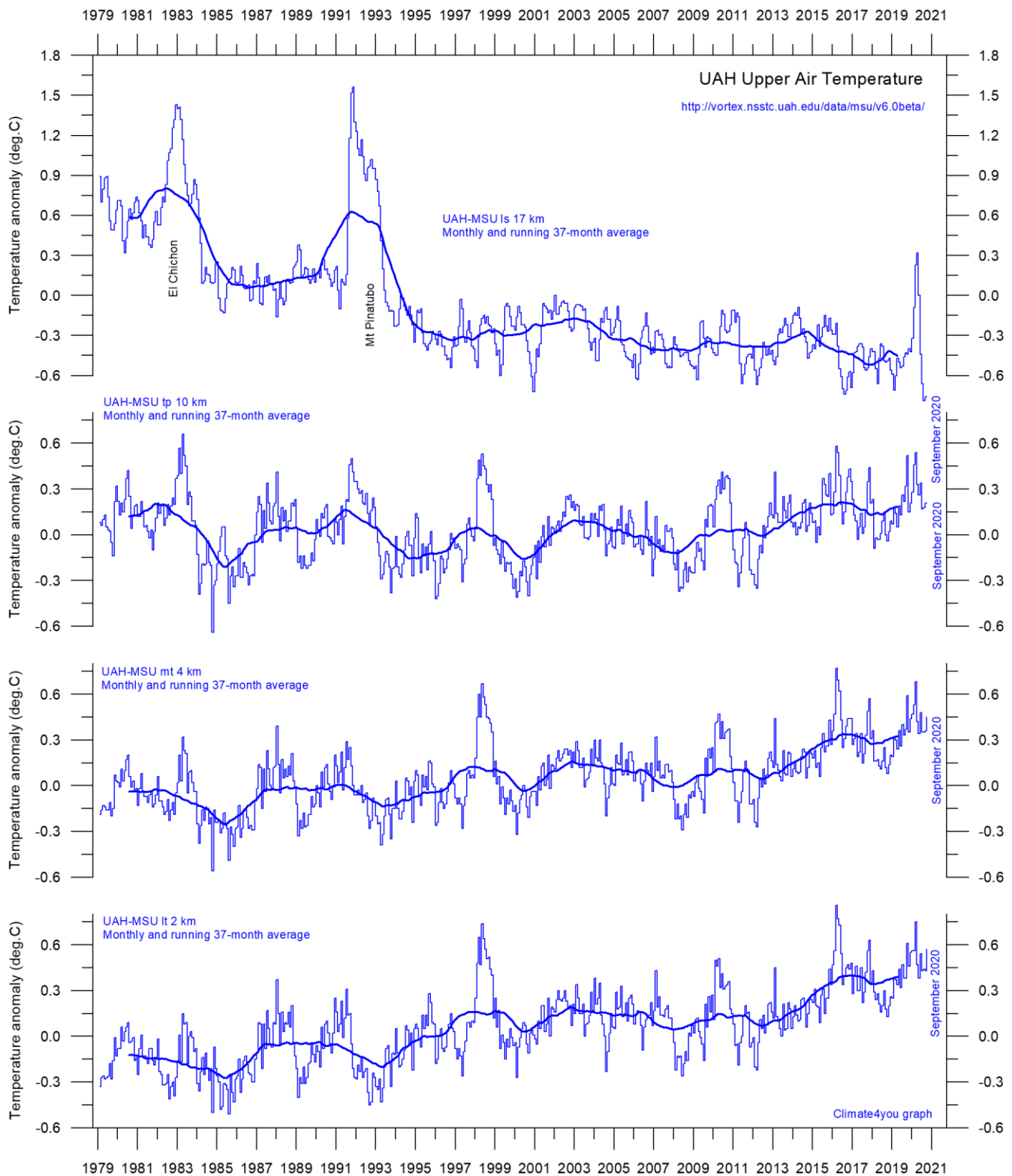
24

Warm ( $>+0.5^{\circ}\text{C}$ ) and cold ( $<-0.5^{\circ}\text{C}$ ) episodes for the [Oceanic Niño Index](#) (ONI), defined as 3 month running mean of ERSSTv4 SST anomalies in the Niño 3.4 region ( $5^{\circ}\text{N}-5^{\circ}\text{S}, 120^{\circ}-170^{\circ}\text{W}$ ). For historical purposes cold and warm episodes are defined when the threshold is met for a minimum of 5 consecutive over-lapping seasons. Anomalies are centred on 30-yr base periods updated every 5 years.

The recent 2015-16 El Niño episode is among the strongest since the beginning of the record in 1950. Considering the entire record, however, recent

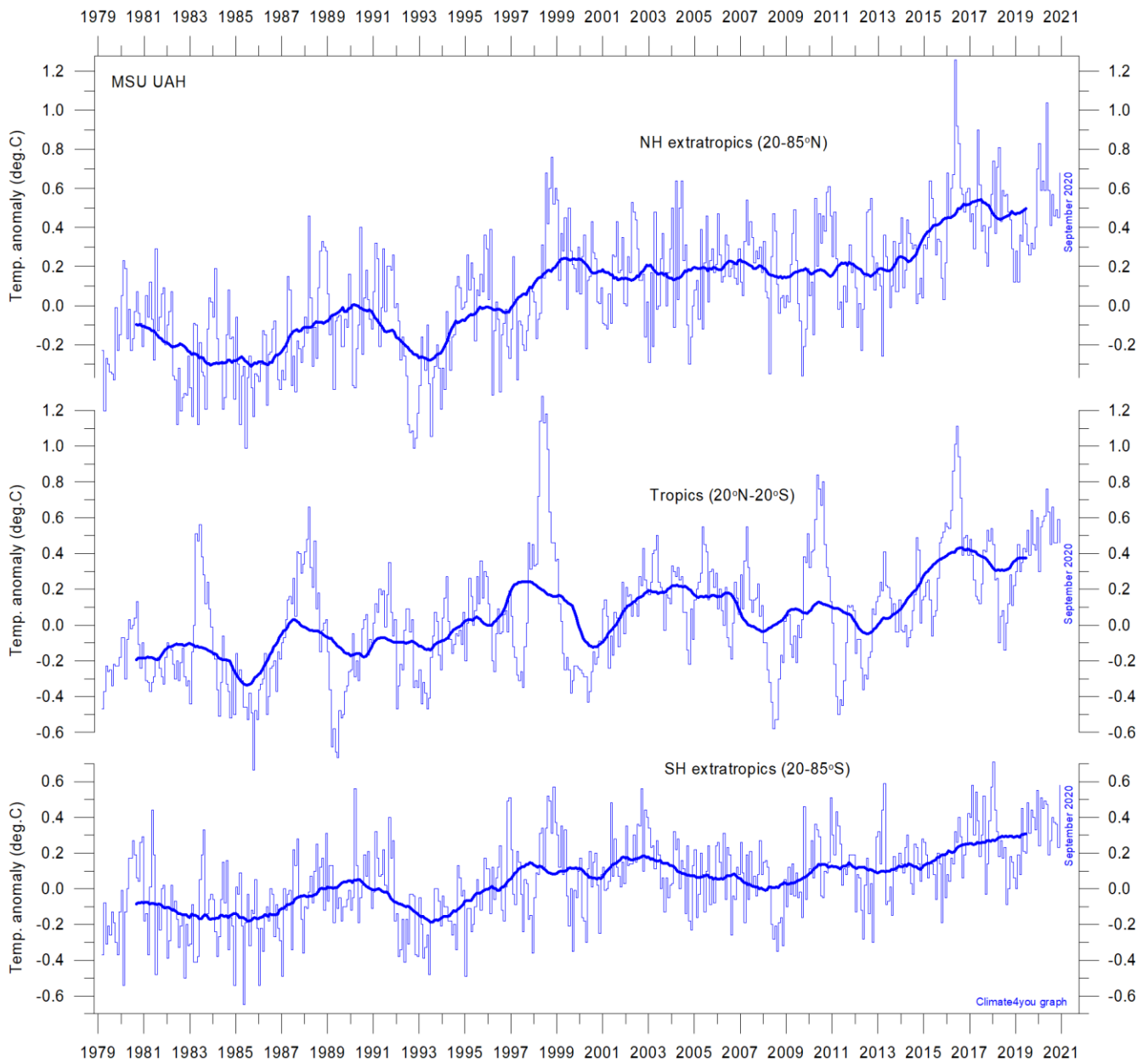
variations between El Niño and La Niña episodes do not appear abnormal in any way.

## Troposphere and stratosphere temperatures from satellites, updated to September 2020



*Global monthly average temperature in different according to University of Alabama at Huntsville, USA. The thin lines represent the monthly average, and the thick line the simple running 37-month average, nearly corresponding to a running 3-year average.*

## Zonal lower troposphere temperatures from satellites, updated to September 2020

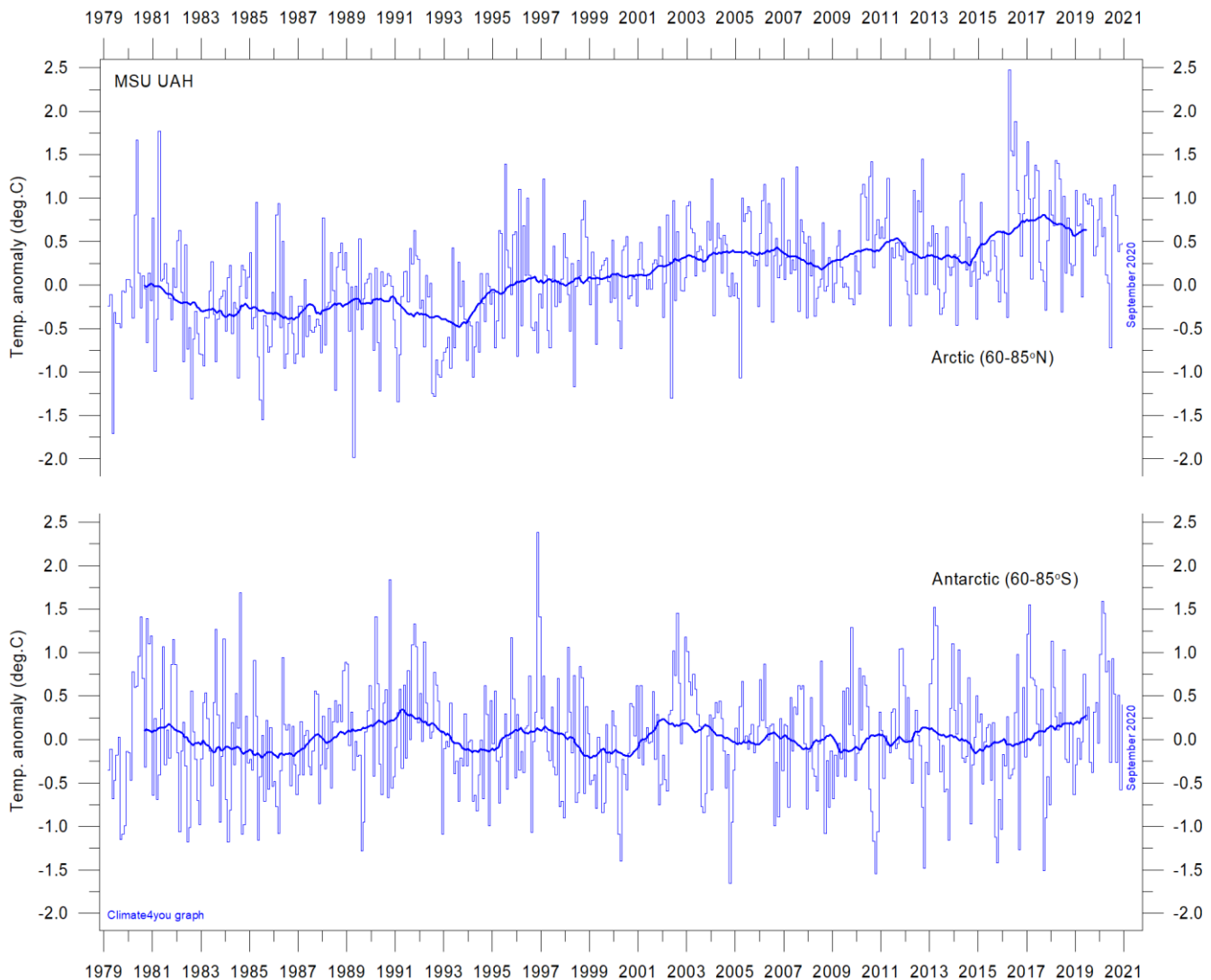


Global monthly average lower troposphere temperature since 1979 for the tropics and the northern and southern extratropics, according to University of Alabama at Huntsville, USA. Thin lines show the monthly temperature. Thick lines represent the simple running 37-month average, nearly corresponding to a running 3-year average. Reference period 1981-2010.

The overall warming since 1980 has dominantly been a northern hemisphere phenomenon, and mainly played out as a marked change between 1994 and 1999. However, this rather rapid temperature change is influenced by the Mt. Pinatubo eruption 1992-93 and the

subsequent 1997 El Niño episode. The diagram also shows the temperature effects of the strong Equatorial El Niño's in 1997 and 2015-16, as well as the moderate El Niño in 2019, apparently were spreading to higher latitudes in both hemispheres with some delay.

## Arctic and Antarctic lower troposphere temperature, updated to September 2020



*Global monthly average lower troposphere temperature since 1979 for the North Pole and South Pole regions, based on satellite observations ([University of Alabama at Huntsville, USA](#)). Thin lines show the monthly temperature. The thick line is the simple running 37-month average, nearly corresponding to a running 3-year average. Reference period 1981-2010.*

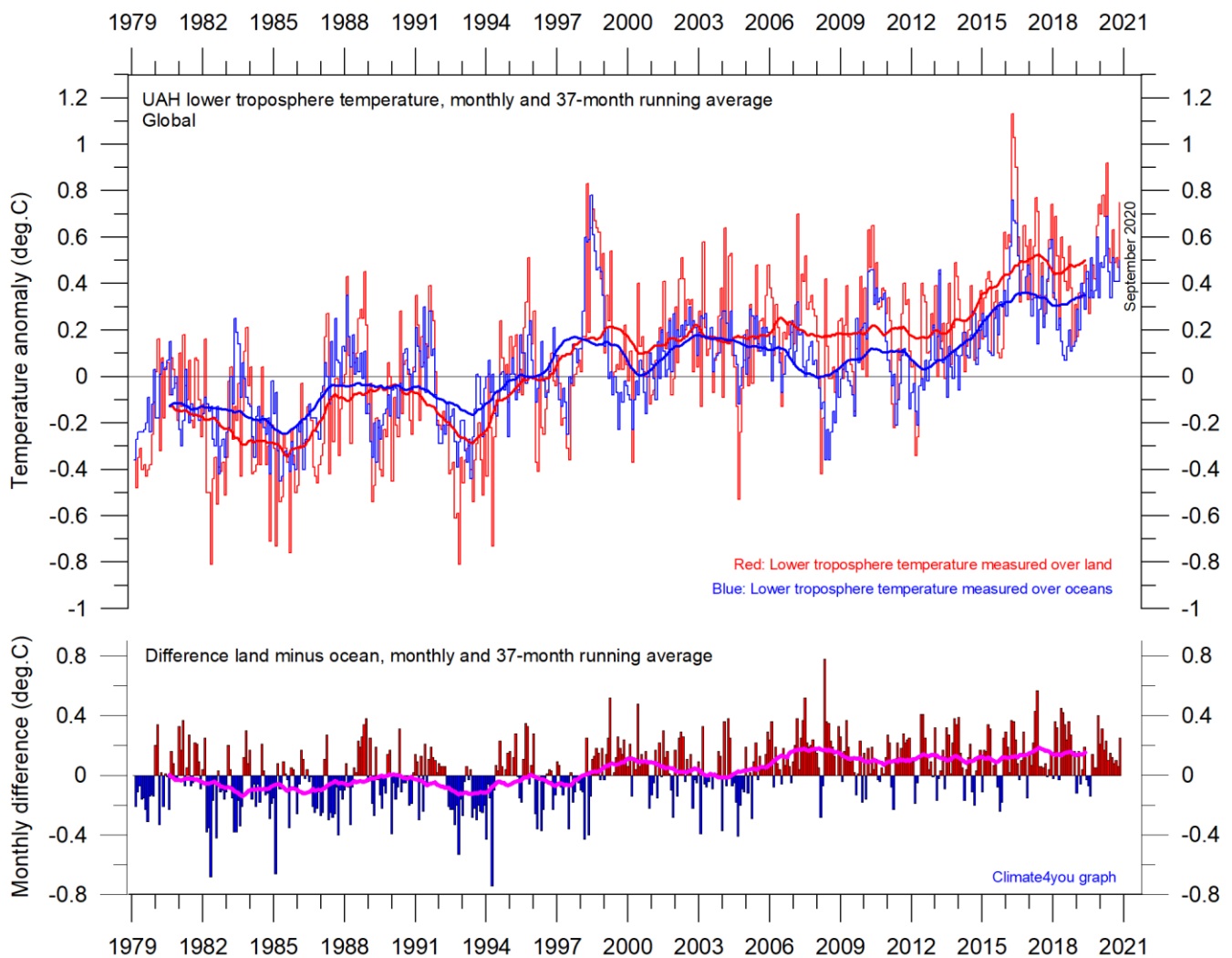
In the Arctic region, warming mainly took place 1994-96, and less so subsequently. In 2016, however, temperatures peaked for several months, presumably because of oceanic heat given off to the atmosphere during the 2015-15 El Niño (see also figure on page 24) and subsequently advected to higher latitudes.

This underscores how Arctic air temperatures may be affected not only by variations in local conditions but also by variations playing out in geographically remote

regions. An overall temperature decrease has characterised the Arctic since 2016 (see also diagrams on page 29-31).

In the Antarctic region, temperatures have essentially remained stable since the onset of the satellite record in 1979. In 2016-17 a small temperature peak visible in the monthly record may be interpreted as the subdued effect of the recent El Niño episode.

## Temperature over land versus over oceans, updated to September 2020



Global monthly average lower troposphere temperature since 1979 measured over land and oceans, respectively, according to [University of Alabama](#) at Huntsville, USA. Thick lines are the simple running 37-month average, nearly corresponding to a running 3-year average. Reference period 1981-2010.

Since 1979, the lower troposphere over land has warmed much more than over oceans, suggesting that the overall warming is derived mainly from incoming solar radiation.

In addition, there may be supplementary reasons for this divergence, such as, e.g., variations in cloud cover and changes in land use.

## Arctic and Antarctic surface air temperature, updated to August 2020

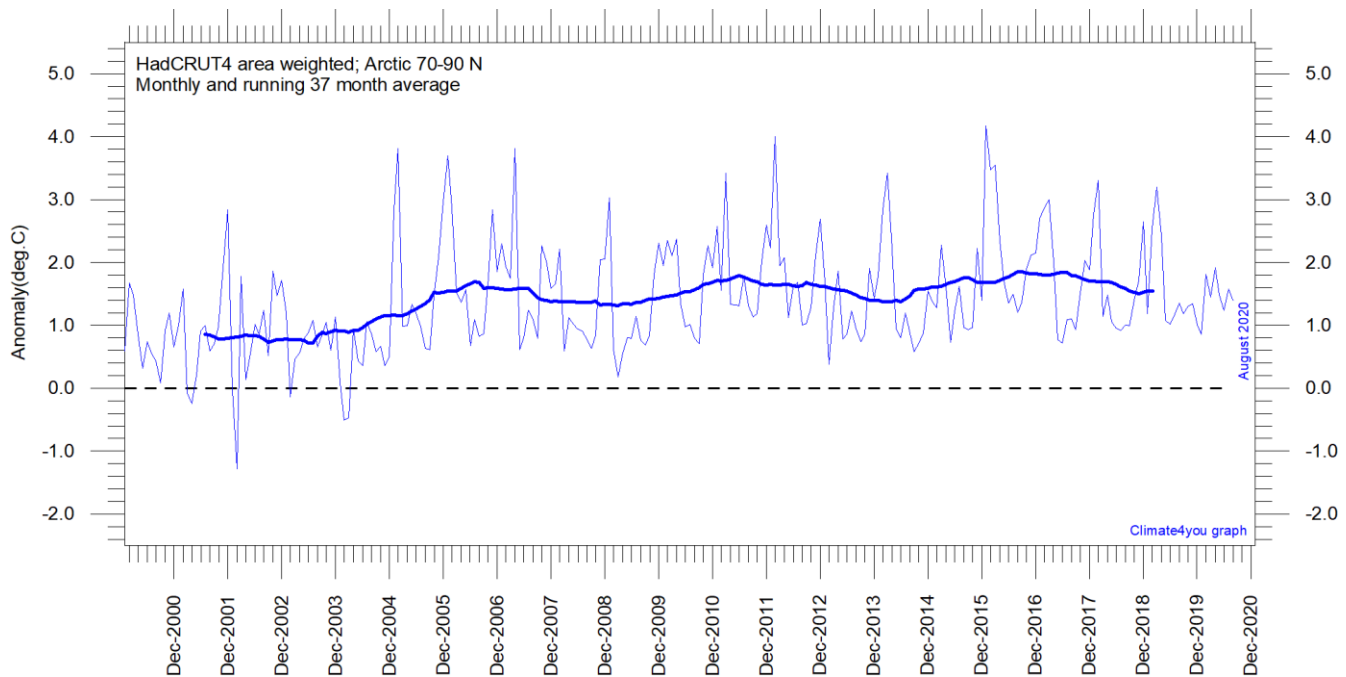


Diagram showing area weighted Arctic (70-90°N) monthly surface air temperature anomalies ([HadCRUT4](#)) since January 2000, in relation to the WMO [normal period](#) 1961-1990. The thin line shows the monthly temperature anomaly, while the thicker line shows the running 37-month (c. 3 year) average.

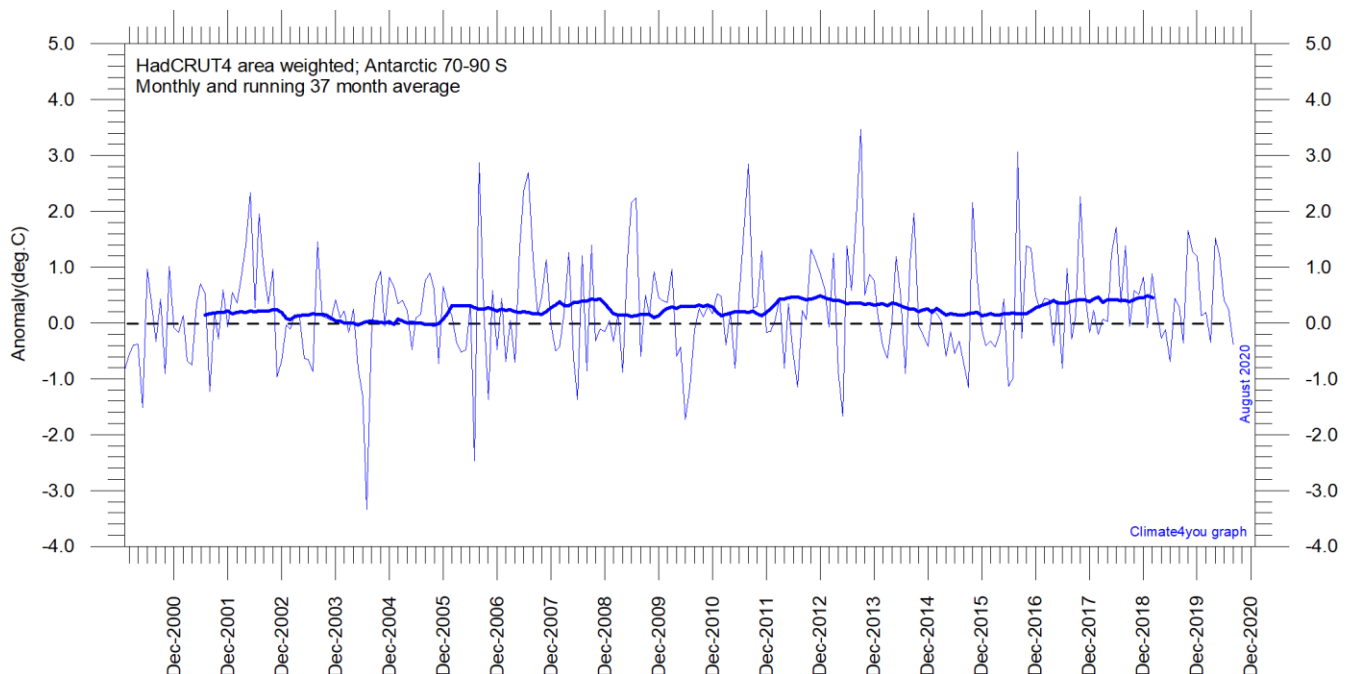


Diagram showing area weighted Antarctic (70-90°S) monthly surface air temperature anomalies ([HadCRUT4](#)) since January 2000, in relation to the WMO [normal period](#) 1961-1990. The thin line shows the monthly temperature anomaly, while the thicker line shows the running 37-month (c. 3 year) average.

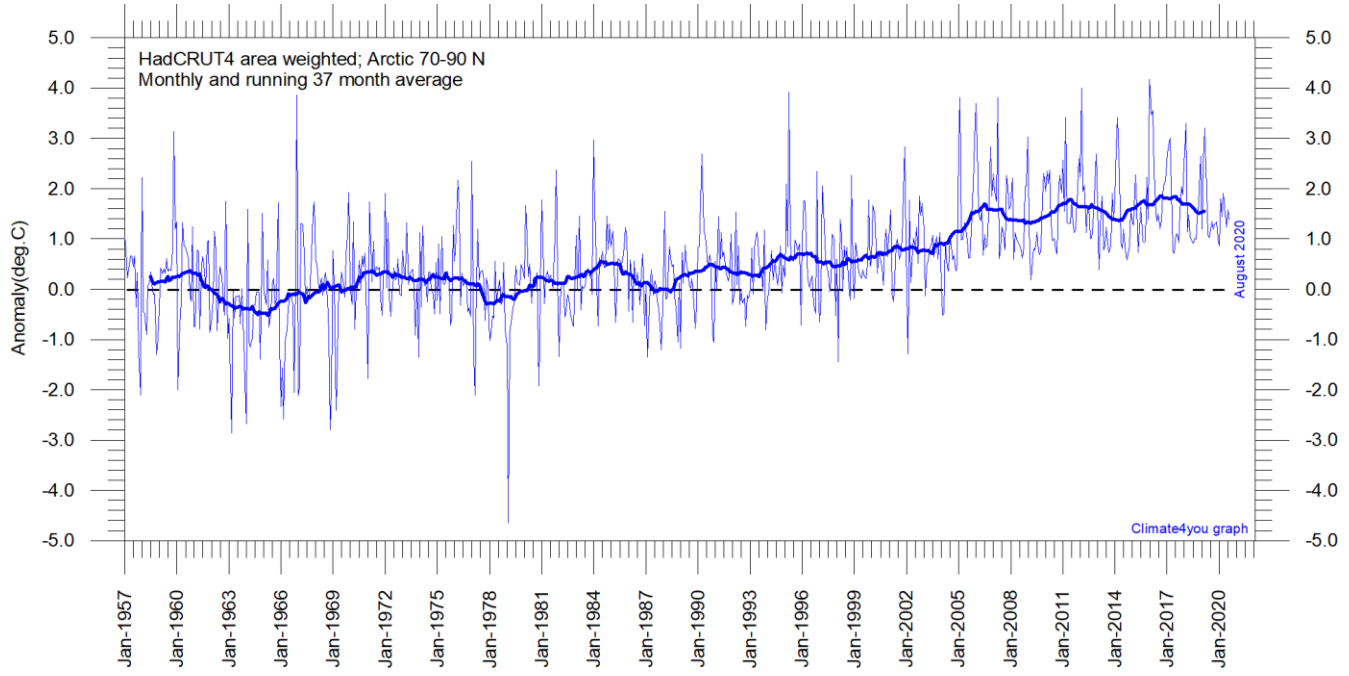


Diagram showing area weighted Arctic ( $70-90^{\circ}\text{N}$ ) monthly surface air temperature anomalies ([HadCRUT4](#)) since January 1957, in relation to the WMO [normal period](#) 1961-1990. The thin line shows the monthly temperature anomaly, while the thicker line shows the running 37-month (c. 3 year) average.

30

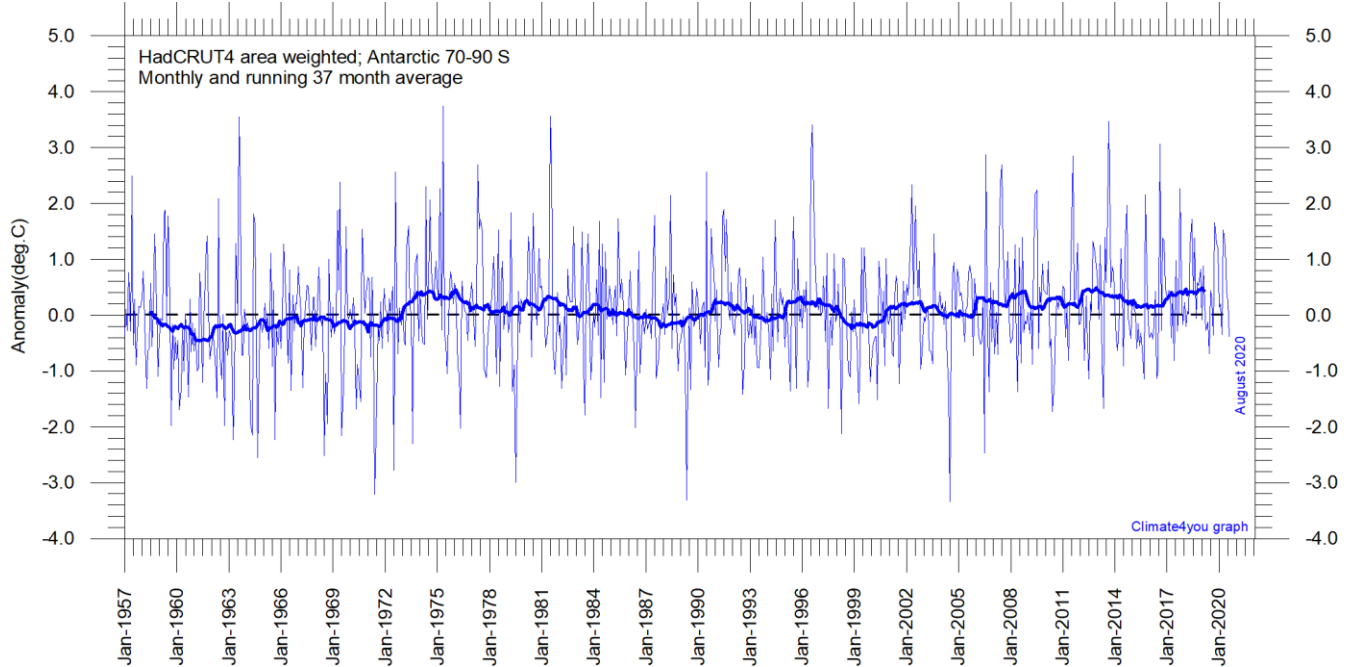


Diagram showing area weighted Antarctic ( $70-90^{\circ}\text{S}$ ) monthly surface air temperature anomalies ([HadCRUT4](#)) since January 1957, in relation to the WMO [normal period](#) 1961-1990. The thin line shows the monthly temperature anomaly, while the thicker line shows the running 37-month (c. 3 year) average.

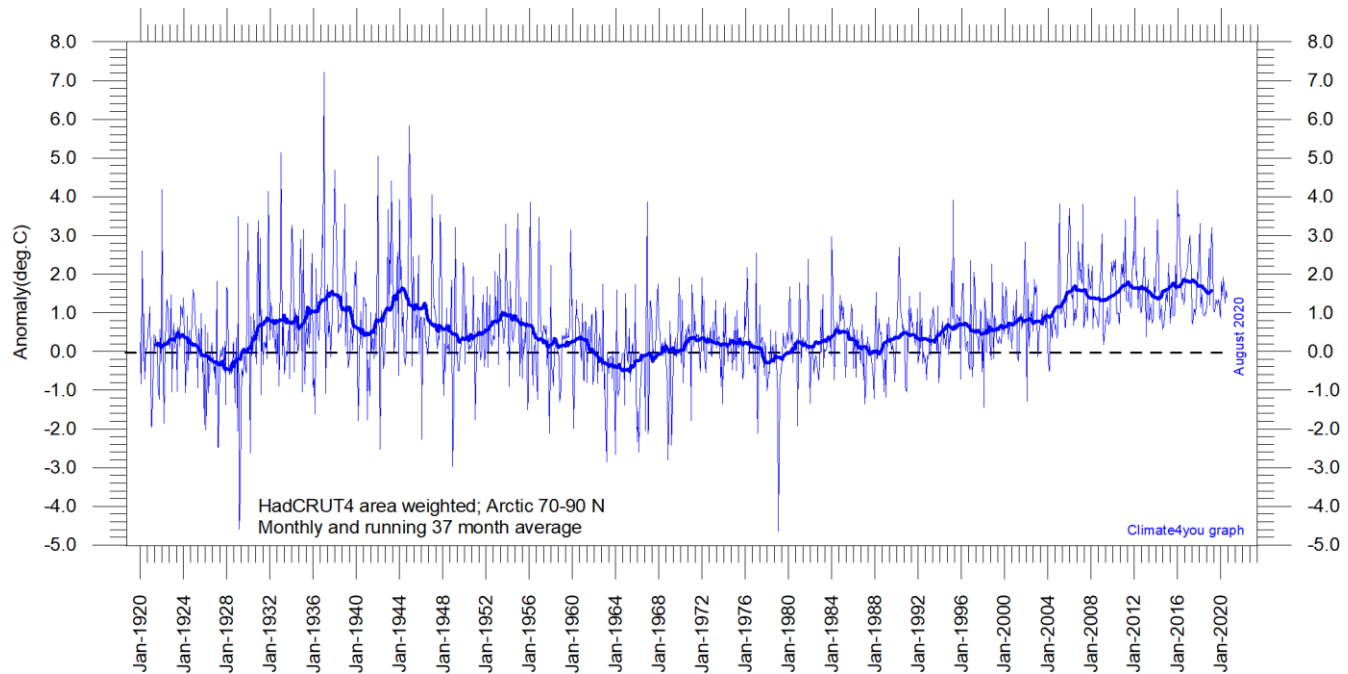


Diagram showing area-weighted Arctic (70-90°N) monthly surface air temperature anomalies ([HadCRUT4](#)) since January 1920, in relation to the WMO [normal period](#) 1961-1990. The thin line shows the monthly temperature anomaly, while the thicker line shows the running 37-month (c. 3 year) average.

31

Because of the relatively small number of Arctic stations before 1930, month-to-month variations in the early part of the Arctic temperature record 1920-2018 are bigger than later (diagram above).

The period from about 1930 saw the establishment of many new Arctic meteorological stations, first in Russia and Siberia, and following the 2<sup>nd</sup> World War, also in North America. The period since 2005 is warm, about as warm as the period 1930-1940.

As the HadCRUT4 data series has improved high latitude coverage data coverage (compared to the HadCRUT3 series), the individual 5°x5° grid cells have been weighted according to their surface area. This area correction is especially important for polar regions. This approach differs from the approach used by Gillett et al. 2008, which

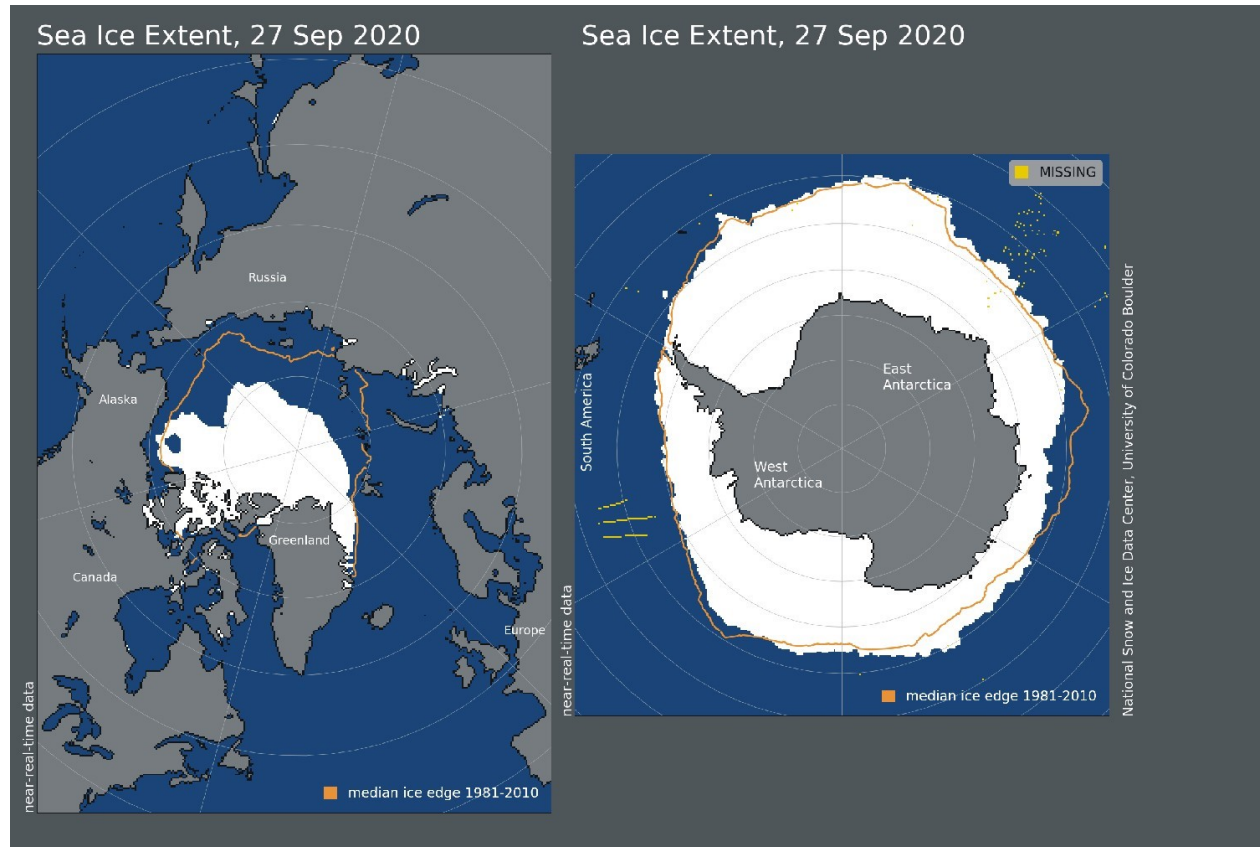
calculated a simple average, with no correction for the substantial latitudinal surface area effect in polar regions.

The area weighted HadCRUT4 surface air temperature records (p.29-31) correspond rather well to the lower troposphere temperature records recorded by satellites (p.27).

Literature:

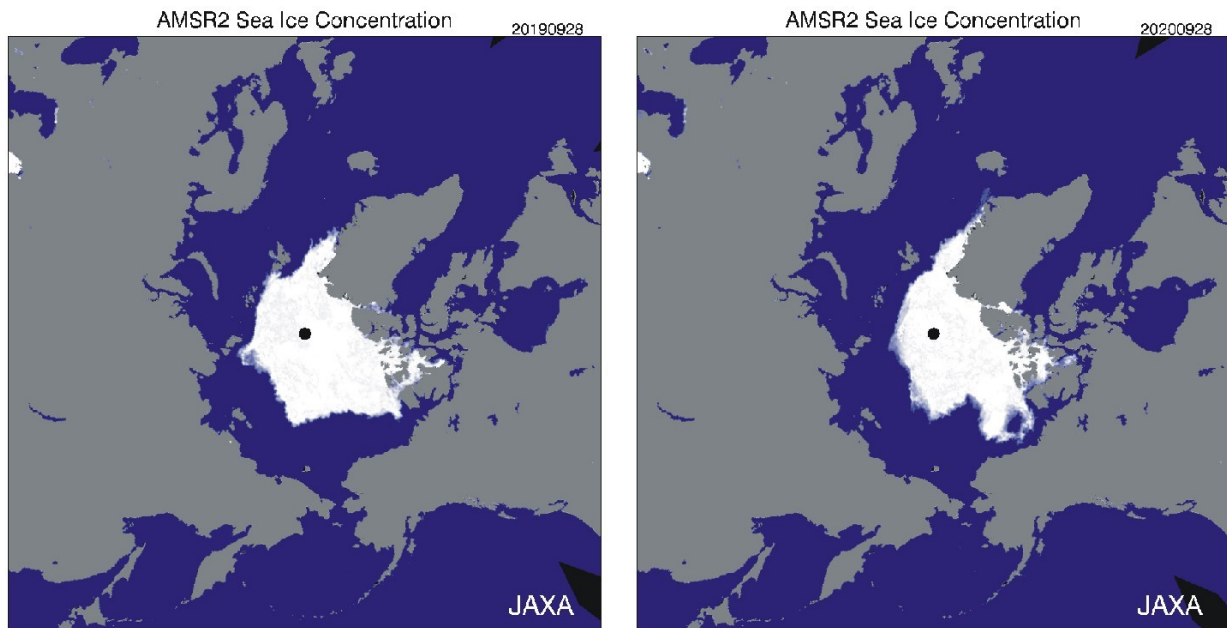
Gillett, N.P., Stone, D.A., Stott, P.A., Nozawa, T., Karpechko, A.Y.U., Hegerl, G.C., Wehner, M.F. and Jones, P.D. 2008. Attribution of polar warming to human influence. *Nature Geoscience* 1, 750-754.

## Arctic and Antarctic sea ice, updated to September 2020

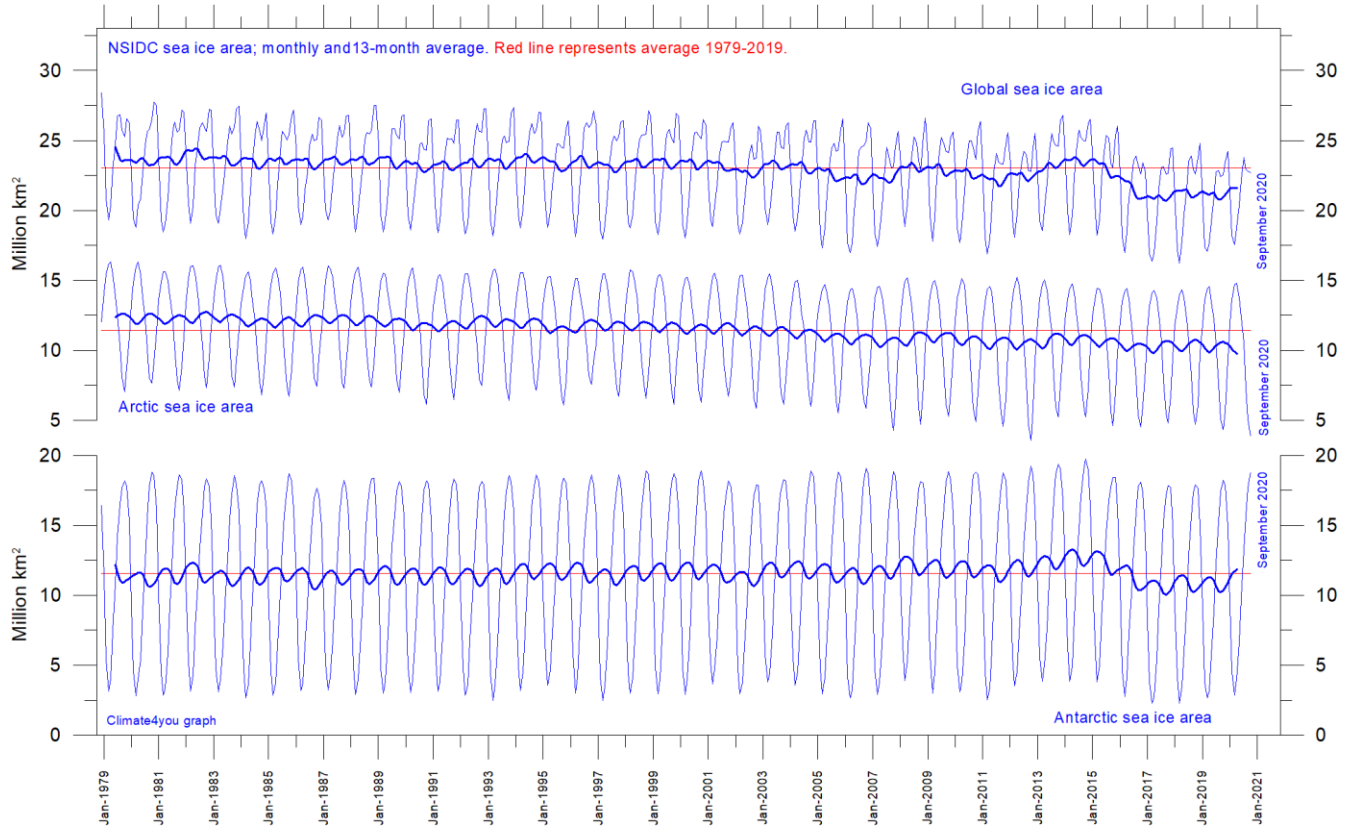


32

*Sea ice extent 27 September 2020. The median limit of sea ice (orange line) is defined as 15% sea ice cover, according to the average of satellite observations 1981-2010 (both years included). Sea ice may therefore well be encountered outside and open water areas inside the limit shown in the diagrams above. Map source: National Snow and Ice Data Center (NSIDC).*



*Diagrams showing Arctic sea ice extent and concentration 28 September 2019 (left) and 2020 (right), according to the Japan Aerospace Exploration Agency (JAXA).*



Graphs showing monthly Antarctic, Arctic and global sea ice extent since November 1978, according to the [National Snow and Ice data Center](#) (NSIDC).

33

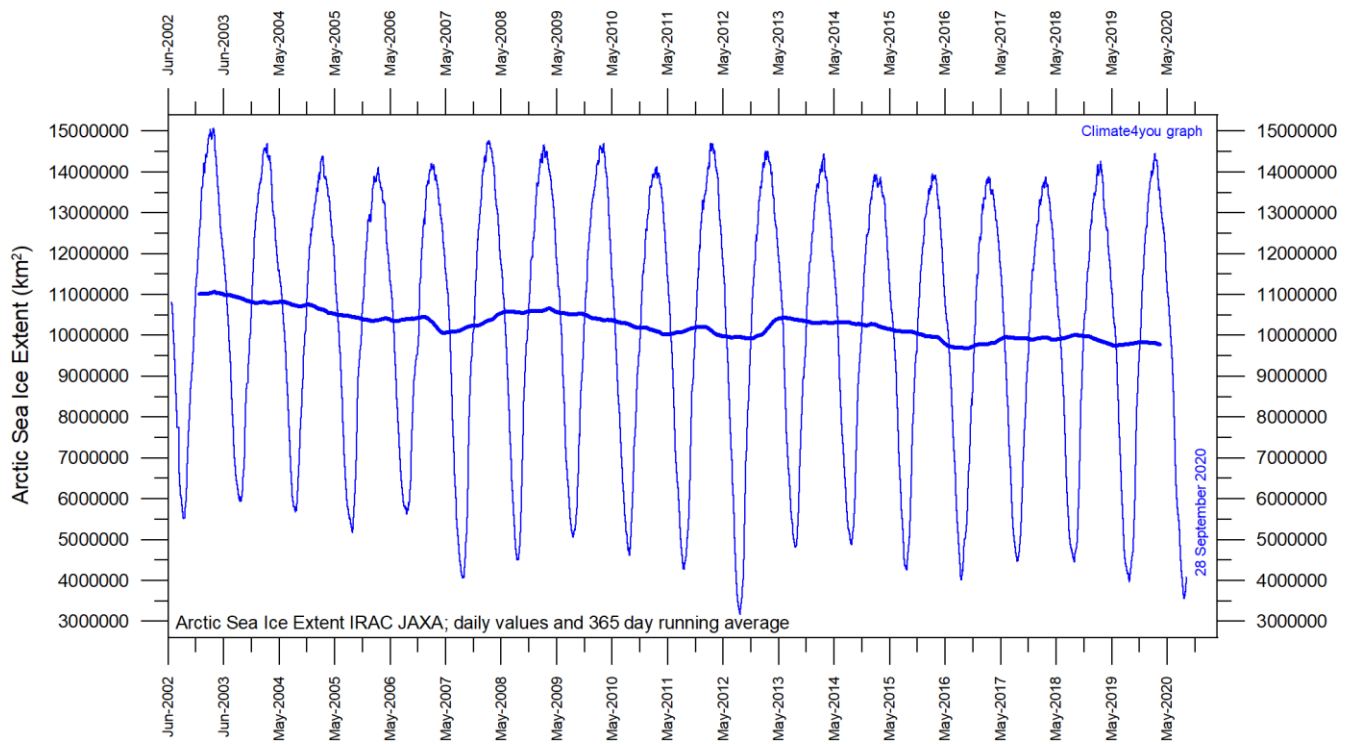
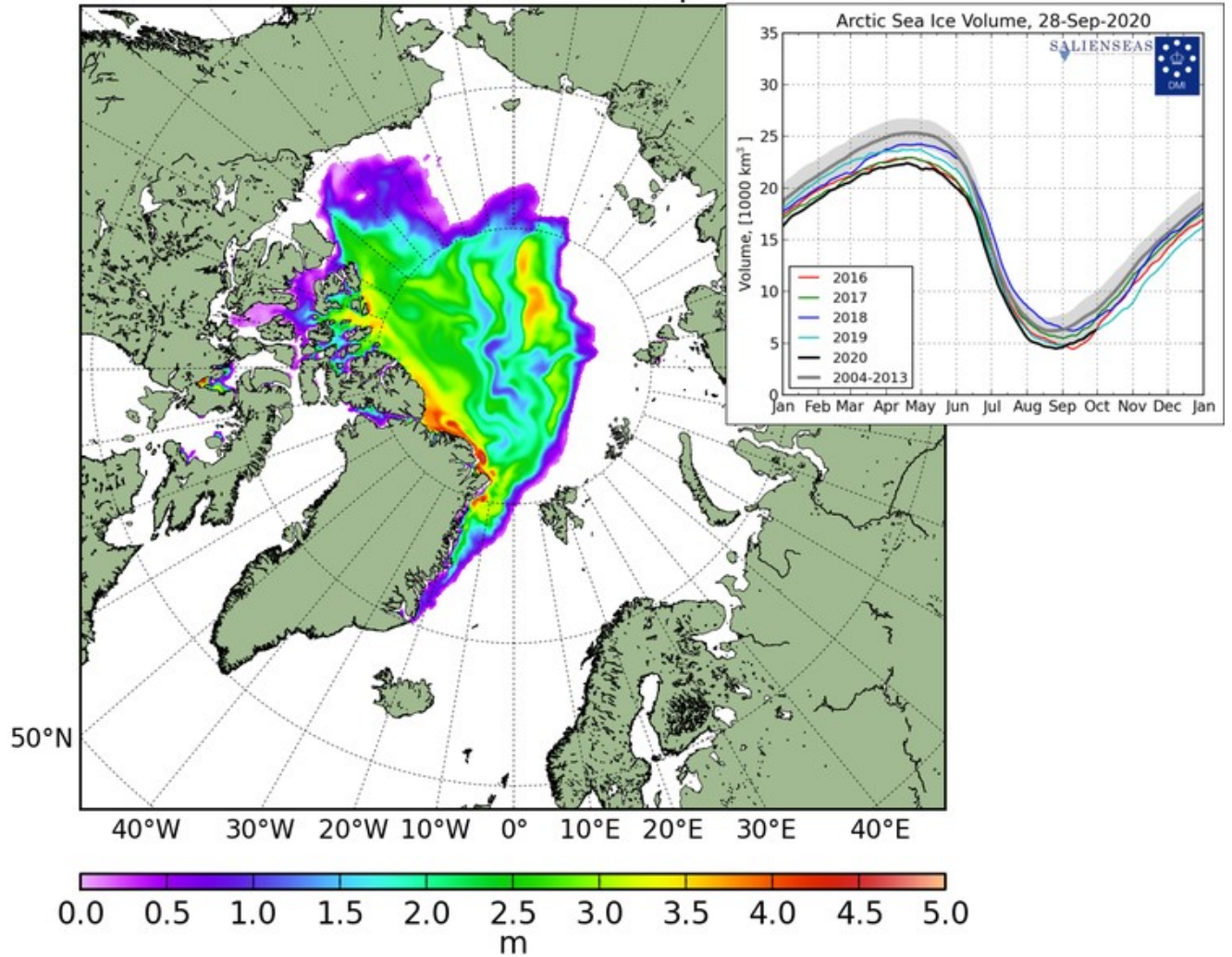
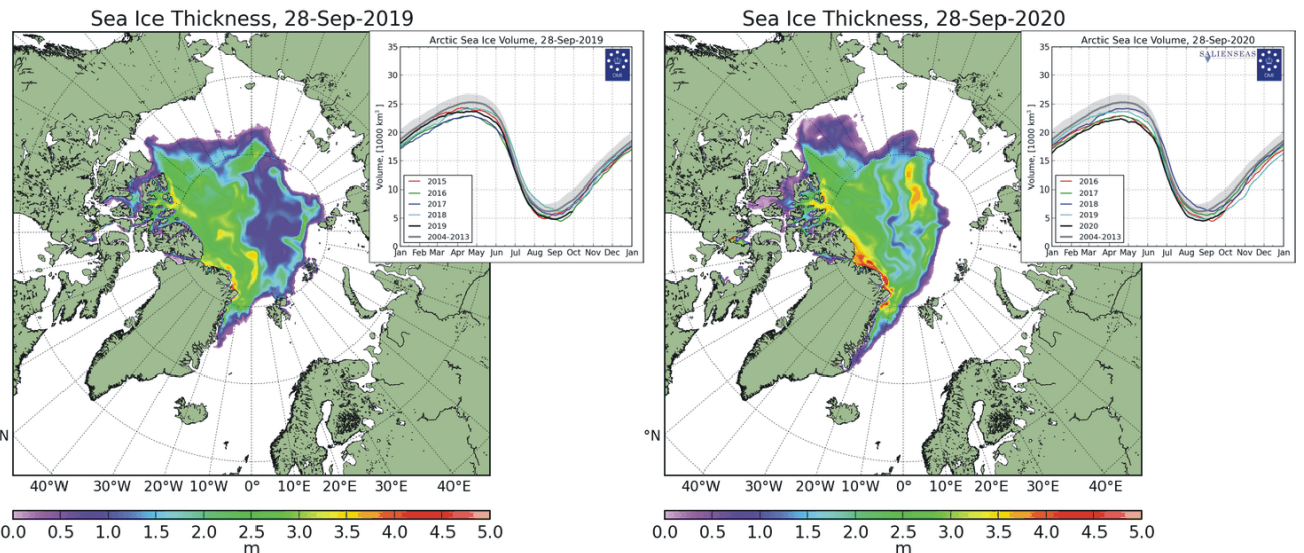


Diagram showing daily Arctic sea ice extent since June 2002, to 28 September 2020, by courtesy of [Japan Aerospace Exploration Agency](#) (JAXA).

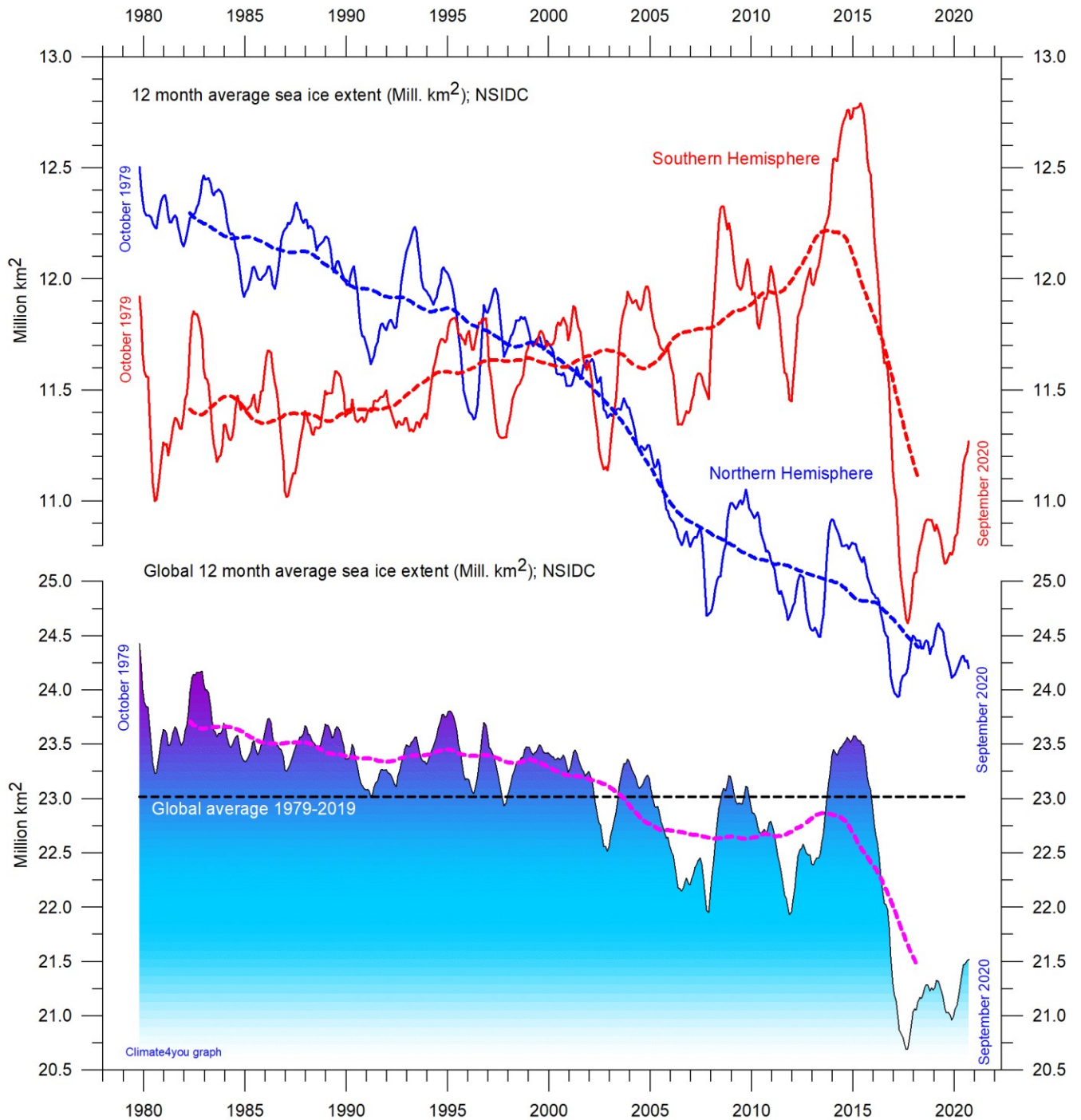
## Sea Ice Thickness, 28-Sep-2020



34



Diagrams showing Arctic sea ice extent and thickness 28 September 2019 (left) and 2020 (right and above) and the seasonal cycles of the calculated total arctic sea ice volume, according to [The Danish Meteorological Institute \(DMI\)](#). The mean sea ice volume and standard deviation for the period 2004-2013 are shown by grey shading.



12 month running average sea ice extension, global and in both hemispheres since 1979, the satellite-era. The October 1979 value represents the monthly 12-month average of November 1978 - October 1979, the November 1979 value represents the average of December 1978 - November 1979, etc. The stippled lines represent a 61-month (ca. 5 years) average. Data source: National Snow and Ice Data Center (NSIDC).

## Sea level in general

Global (or eustatic) sea-level change is measured relative to an idealised reference level, the geoid, which is a mathematical model of planet Earth's surface (Carter et al. 2014). Global sea-level is a function of the volume of the ocean basins and the volume of water they contain. Changes in global sea-level are caused by – but not limited to - four main mechanisms:

1. Changes in local and regional air pressure and wind, and tidal changes introduced by the Moon.
2. Changes in ocean basin volume by tectonic (geological) forces.
3. Changes in ocean water density caused by variations in currents, water temperature and salinity.
4. Changes in the volume of water caused by changes in the mass balance of terrestrial glaciers.

In addition to these there are other mechanisms influencing sea-level; such as storage of ground water, storage in lakes and rivers, evaporation, etc.

Mechanism 1 is controlling sea-level at many sites on a time scale from months to several years. As an example, many coastal stations show a pronounced annual variation reflecting seasonal changes in air pressures and wind speed. Longer-term climatic changes playing out over decades or centuries will also affect measurements of sea-level changes. Hansen et al. (2011, 2015) provide excellent analyses of sea-level changes caused by recurrent changes of the orbit of the Moon and other phenomena.

Mechanism 2 – with the important exception of earthquakes and tsunamis - typically operates over long (geological) time scales and is not significant on human time scales. It may relate to variations in the seafloor spreading rate, causing volume changes in mid-ocean mountain ridges, and to the slowly changing configuration of land and oceans. Another effect may be the slow rise of basins due to isostatic offloading by deglaciation after an ice age. The floor of the Baltic Sea and the Hudson Bay are presently rising, causing a slow net transfer of

water from these basins into the adjoining oceans. Slow changes of very big glaciers (ice sheets) and movements in the mantle will affect the gravity field and thereby the vertical position of the ocean surface. Any increase of the total water mass as well as sediment deposition into oceans increase the load on their bottom, generating sinking by viscoelastic flow in the mantle below. The mantle flow is directed towards the surrounding land areas, which will rise, thereby partly compensating for the initial sea level increase induced by the increased water mass in the ocean.

Mechanism 3 (temperature-driven expansion) only affects the uppermost part of the oceans on human time scales. Usually, temperature-driven changes in density are more important than salinity-driven changes. Seawater is characterised by a relatively small coefficient of expansion, but the effect should however not be overlooked, especially when interpreting satellite altimetry data. Temperature-driven expansion of a column of seawater will not affect the total mass of water within the column considered and will therefore not affect the potential at the top of the water column. Temperature-driven ocean water expansion will therefore not in itself lead to any lateral displacement of water, but only locally lift the ocean surface. Near the coast, where people are living, the depth of water approaches zero, so no measurable temperature-driven expansion will take place here (Mörner 2015). Mechanism 3 is for that reason not important for coastal regions.

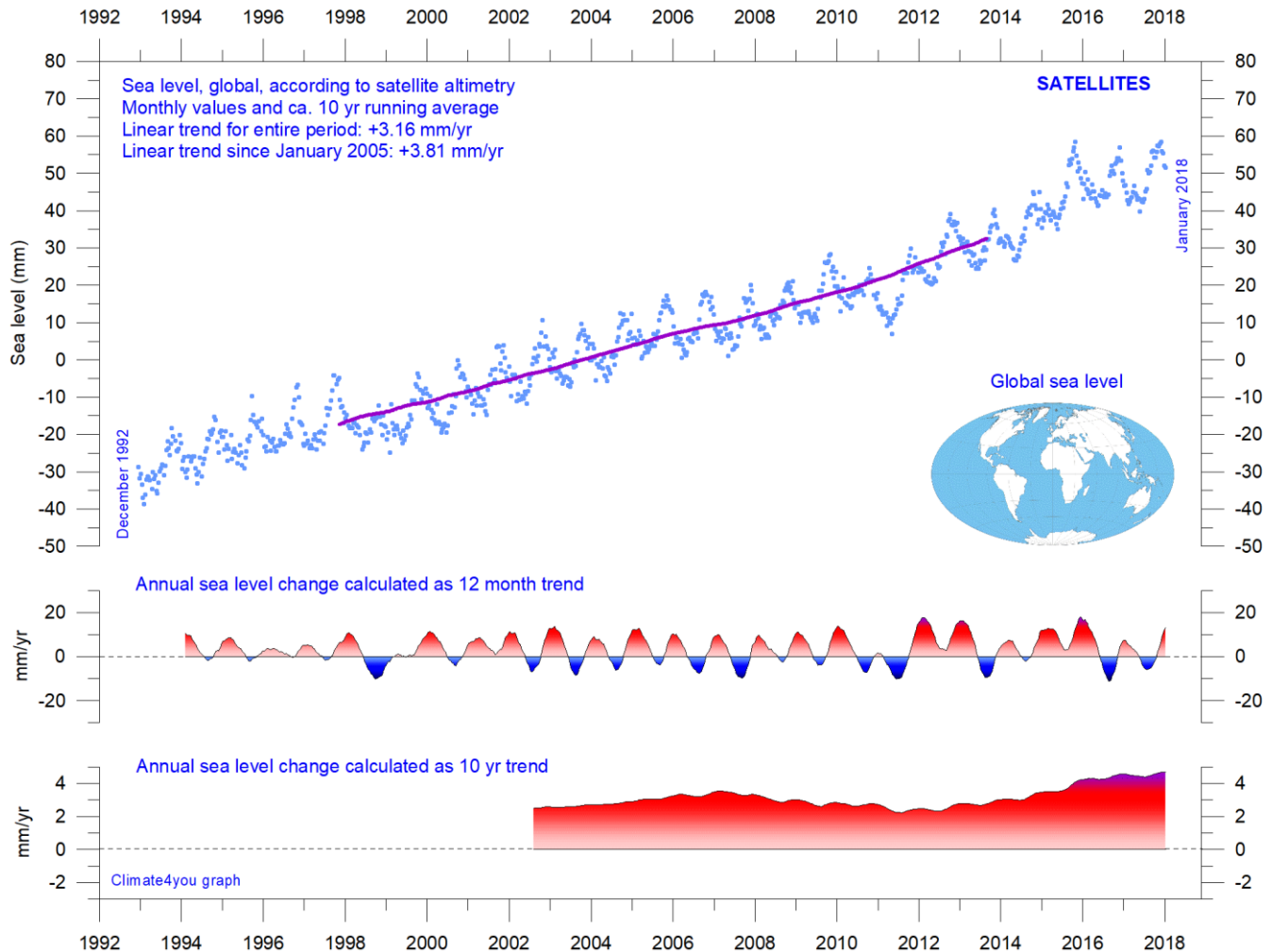
Mechanism 4 (changes in glacier mass balance) is an important driver for global sea-level changes along coasts, for human time scales. Volume changes of floating glaciers – ice shelves – has no influence on the global sea-level, just like volume changes of floating sea ice has no influence. Only the mass-balance of grounded or land-based glaciers is important for the global sea-level along coasts.

Summing up: Presumably, mechanism 1 and 4 are the most important for understanding sea-level changes along coasts.

### References:

- Carter R.M., de Lange W., Hansen, J.M., Humlum O., Idso C., Kear, D., Legates, D., Mörner, N.A., Ollier C., Singer F. & Soon W. 2014. Commentary and Analysis on the Whitehead& Associates 2014 NSW Sea-Level Report. Policy Brief, NIPCC, 24. September 2014, 44 pp. <http://climatechangereconsidered.org/wp-content/uploads/2014/09/NIPCC-Report-on-NSW-Coastal-SL-9z-corrected.pdf>
- Hansen, J.-M., Aagaard, T. and Binderup, M. 2011. Absolute sea levels and isostatic changes of the eastern North Sea to central Baltic region during the last 900 years. *Boreas*, 10.1111/j.1502-3885.2011.00229.x. ISSN 0300–9483.
- Hansen, J.-M., Aagaard, T. and Huijpers, A. 2015. Sea-Level Forcing by Synchronization of 56- and 74-YearOscillations with the Moon's Nodal Tide on the Northwest European Shelf (Eastern North Sea to Central Baltic Sea). *Journ. Coastal Research*, 16 pp.
- Mörner, Nils-Axel 2015. Sea Level Changes as recorded in nature itself. *Journal of Engineering Research and Applications*, Vol.5, 1, 124-129.

## Global sea level from satellite altimetry, updated to January 2018



37

Global sea level since December 1992 according to the Colorado Center for Astrodynamics Research at University of Colorado at Boulder. The blue dots are the individual observations, and the purple line represents the running 121-month (ca. 10 year) average. The two lower panels show the annual sea level change, calculated for 1 and 10-year time windows, respectively. These values are plotted at the end of the interval considered. Data from the TOPEX/Poseidon mission have been used before 2002, and data from the Jason-1 mission (satellite launched December 2001) after 2002.

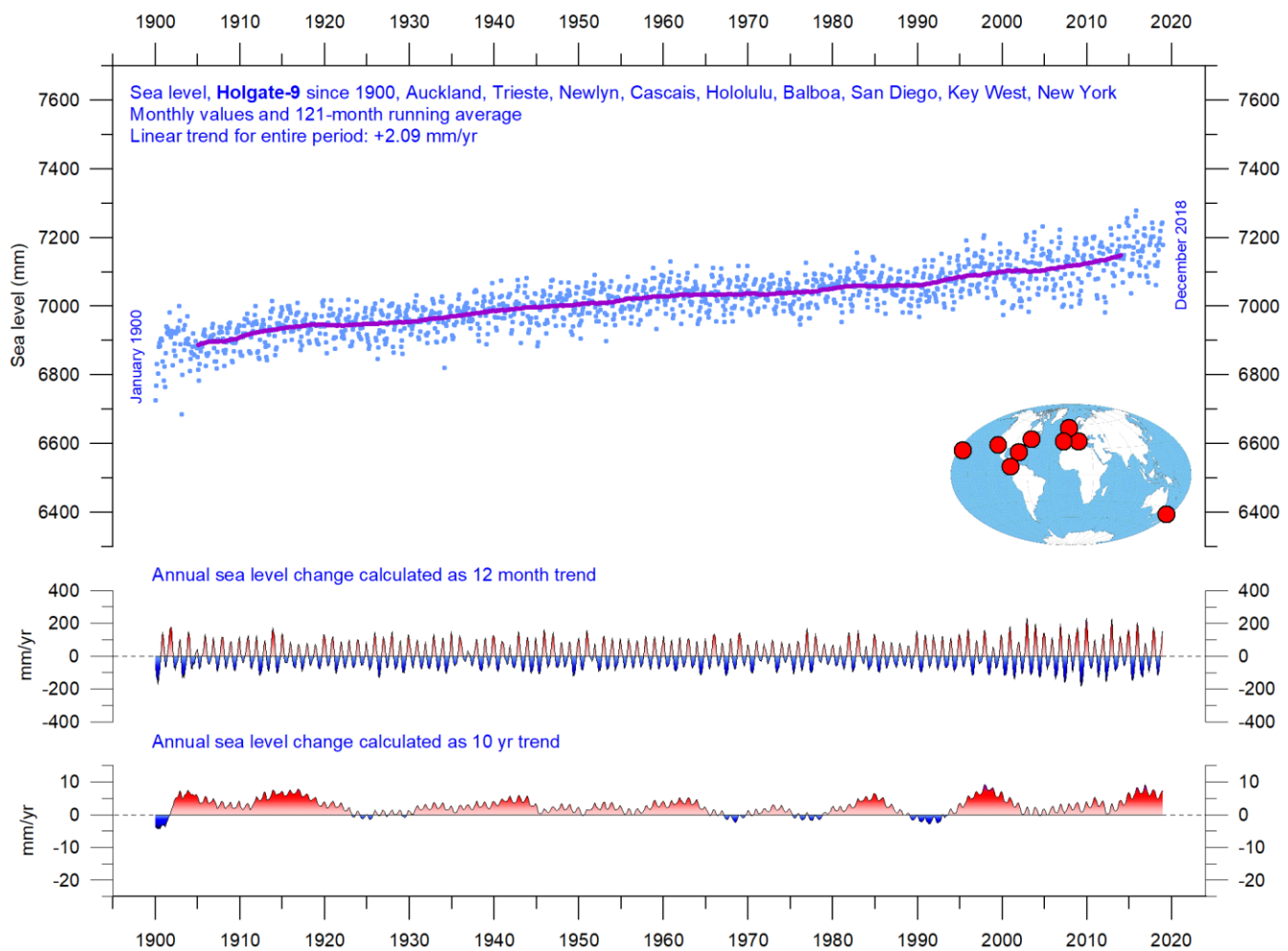
Ground truth is a term used in various fields to refer to information provided by direct observation as opposed to information provided by inference, such as, e.g., by satellite observations.

In remote sensing using satellite observations, ground truth data refers to information collected on location. Ground truth allows the satellite data to be related to real features observed on the planet surface. The collection of ground truth data enables calibration of remote-sensing

data, and aids in the interpretation and analysis of what is being sensed or recorded by satellites. Ground truth sites allow the remote sensor operator to correct and improve the interpretation of satellite data.

For satellite observations on sea level ground true data are provided by the classical tide gauges (example diagram on next page), that directly measures the local sea level many places distributed along the coastlines on the surface of the planet.

## Global sea level from tide-gauges, updated to December 2018



Holgate-9 monthly tide gauge data from PSMSL Data Explorer. Holgate (2007) suggested the nine stations listed in the diagram to capture the variability found in a larger number of stations over the last half century studied previously. For that reason, average values of the Holgate-9 group of tide gauge stations are interesting to follow, even though Auckland (New Zealand) has not reported data since 2000, and Cascais (Portugal) not since 1993. Unfortunately, by this data loss the Holgate-9 series since 2000 is underrepresented with respect to the southern hemisphere. The blue dots are the individual average monthly observations, and the purple line represents the running 121-month (ca. 10 year) average. The two lower panels show the annual sea level change, calculated for 1 and 10-year windows, respectively. These values are plotted at the end of the interval considered.

Data from tide-gauges all over the world suggest an average global sea-level rise of 1-1.5 mm/year, while the satellite-derived record (page 37) suggest a rise of about 3.2 mm/year, or more. The noticeable difference (at least 1:2) between the two data sets is remarkable but has no

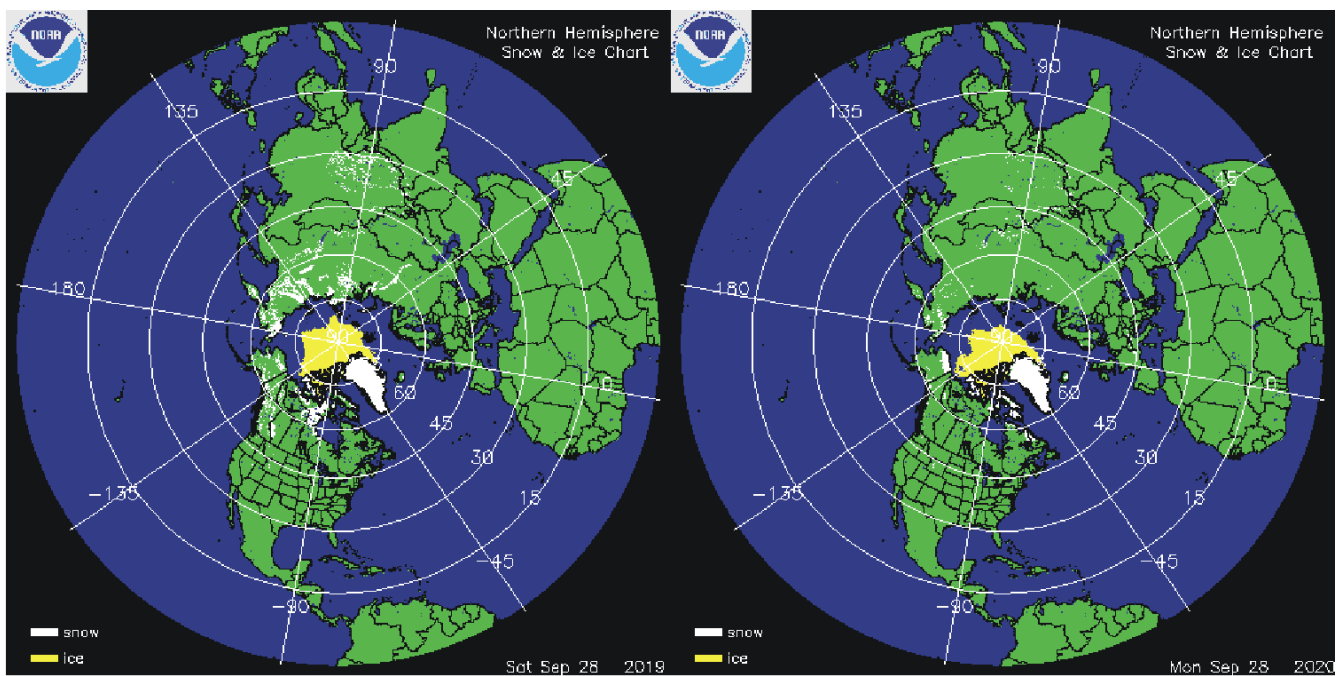
broadly accepted explanation. It is however known that satellite observations are facing several complications in areas near the coast. Vignudelli et al. (2019) provide an updated overview of the current limitations of classical satellite altimetry in coastal regions.

### References:

Holgate, S.J. 2007. On the decadal rates of sea level change during the twentieth century. *Geophys. Res. Letters*, 34, L01602, doi:10.1029/2006GL028492

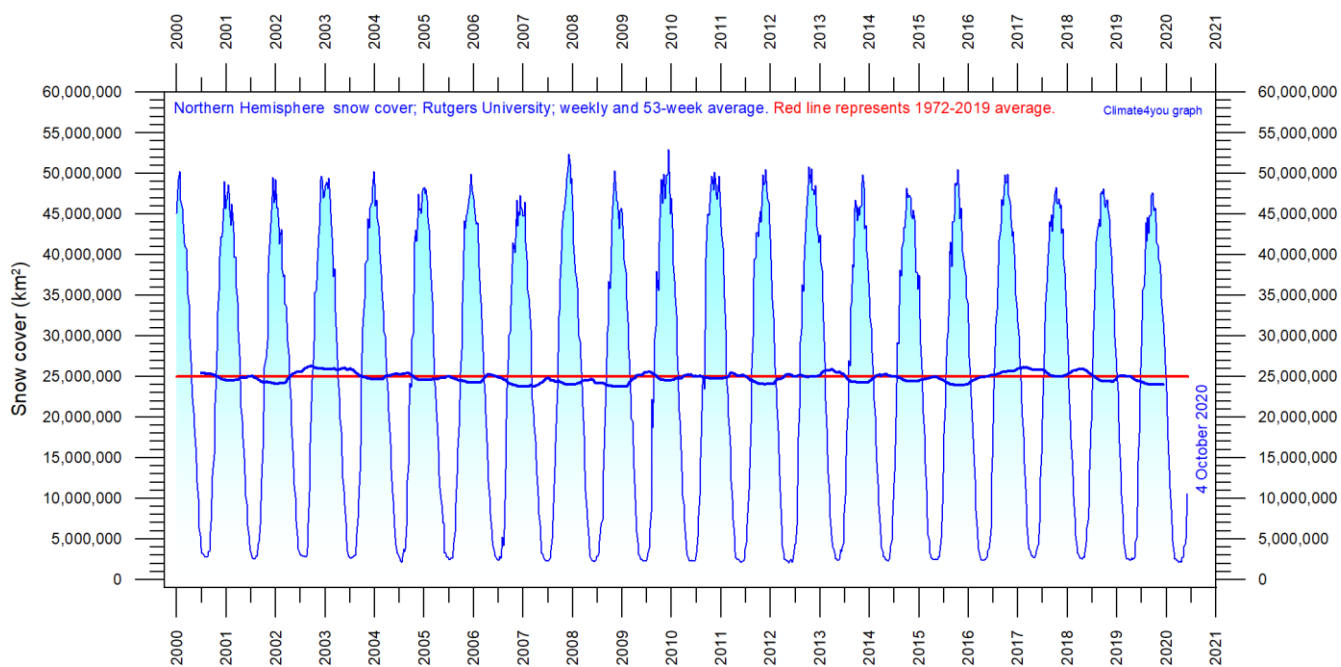
Vignudelli et al. 2019. Satellite Altimetry Measurements of Sea Level in the Coastal Zone. *Surveys in Geophysics*, Vol. 40, p. 1319–1349. <https://link.springer.com/article/10.1007/s10712-019-09569-1>

## Northern Hemisphere weekly and seasonal snow cover, updated to September 2020

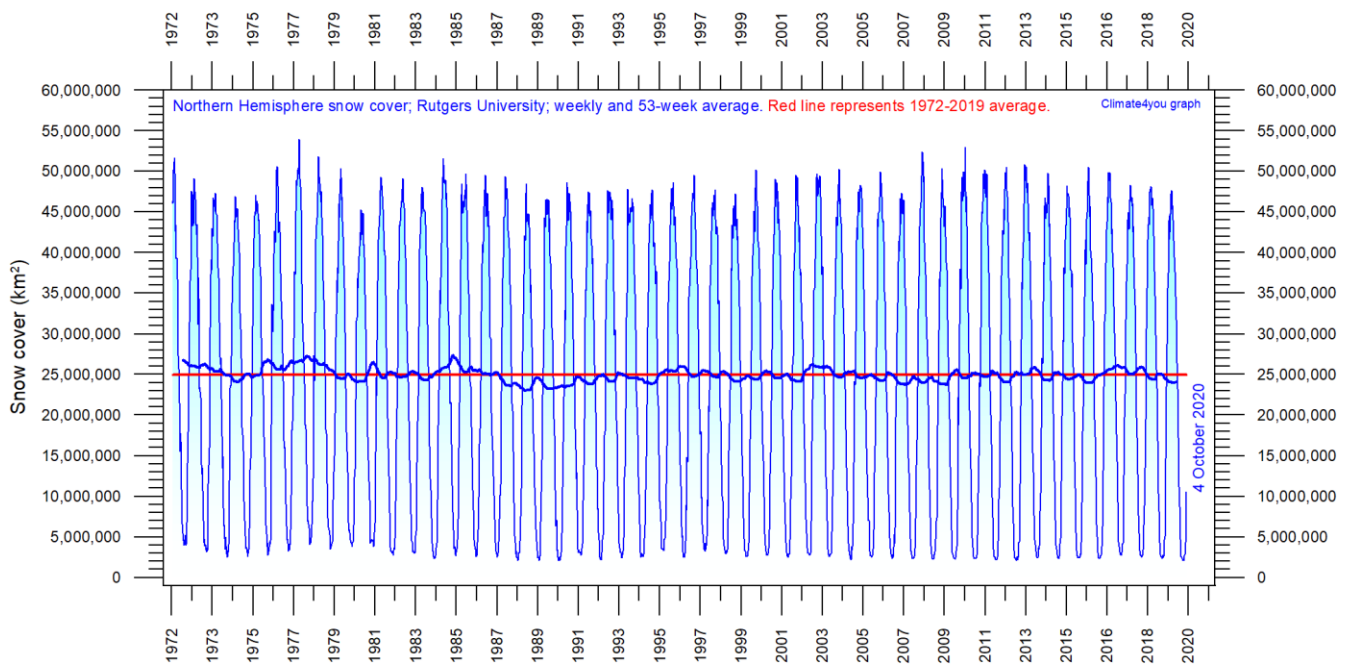


*Northern hemisphere snow cover (white) and sea ice (yellow) 28 September 2019 (left) and 2020 (right). Map source: [National Ice Center \(NIC\)](#).*

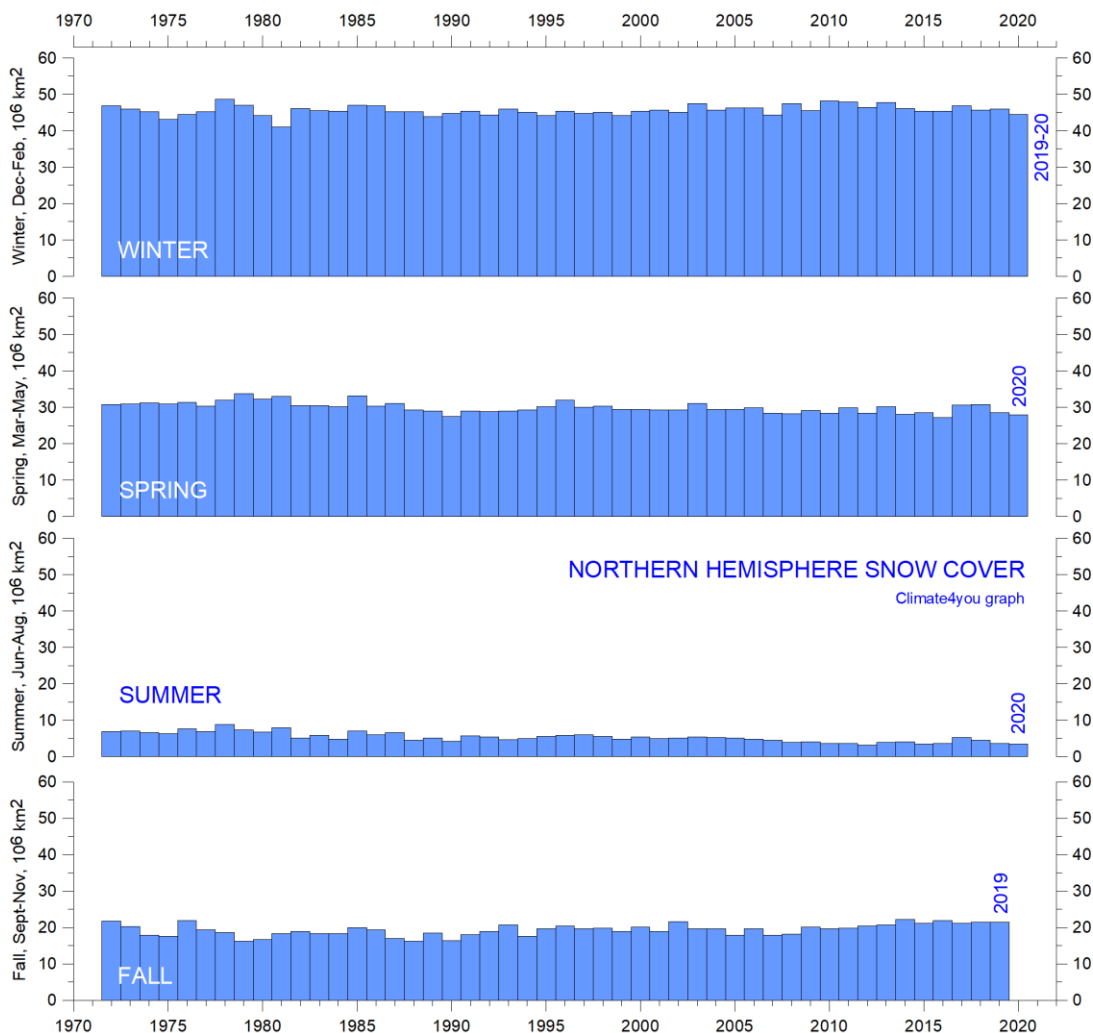
39



*Northern hemisphere weekly snow cover since January 2000 according to Rutgers University Global Snow Laboratory. The thin blue line is the weekly data, and the thick blue line is the running 53-week average (approximately 1 year). The horizontal red line is the 1972-2019 average.*

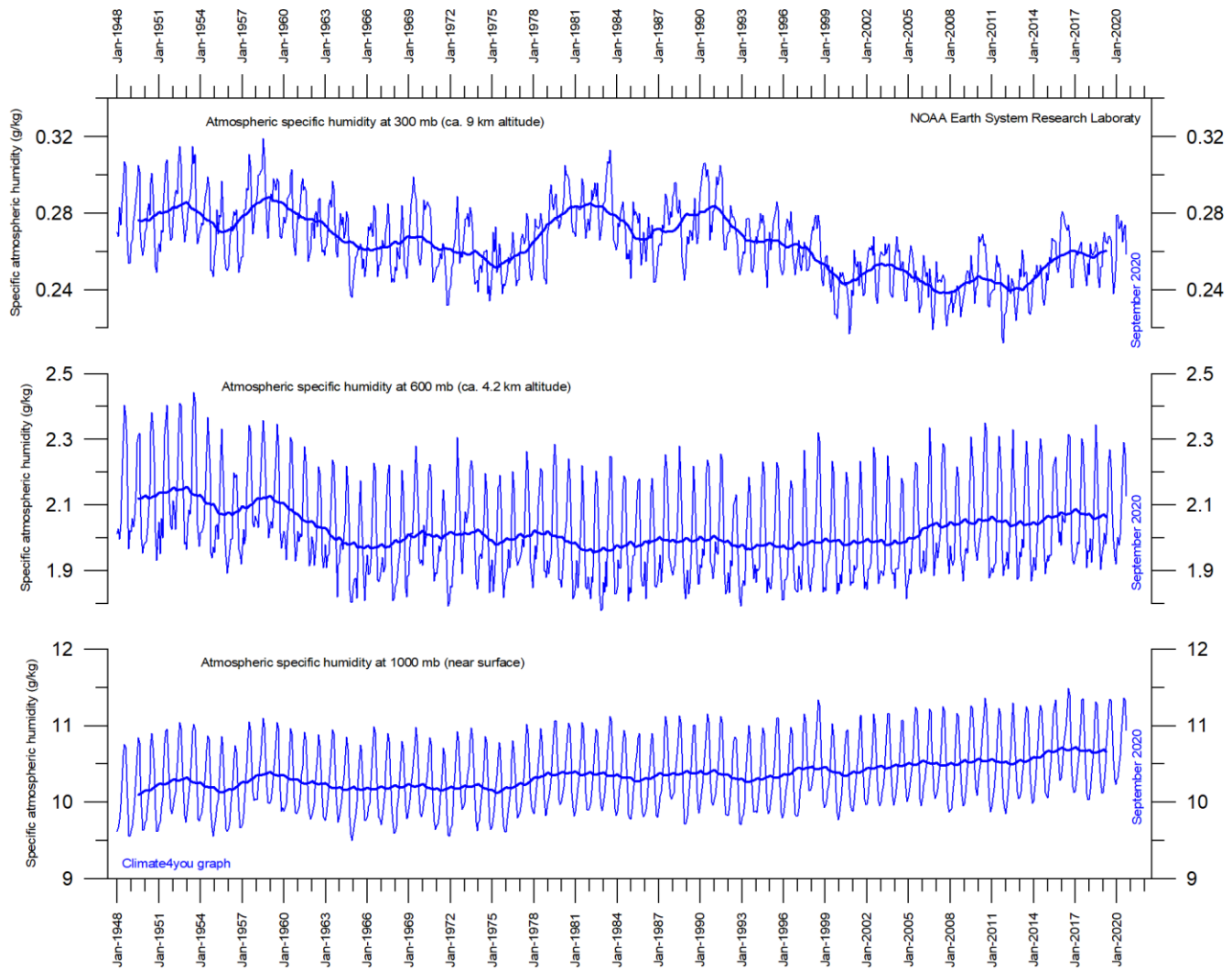


Northern hemisphere weekly snow cover since January 1972 according to Rutgers University Global Snow Laboratory. The thin blue line is the weekly data, and the thick blue line is the running 53-week average (approximately 1 year). The horizontal red line is the 1972-2019 average.



Northern hemisphere seasonal snow cover since January 1972 according to Rutgers University Global Snow Laboratory.

## Atmospheric specific humidity, updated to September 2020



Specific atmospheric humidity (g/kg) at three different altitudes in the lower part of the atmosphere ([the Troposphere](#)) since January 1948 ([Kalnay et al. 1996](#)). The thin blue lines show monthly values, while the thick blue lines show the running 37-month average (about 3 years). Data source: [Earth System Research Laboratory \(NOAA\)](#).

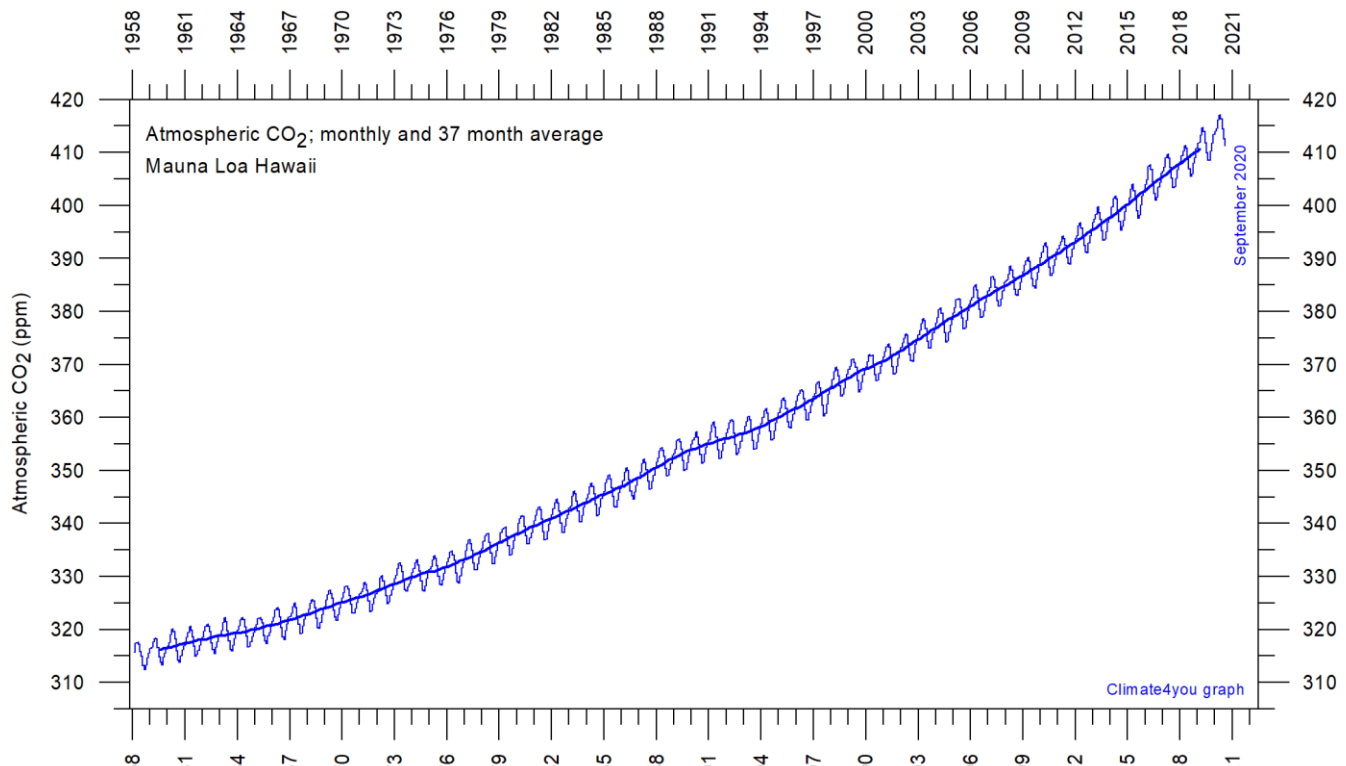
Water vapor is the most important greenhouse gas in the Troposphere. The highest concentration is found within a latitudinal range from 50°N to 60°S. The two polar regions of the Troposphere are comparatively dry.

The diagram above shows the specific atmospheric humidity to be stable or slightly increasing up to about 4–5 km altitude. At higher levels in the Troposphere (about 9 km), the specific humidity has been decreasing for the duration of the record (since 1948), but with shorter

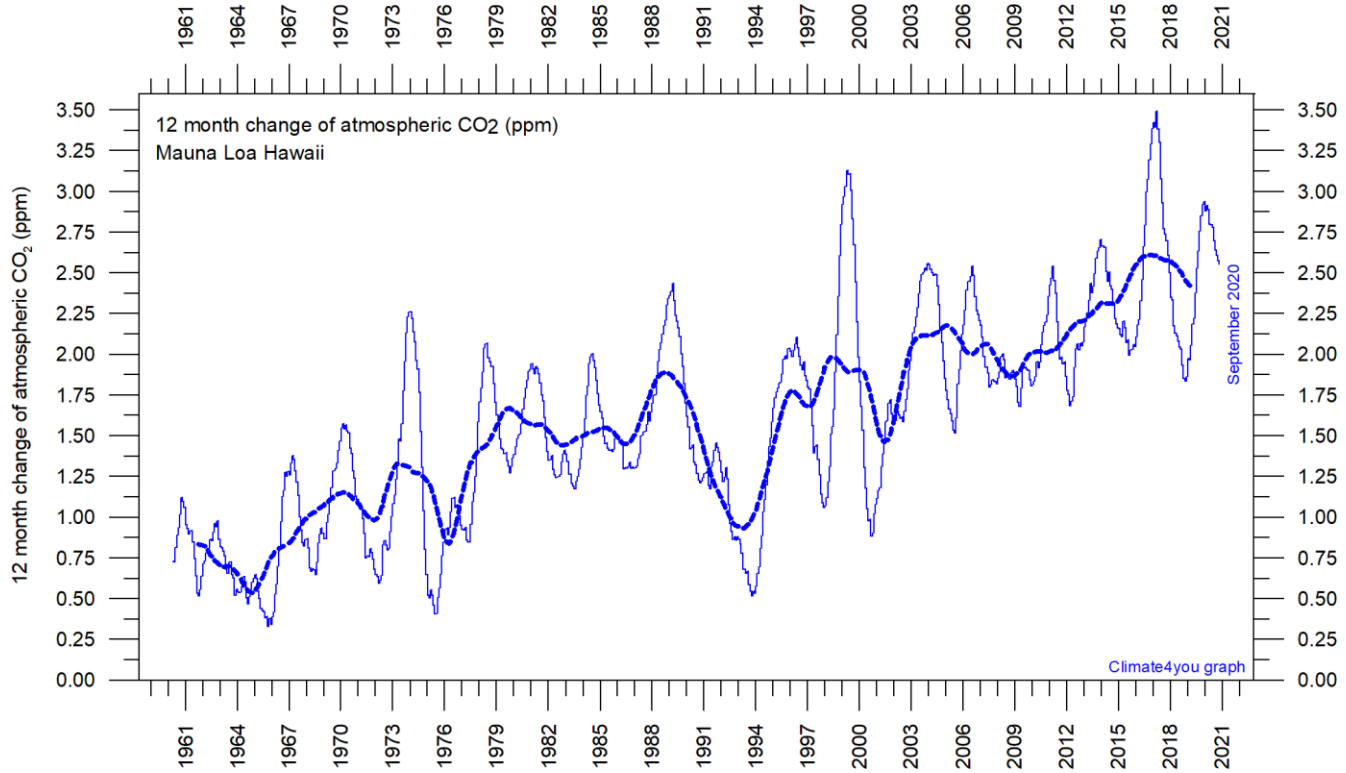
variations superimposed on the falling trend. A Fourier frequency analysis (not shown here) shows these variations to be influenced especially by a periodic variation of about 3.7-year duration.

The persistent decrease in specific humidity at about 9 km altitude is particularly noteworthy, as this altitude roughly corresponds to the level where the theoretical temperature effect of increased atmospheric CO<sub>2</sub> is expected initially to play out.

## Atmospheric CO<sub>2</sub>, updated to September 2020

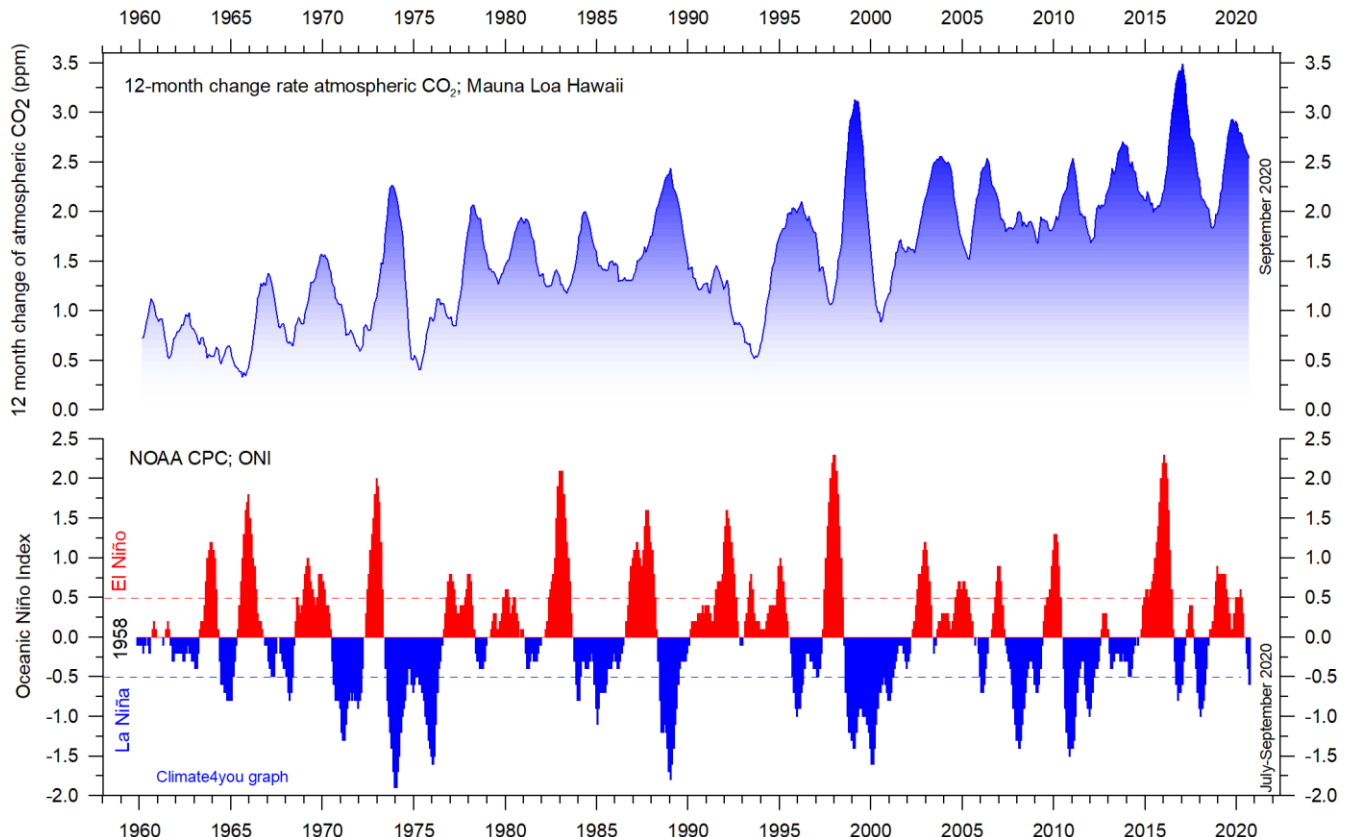


42



Monthly amount of atmospheric CO<sub>2</sub> (upper diagram) and annual growth rate (lower diagram); average last 12 months minus average preceding 12 months, thin line) of atmospheric CO<sub>2</sub> since 1959, according to data provided by the [Mauna Loa Observatory](#), Hawaii, USA. The thick, stippled line is the simple running 37-observation average, nearly corresponding to a running 3-year average. A Fourier frequency analysis (not shown here) shows the 12-month change of Tropospheric CO<sub>2</sub> to be influenced especially by periodic variations of 2.5- and 3.8-years' duration.

## The relation between annual change of atmospheric CO<sub>2</sub> and La Niña and El Niño episodes, updated to September 2020



*Visual association between annual growth rate of atmospheric CO<sub>2</sub> (upper panel) and Oceanic Niño Index (lower panel). See also diagrams on page 40 and 22, respectively.*

Changes in the global atmospheric CO<sub>2</sub> is seen to vary roughly in concert with changes in the Oceanic Niño Index. The typical sequence of events is that changes in the global atmospheric CO<sub>2</sub> to a certain degree follows changes in the Oceanic Niño Index, but clearly not in all details. Many processes, natural as well as anthropogenic, controls the amount of atmospheric CO<sub>2</sub>, but oceanographic processes are clearly highly important (see also diagram on next page).

### Atmospheric CO<sub>2</sub> and the present coronavirus pandemic

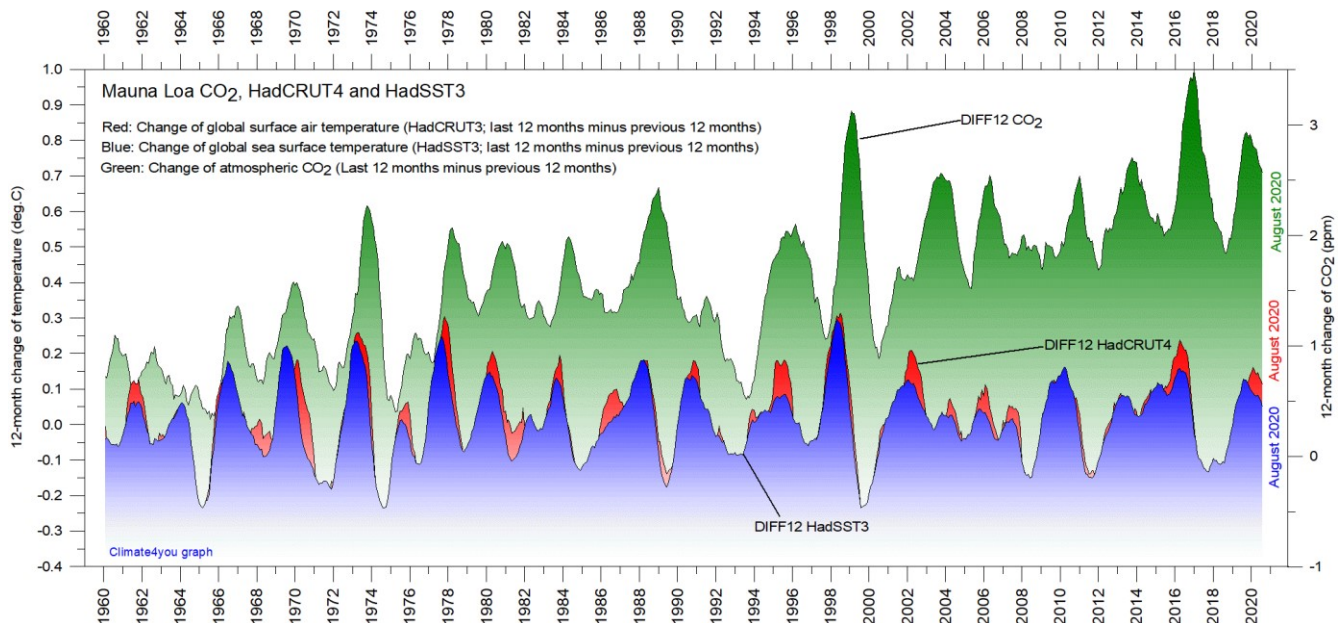
Modern political initiatives usually assume the human influence (mainly the burning of fossil fuels) to represent

the core reason for the observed increase in atmospheric CO<sub>2</sub> since 1958 (see diagrams on page 41).

The present (since January 2020) coronavirus pandemic has resulted in a marked reduction in the global consumption of fossil fuels, as is well reflected by plummeting value of oil and gas. It is interesting to follow the effect of this on the amount of atmospheric CO<sub>2</sub>.

By the end of June 2020 there is still no clear effect to be seen. The simple explanation for this is that the human contribution is too small compared to the numerous natural sources and sinks for atmospheric CO<sub>2</sub> to appear in diagrams showing the amount of atmospheric CO<sub>2</sub> (see, e.g., the diagrams on p. 42-44).

## The phase relation between atmospheric CO<sub>2</sub> and global temperature, updated to August 2020



12-month change of global atmospheric CO<sub>2</sub> concentration ([Mauna Loa](#); green), global sea surface temperature ([HadSST3](#); blue) and global surface air temperature ([HadCRUT4](#); red dotted). All graphs are showing monthly values of DIFF12, the difference between the average of the last 12 month and the average for the previous 12 months for each data series.

44

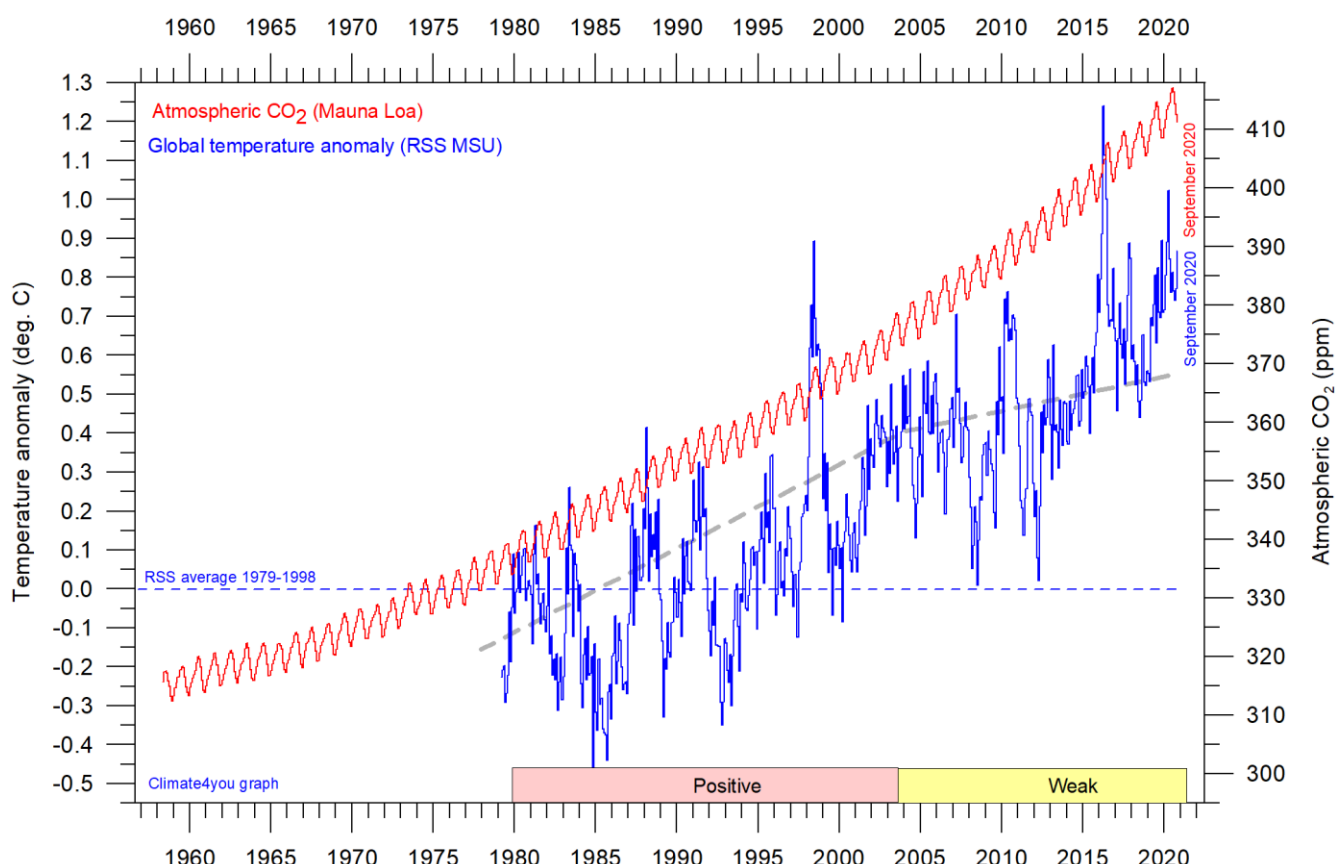
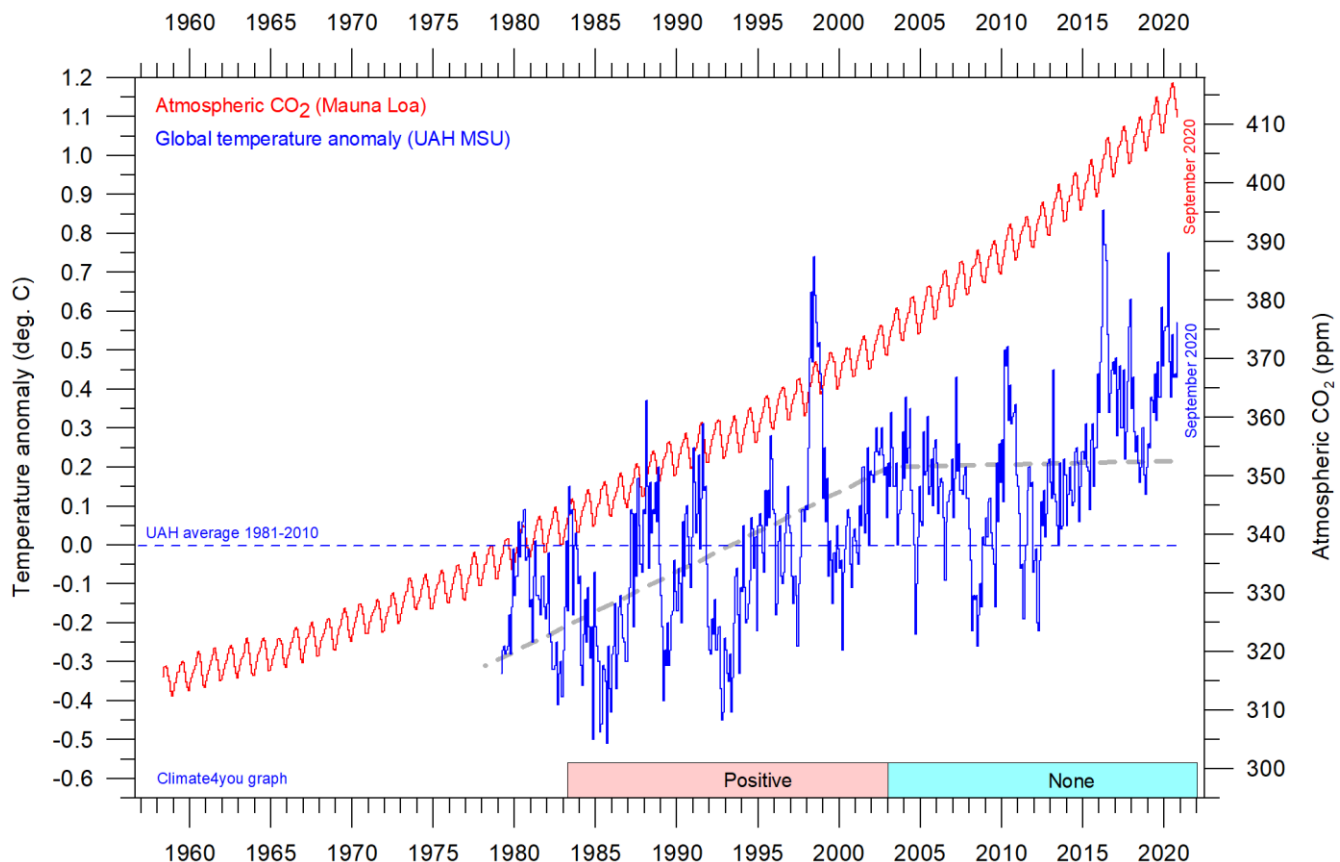
The typical sequence of events is seen to be that changes in the global atmospheric CO<sub>2</sub> follow changes in global surface air temperature, which again follow changes in global ocean surface temperatures. Thus, changes in

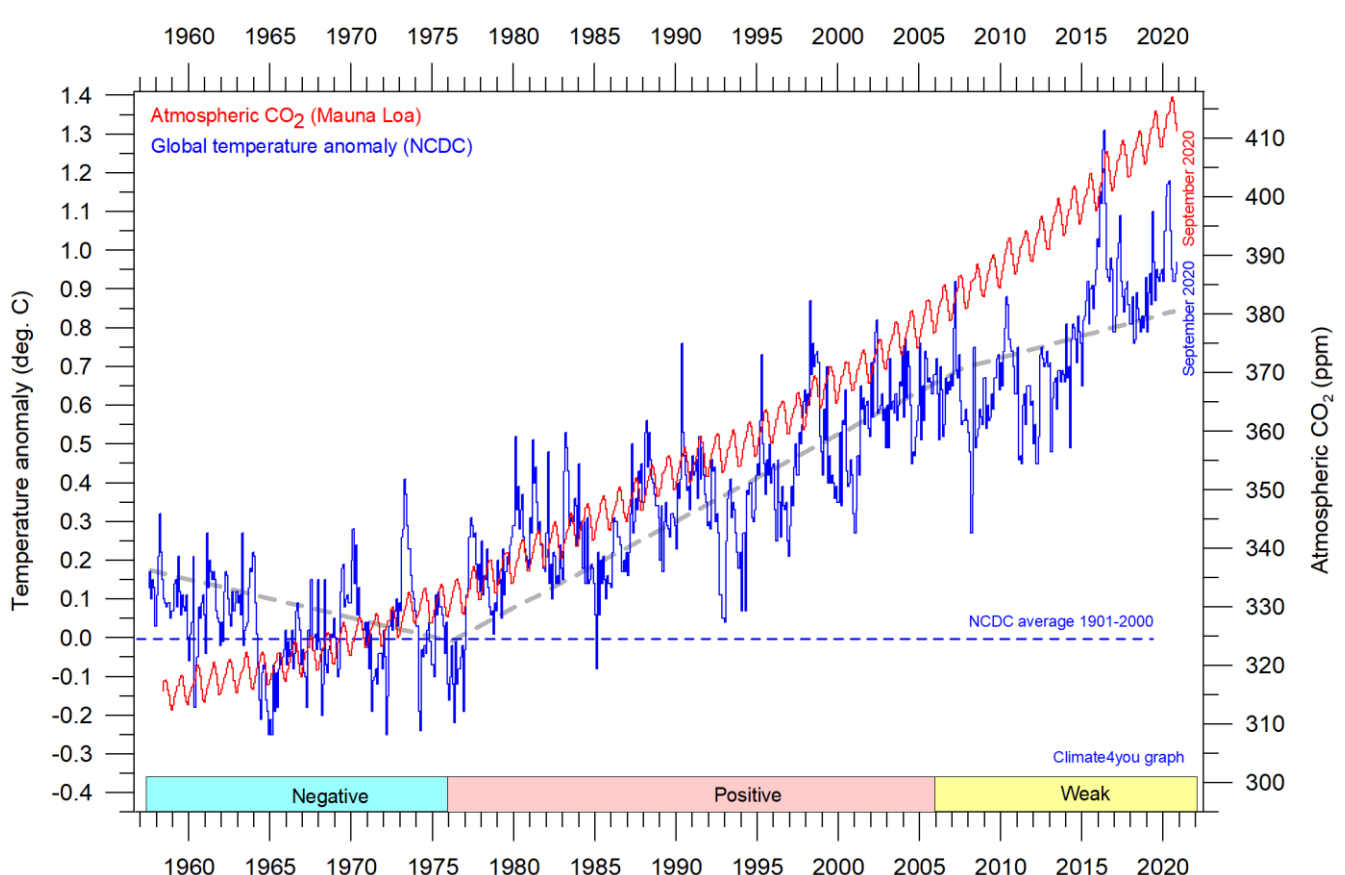
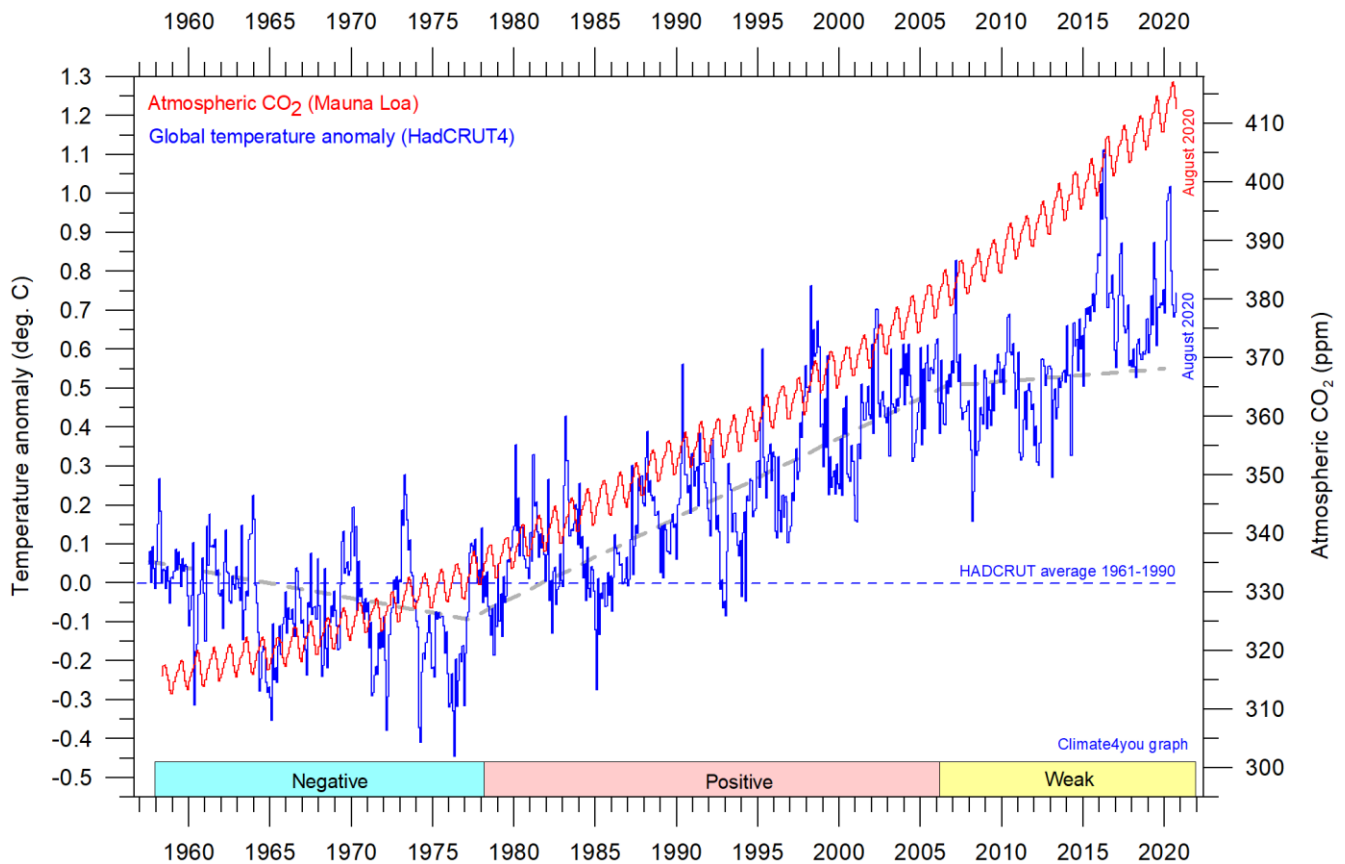
global atmospheric CO<sub>2</sub> are lagging 9.5–10 months behind changes in global air surface temperature, and 11–12 months behind changes in global sea surface temperature.

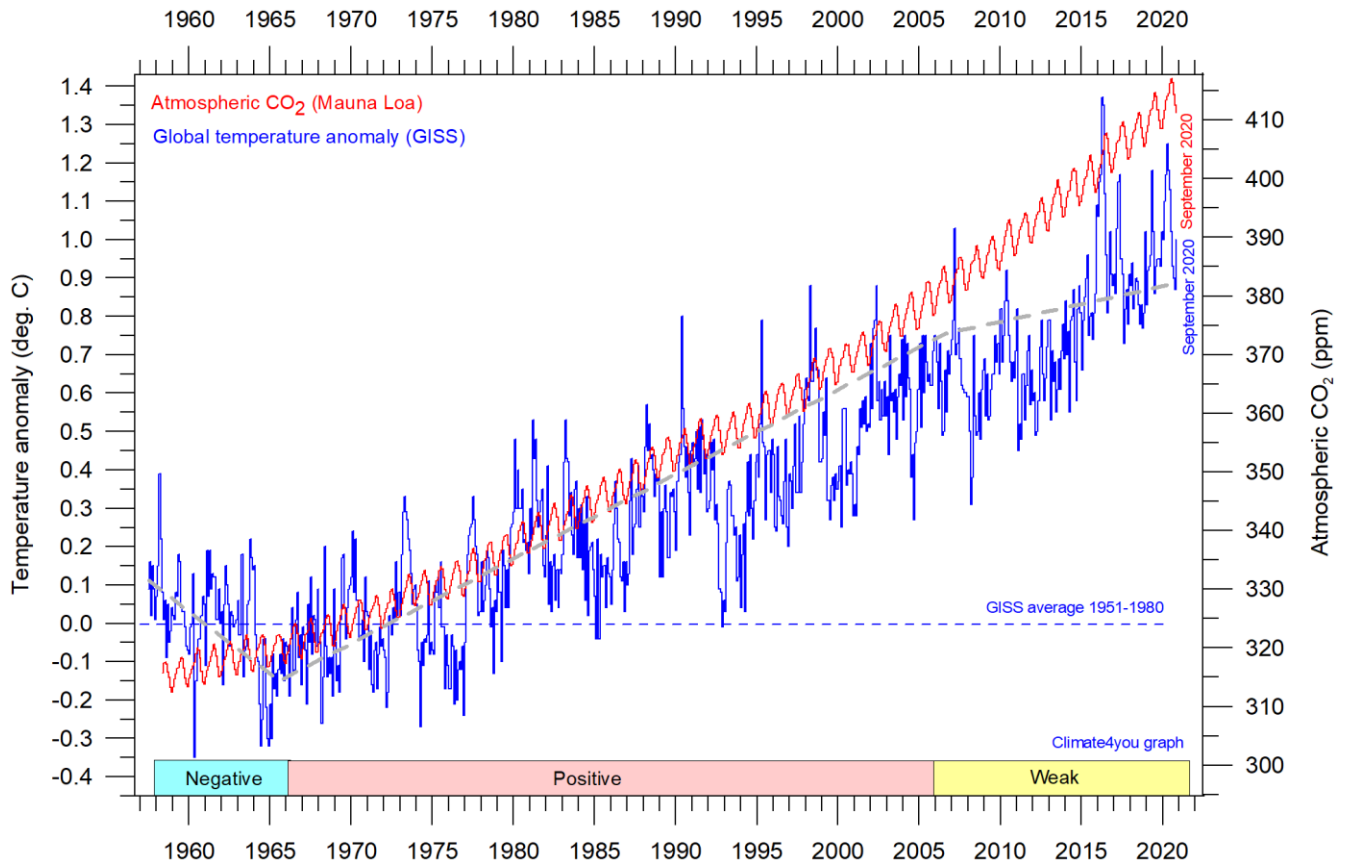
### References:

- Humlum, O., Stordahl, K. and Solheim, J-E. 2012. The phase relation between atmospheric carbon dioxide and global temperature. *Global and Planetary Change*, August 30, 2012.  
<http://www.sciencedirect.com/science/article/pii/S0921818112001658?v=s5>

## Global air temperature and atmospheric CO<sub>2</sub>, updated to September 2020







Diagrams showing UAH, RSS, HadCRUT4, NCDC and GISS monthly global air temperature estimates (blue) and the monthly atmospheric CO<sub>2</sub> content (red) according to the [Mauna Loa Observatory](#), Hawaii. The Mauna Loa data series begins in March 1958, and 1958 was therefore chosen as starting year for all diagrams above. Reconstructions of past atmospheric CO<sub>2</sub> concentrations (before 1958) are not incorporated in this diagram, as such past CO<sub>2</sub> values are derived by other means (ice cores, stomata, or older measurements using different methodology), and therefore are not directly comparable with direct atmospheric measurements. The dotted grey line indicates the approximate linear temperature trend, and the boxes in the lower part of the diagram indicate the relation between atmospheric CO<sub>2</sub> and global surface air temperature, negative or positive.

Most climate models are programmed to give the greenhouse gas carbon dioxide CO<sub>2</sub> significant influence on the modelled global temperature. It is therefore relevant to compare different temperature records with measurements of atmospheric CO<sub>2</sub>, as shown in the diagrams above.

Any comparison, however, should not be made on a monthly or annual basis, but for a longer time, as other effects (oceanographic, cloud cover, etc.) may override the potential influence of CO<sub>2</sub> on short time scales such as just a few years.

It is of course equally inappropriate to present new meteorological record values, whether daily, monthly, or

annual, as demonstrating the legitimacy of the hypothesis ascribing high importance of atmospheric CO<sub>2</sub> for global temperatures. Any such meteorological record value may well be the result of other phenomena. Unfortunately, many news media repeatedly fall into this trap.

What exactly defines the critical length of a relevant period length to consider for evaluating the alleged importance of CO<sub>2</sub> remains elusive and represents a theme for discussion.

Nonetheless, the length of the critical period must be inversely proportional to the temperature sensitivity of CO<sub>2</sub>, including feedback effects. Thus, if the net temperature effect of atmospheric CO<sub>2</sub> is strong, the critical period will be short, and vice versa.

However, past climate research history provides some clues as to what has traditionally been considered the relevant length of period over which to compare temperature and atmospheric CO<sub>2</sub>.

After about 10 years of concurrent global temperature- and CO<sub>2</sub>-increase, IPCC was established in 1988. For obtaining public and political support for the CO<sub>2</sub>-hypothesis the 10-year warming period leading up to 1988 most likely was considered important. Had the global temperature instead been decreasing at that time, politic support for the hypothesis would have been difficult to obtain in 1988.

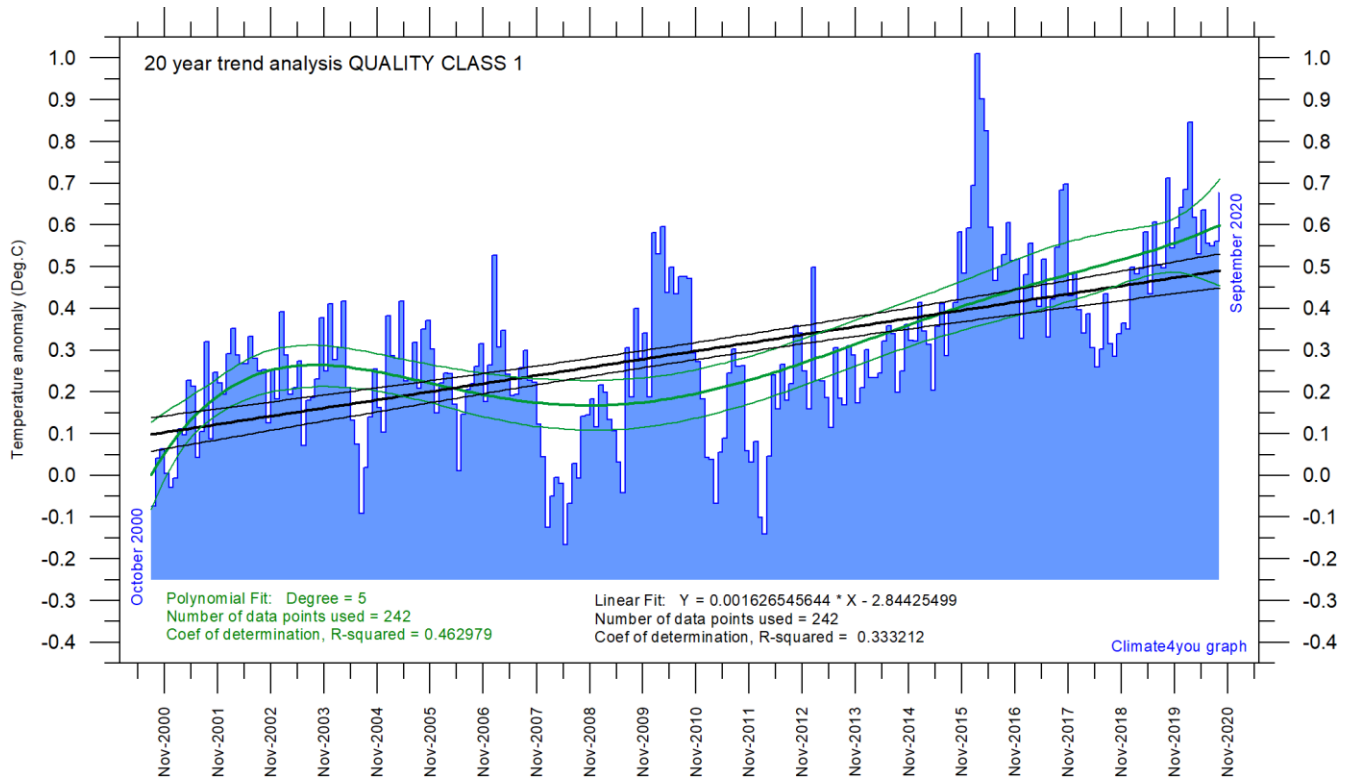
Based on the previous 10 years of concurrent temperature- and CO<sub>2</sub>-increase, many climate

scientists in 1988 presumably felt that their understanding of climate dynamics was enough to conclude about the importance of CO<sub>2</sub> for affecting observed global temperatures.

Thus, it may safely be concluded that 10 years in 1988 was considered a period long enough to demonstrate the effect of increasing atmospheric CO<sub>2</sub> on global temperatures. The 10-year period is also basis for the anomaly diagrams shown on page 2.

Adopting this approach as to critical time length (at least 10 years), the varying relation (positive or negative) between global temperature and atmospheric CO<sub>2</sub> has been indicated in the lower panels of the diagrams above.

## Latest 20-year QC1 global monthly air temperature changes, updated to September 2020



49

Last 20 years' global monthly average air temperature according to Quality Class 1 (UAH and RSS; see p.10) global monthly temperature estimates. The thin blue line represents the monthly values. The thick black line is the linear fit, with 95% confidence intervals indicated by the two thin black lines. The thick green line represents a 5-degree polynomial fit, with 95% confidence intervals indicated by the two thin green lines. A few key statistics are given in the lower part of the diagram (please note that the linear trend is the monthly trend).

In the enduring scientific climate debate, the following question is often put forward: Is the surface air temperature still increasing or has it basically remained without significant changes during the last 15-16 years?

The diagram above may be useful in this context and demonstrates the differences between two often used statistical approaches to determine recent temperature trends. Please also note that such fits only attempt to describe the past, and usually have small, if any, predictive power.

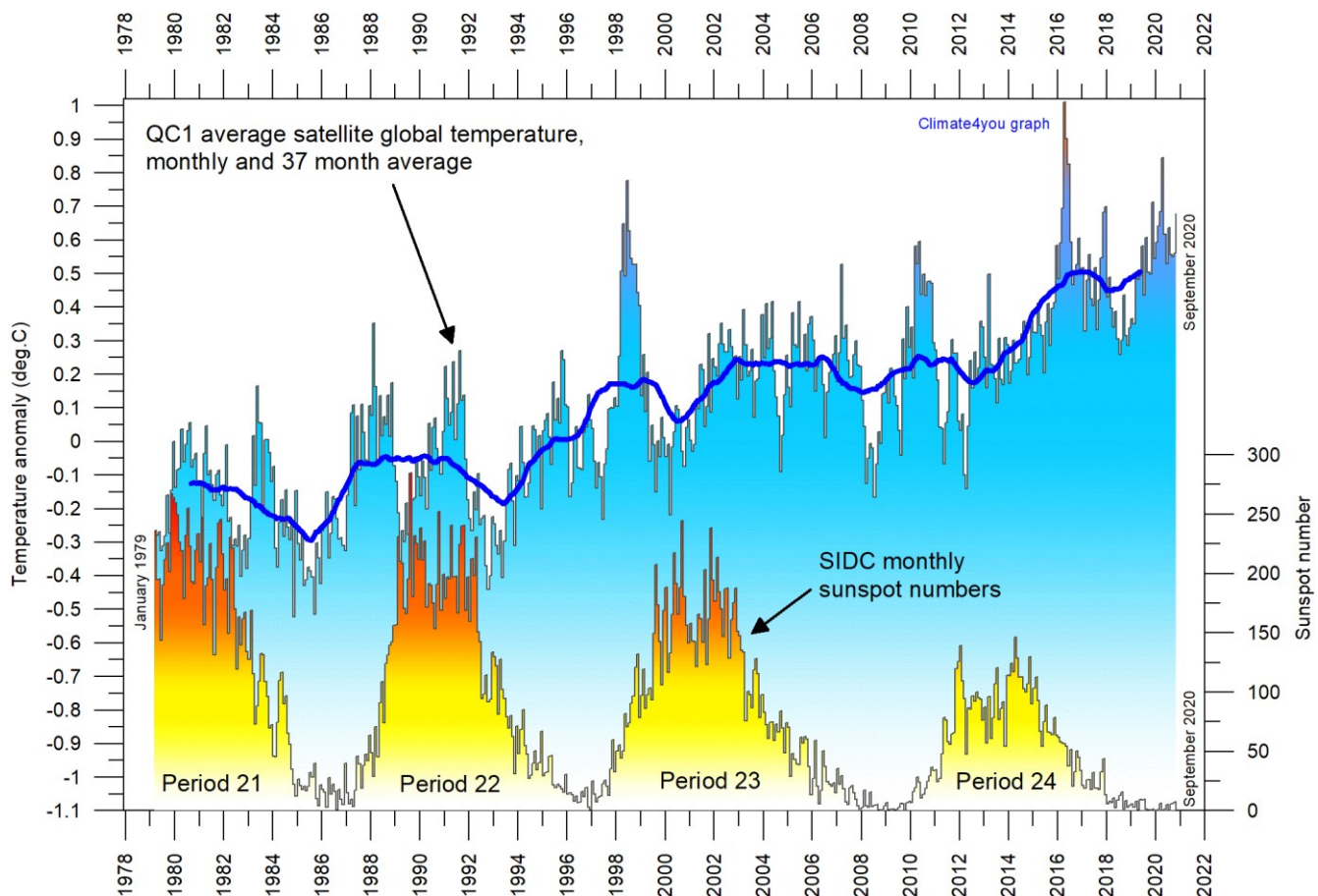
In addition, before using any linear trend (or other) analysis of time series a proper statistical model should be chosen, based on statistical justification.

For temperature time series, there is no *a priori* physical reason why the long-term trend should be linear in time. In fact, climatic time series often have trends for which a straight line is not a good approximation, as is clearly demonstrated by several of the diagrams shown in the present report.

For an admirable description of problems often encountered by analyses of temperature time series analyses, please see [Keenan, D.J. 2014: Statistical Analyses of Surface Temperatures in the IPCC Fifth Assessment Report.](#)

See also diagrams on page 12.

## Sunspot activity and QC1 average satellite global air temperature, updated to September 2020



Variation of global monthly air temperature according to Quality Class 1 (UAH and RSS; see p.4) and observed sunspot number as provided by the Solar Influences Data Analysis Center (SIDC), since 1979. The thin lines represent the monthly values, while the thick line is the simple running 37-month average, nearly corresponding to a running 3-year average. The asymmetrical temperature 'bump' around 1998 is influenced by the oceanographic El Niño phenomenon in 1998, as is the case also for 2015-16. Temperatures in year 2019 was influenced by a moderate El Niño.

## Climate and history; one example among many

**The ‘Zweite Mandrenke 1634 AD’. Ocean-land dynamics in the Frisian area, SE North Sea.**



51

*Figure 1. Scenery from modern Nordstrand. Picture source: Wikimedia.*

Nordstrand (figure 1 and 2) is one of the many Frisian islands (or Wadden Sea Islands) extending from the Netherlands to south-west Denmark, with the islands north of the German Bight are known as the North Frisian Islands. Until the German-Austrian-Danish war in year 1864, the North Frisian Islands were under the Kingdom of Denmark (Herzogtum Schleswig in Personalunion). Except for the three northernmost islands, the North Frisian Islands today are part of Germany. The entire row of Frisian islands is a nice example of what among coastal geomorphologists is known as Barrier islands.

As can be seen from figure 2, Nordstrand used to be part of a much more extensive land area, extending far into the present North Sea. Slow regional tectonic sinking in combination with the overall Holocene global sea level rise have caused a large-

scale flooding of vast land areas in this region of NW Europe over the past 12,000 years. On global scale, the surface level of oceans has risen about 120 m during this period. The melting of the former huge Ice Sheets in North America and in northern Europe is the main reason for this, with major global coastal effects.

About 12,000 years ago, most of the present North Sea was dry land. The northern coast of this huge land area extended roughly from Hanstholm in NW Denmark towards Edinburgh in Scotland (figure 2). Since then, most of this extensive land area has been flooded by the rising ocean, gradually forming the modern North Sea, today roughly measuring 600 km from east to west. In a geological context, this has been a rapid change.

In the North Sea region, the relative (in relation to land) sea level rise initially was very rapid, at least until about 9,000 years ago. In the southern North Sea, the relative sea level rise probably was about 12-13 mm per year (Behre 2007). Subsequently, the relative sea level rise gradually declined to about 1-2 mm/yr, although with important variations playing out over periods of several centuries (Behre 2007). So, the overall development during the past 12,000 years has certainly been transgression (relative sea level rise), but from time to time there has also been periods of regression (relative sea level drop). Nature rarely operates in a simple, linear way.



**Figure 2. Reconstructed former North Sea shorelines between 12,000 and 6,000 yr B.C. (Behre 2007).** Please note that B.C. indicates years before Christ. UK is to the left, and Denmark to the right. The red ellipse indicates the position of the Nordstrand region. The present North Sea measures about 600 km from east to west.

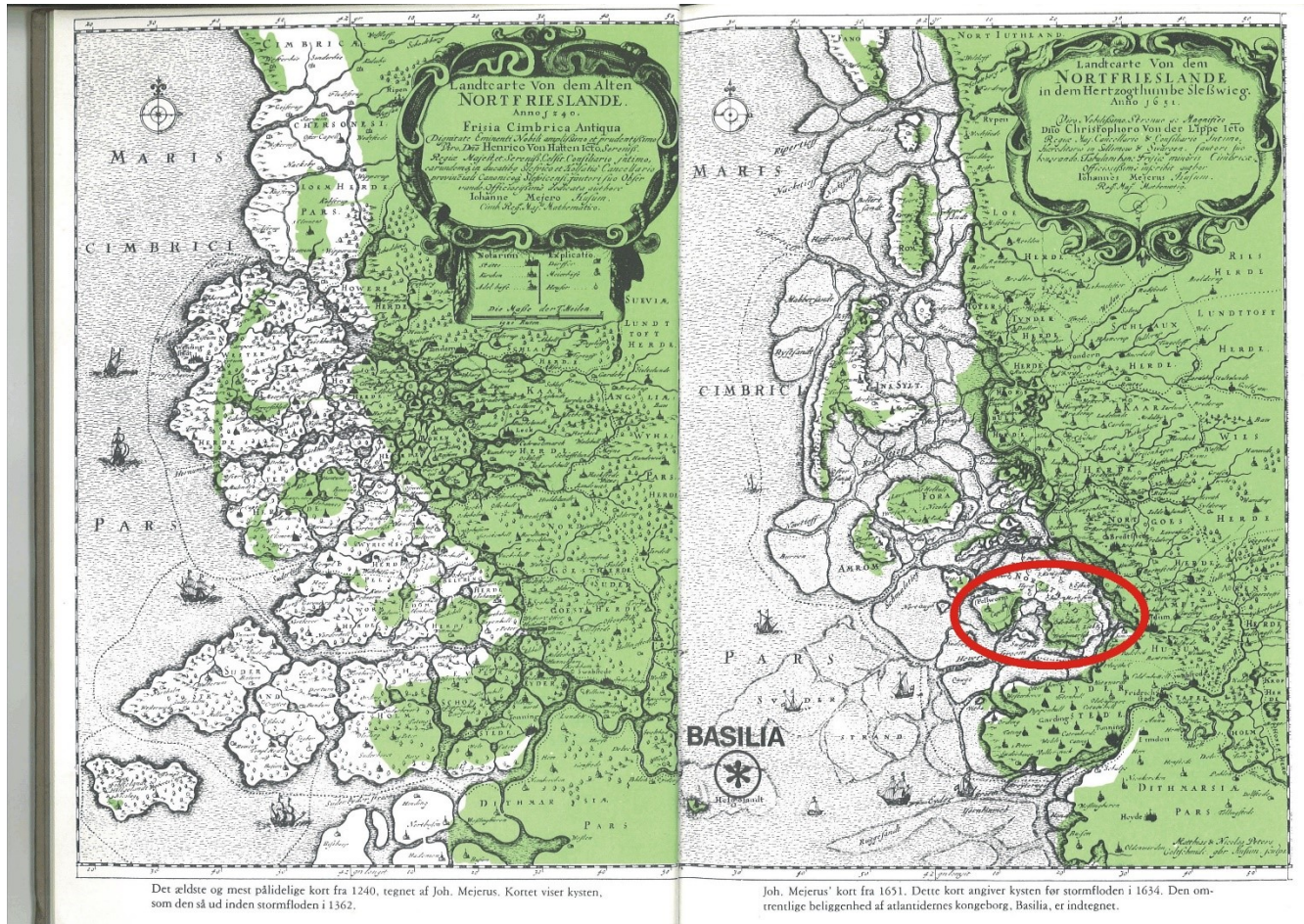
In year 1240, in the Medieval Period, the coast in the Nordstrand region was still located about 30-40 km

west of the modern position (figure 3). The following spectacular coastal recession until today's geographical situation is documented by various sources. Over centuries, but especially during relatively cold periods, strong storms contributed to this stunning loss of land, as is illustrated below by a large flood in the Nordstrand region in the year 1634. This flood is also known as the 'Zweite Mandrenke'.

The summer of 1634 is known to have been warm and dry, with excellent growing conditions on the farming fields of Nordstrand, which at that time was a coherent land area consisting of present Nordstrand and Pellworm (figure 5), as well as the sea today separating them (figure 4). At that time Nordstrand had a population of about 8800 people, distributed on 1745 houses and farms. The people on Nordstrand was doing well, and each year large quantities of farm products were exported to nearby parts of Europe (Pedersen 1977).

Floods is known to have affected Nordstrand several times before 1634, among others the 'Grote Mandränke' in 1362, and also just a few years before 1634 there had been a strong storm, resulting in many parts in Nordstrand being flooded. For that reason, the Danish government had hired the Dutch expert *Jan Adriaansz Leeghwater* to supervise a significant land reclamation project, including the construction of stronger and higher dikes around Nordstrand. The outline of Nordstrand shortly before 1634 is shown in figure 5.

The first weeks of October 1634 were dominated by stable weather and easterly and south-easterly winds, but on 11 October the wind turned towards southwest, increasing in strength, and it soon began to rain. In the evening of 11 October, a fierce storm was blowing with rain, hail, and thunder (Pedersen, 1977). Slowly the fiery wind began turning towards northwest, which typically is fairly alarming in this part of the North Sea, as the wind then forces large water masses into the confined German Bight, leading to rapid increase in sea level along the adjoining coasts. Especially if this timewise matches a normal high tide, this may develop into a profoundly serious situation.



53

*Figure 3. Geography of southern Denmark and northern Germany, showing (left) the coastal outline in 1240 AD, and (right) the outline in 1651 AD, both maps compiled by Johannes Mejerus. The green area shows the modern outline of land. The red ellipse shows the location of the islands Nordstrand and Pellworm today. Each map covers about 95 km from west to east. Map source: Pedersen (1977).*

Around 22 hr in the evening of 11 October the dike near the small town Strintebøl, at the head of the embayment cutting into the southern part of the island (figure 5), was overrun by the rising sea. This was not entirely unexpected as this was where the dikes still were in a relatively bad and unrepaired condition, but within one hour also other and higher dikes were broken at 44 different places along the coast of the island. In addition to the outer dikes, Nordstrand possessed several inner protective dikes, but also these were rapidly overrun by the water.

Around midnight between 11 and 12 October, almost the entire island was covered by several meters of water in rapid movement. People had to evacuate to the uppermost levels in their houses,

but the rapid flowing water and high waves eroded the foundation of the houses, leading to collapse and drowning of the inhabitants. Any rescue attempts from the mainland further to the east were quite impossible under these circumstances, and, eventually, most inhabitants on Nordstrand perished during this dreadful night.

Next morning the Nordstrand island had basically changed into a desert covered by sandy flood sediments. Few areas escaped this flood-driven sand sedimentation, but they all remained covered by sea water for some time. When they eventually dried out, the fields were utterly unsuitable for farming because of the high salt content in the soil (Pedersen 1977).



*Figure 4. The islands Pellworm (left) and Nordstrand (right) in northern Germany. The dark channels between the two land areas are large tidewater channels. Today Nordstrand is connected to the mainland by ongoing land reclamation projects, and therefore formally again a peninsula. Picture source: Google earth.*

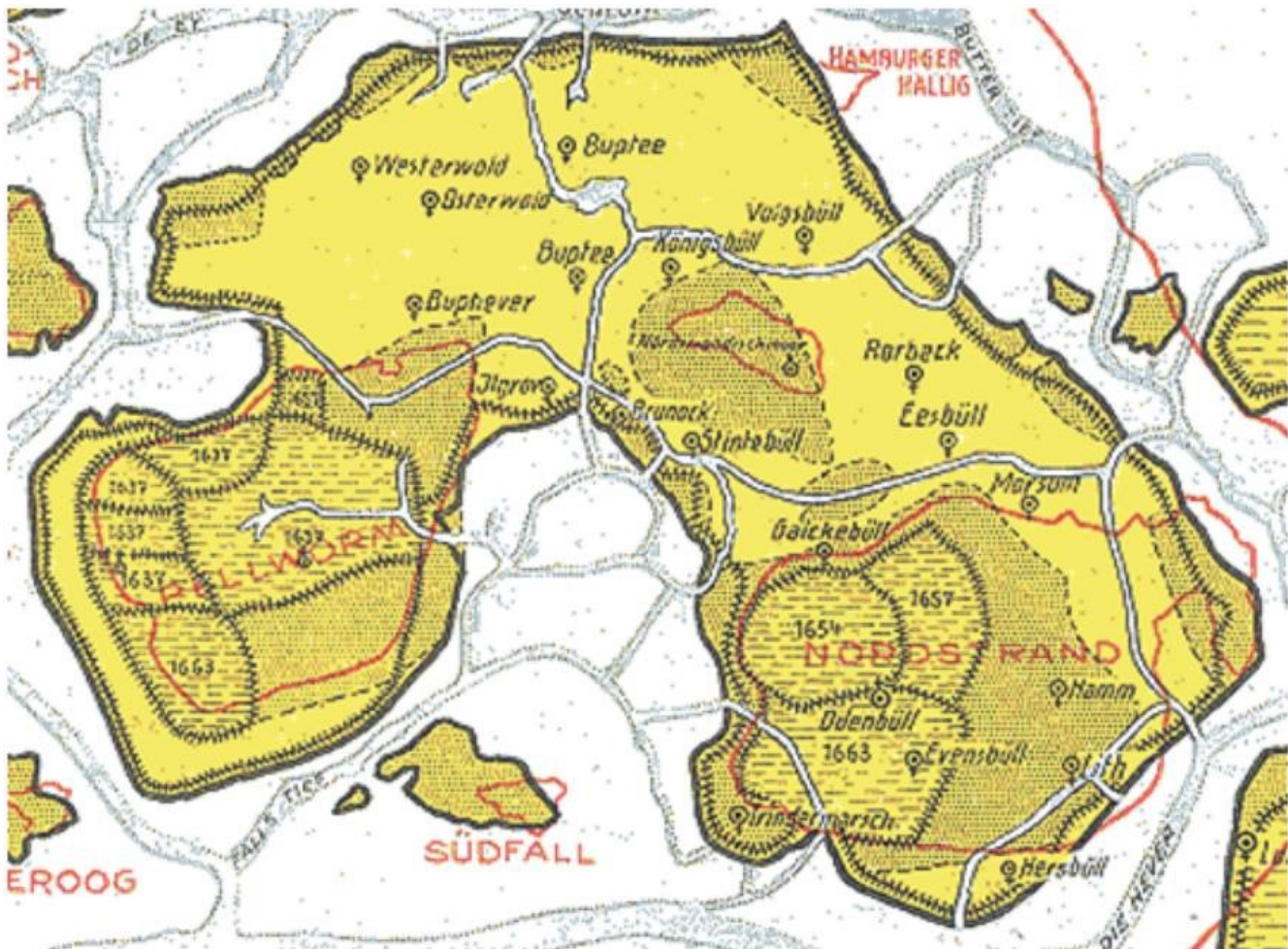
54

After the storm it was discovered that 6035 persons of the about 8800 inhabitants perished during the flood. Of the 1754 houses and farms 1335 were destroyed. About 50,000 animals were lost. Before the flood there was 22 churches on the island, but due to their robust construction none of these was entirely destroyed, and many of the survivors actually made it through this night because they had taken refuge in the churches. However, only three of the 22 churches came into use after the flood. Most of the survivors left Nordstrand and moved east to the mainland, or to the Netherlands.

The northern and central parts of what used to be Nordstrand were given up, and dikes never rebuilt. The western part, today called Pellworm, and the eastern part, todays Nordstrand, was slowly reclaimed from the sea by construction of new dikes. Big tidewater channels developed across the former land areas in the central part of the former Nordstrand, as can be seen from figure 4.

After the 1634 disaster, the Dutch dike expert *Quirinus Indervelde* was hired to lead the construction of new and improved dikes. As reward *Indervelde* and his hundreds of Dutch dike workers could take ownership of the reclaimed land (Rabbel.nl 2012). The reclaiming of land was, however, an awfully slow process, and it was first in 1654 that the dikes around the first polder (reclaimed land) were finished. This became the polder Alterkoog in present day Nordstrand (see figure 5). In 1657 and 1663, the polders Osterkoog and Trindermarschkoog were next to be reclaimed.

By the reclaiming process extensive parts of Nordstrand and Pellworm became owned by Dutch people, and they could freely practice their Roman Catholic religion, although the Danish Kingdom mainly was Lutheran. In fact, the Catholic Church on Nordstrand was under the jurisdiction of the archbishopric of Utrecht in the Netherlands. Today, the archbishopric of Utrecht still owns about 100 acres of land on the now German island Nordstrand (Rabbel.nl 2012).



55

*Figure 5. The geography of Nordstrand before the 1634 flood. The red lines indicate what is left today of the previous much larger Nordstrand Island: the present-day island Pellworm (W) and the small island Nordstrandischmoor (N) and Nordstrand (SE). Compare with figure 3. Before the 1634 flood the island measured about 25 km from east to west. Later reclaimed areas (polders) are shown by the year of reclamation. Map source: Rabbel.nl 2012.*

#### References:

Behre, K.-E. 2007. A new Holocene sea-level curve for the southern North Sea. *Boreas*, Vol. 36, p. 82-102.

Pedersen, K. 1977. *Det tabte land I vest* (Engl.: The lost land in the west). Vestkystens Forlag, Esbjerg, Denmark, 125 pp., ISBN 87-980485-1-1.

Rabbel.nl 2012. Cor Snabel's story of the Nordstrand flood of 1634. <http://rabbel.nl/nordstrand.html>

\*\*\*\*\*

All diagrams in this report, along with any supplementary information, including links to data sources and previous issues of this newsletter, are freely available for download on [www.climate4you.com](http://www.climate4you.com)

Yours sincerely,

Ole Humlum (Ole.Humlum@gmail.com)

Arctic Historical Evaluation and Research Organisation, Longyearbyen, Svalbard

20 October 2020.